1994

Synthesis of Malathion, Malaoxon, and Isomalathion Enantiomers and Examination of Their Interactions with Acetylcholinesterase

Clifford E. Berkman
Loyola University Chicago

LOYOLA UNIVERSITY OF CHICAGO

SYNTHESIS OF MALATHION, MALAOXON, AND ISOMALATHION ENANTIOMERS AND EXAMINATION OF THEIR INTERACTIONS WITH ACETYLCHOLINESTERASE

A DISSERTATION SUBMITTED TO

THE FACULTY OF THE GRADUATE SCHOOL

IN PARTIAL FULFILLMENT OF THE REQUIREMENTS FOR

THE DEGREE OF DOCTOR OF PHILOSOPHY

DEPARTMENT OF CHEMISTRY

BY

CLIFFORD E. BERKMAN

CHICAGO, IL

MAY 1994

Clifford E. Berkman

Loyola University of Chicago

SYNTHESIS OF MALATHION, MALAOXON, AND ISOMALATHION ENANTIOMERS AND EXAMINATION OF THEIR INTERACTIONS WITH ACETYLCHOLINESTERASE

The first synthesis of the individual stereoisomers of malathion [S-(1,2-dicarboethoxyethyl) O,O-dimethyl phosphorodithioate], malaoxon [S-(1,2-dicarboethoxyethyl) O,O-dimethyl phosphorothiolate], and isomalathion [S-(1,2-dicarboethoxyethyl) O,S-dimethyl phosphorodithiolate] has been accomplished. Malathion enantiomers were prepared from malic acid enantiomers in three steps. Malaoxon enantiomers were prepared from the corresponding malathion enantiomers via oxidative desulfuration with MMPP. Isomalathion stereoisomers were prepared by two separate paths employing fractional crystallization of alkaloid phosphorothioic acid salts.

No *in vitro* AChE inhibition data could be obtained for the malathion enantiomers owing to limited solubility. (*R*)-malathion was shown to be a more potent insecticide against *Drosophila Melanogaster*. The bimolecular reaction constant (k_i), dissociation constant (K_D), and phosphorylation constant (k_p) for the inhibition of rat brain acetylcholinesterase by malaoxon enantiomers and for the

inhibition of rat brain acetylcholinesterase and electric eel acetylcholinesterase by isomalathion enantiomers were determined. (*R*)-Malaoxon was an 8-fold stronger inhibitor than (*S*)-malaoxon. Isomalathion stereoisomers with the *R* configuration at phosphorus were 4.3 to 8.8-fold stronger inhibitors of rat brain acetylcholinesterase but 3.4 to 5.8-fold weaker inhibitors of electric eel acetylcholinesterase than the stereoisomers with the *S* configuration at phosphorus. Spontaneous (k_0) and oxime-mediated (k_{oxime}) reactivation rate constants were obtained for rat brain acetylcholinesterase inhibited by the isomalathion stereoisomers. Reactivation rate constants for acetylcholinesterase inhibited by the *R* at phosphorus isomalathion stereoisomers were comparable to those of acetylcholinesterase inhibited by (*S*)-isoparathion methyl, which supports a common phosphorylation mechanism, namely, formation of identical O,S-dimethyl phosphorylated enzymes. Rat brain acetylcholinesterase inhibited by the *S* at phosphorus isomalathion stereoisomers was refractory to reactivation suggesting an alternate mechanism of inhibition, i.e., the loss of the thiomethyl ligand. Several mechanisms are proposed to account for this nonreactivation observed with the *S* at phosphorus isomalathion stereoisomers. Rate constants for non-reactivatability (k_{NR}) were determined for rat brain acetylcholinesterase inhibited by isoparathion methyl enantiomers as a model for acetylcholinesterase inhibitors resulting in an asymmetric O,S-dimethyl phosphorothiolated enzyme. Rat brain acetylcholinesterase inhibited by (*R*)-isoparathion methyl underwent a time-dependent decrease of reactivatability twice that of (*S*)-isoparathion.

ACKNOWLEDGMENTS

My thanks to Chuck Thompson are manifold; first, for providing me with a globally relevant research project with unanticipated nuances that continue to stir my curiosity; second, for his benevolent guidance throughout my graduate studies; and third, for his nearly endless supply of gourmet coffee. I wish to acknowledge the Thompson Group for their esprit de corps, especially Nam Huh, Diana Green, Jeff Frick, Seungmin Ryu, Jing Lin, John Jackson, Jim Kiddle, with special thanks to Debra Quinn for her expert assistance. Acknowledgements are also due to: Stephen Pavkovic and Elias Fernandez for solving the structure to the desmethyl malathion-strychnine salt whose configurational assignment was invaluable; Scott Perrin of Regis Chemical Company for developing a technique to resolve the four stereoisomers of isomalathion; Ib Winckelmann of Cheminova Agro for examining the insecticidal activities of the malathion enantiomers; and John Cashman for helpful discussions. I would also like to thank my parents for their support and continued concern over my "exposure" to nerve gas agents. Importantly, I wish to thank Noreen Ryan for her tireless support, love, and tolerance throughout the duration of my graduate studies.

TABLE OF CONTENTS

LIST OF ABBREVIATIONS

Abs.	absorbance
AChE	acetylcholinesterase
Anal.	combustion elemental analysis
ATCh-I	acetylthiocholine iodide
BEAChE	bovine erythrocyte acetylcholinesterase
c	concentration (g/100 mL)
d	doublet
dd	doublet of doublets
dq	doublet of quartets
DMF	dimethylformamide
dt	doublet of triplets
DTNB	5,5'-dithiobis(2-nitrobenzoic acid)
EEAChE	electric eel acetylcholinesterase
Et	ethyl
equiv	equivalents
g	gram
h	hour

HEAChE	human erythrocyte acetylcholinesterase
HPLC	high performance liquid chromatography
Hz	hertz
J	NMR coupling constant (in Hz)
L	liter
m	multiplet
m	meta
M	molar (molarity)
*m*CPBA	*m*-chloroperoxybenzoic acid
MeOH	methanol
MHz	megahertz
MMPP	monoperoxyphthalic acid magnesium salt
min	minute
mL	milliliter
uL	microliter
mmol	millimole
mol	mole
mp	melting point
NMR	nuclear magnetic resonance
OP	organophosphorus
PTS	Peets

p	para
2-PAM	2-pyridinium aldoxime methiodide
Ph	phenyl
ppm	parts per million
RBAChE	rat brain acetylcholinesterase
s	singlet
SBC	Seattle's Best
STB	Starbucks
t	triplet
TEA	triethylamine
THF	tetrahydrofuran
TLC	thin layer chromatography

LIST OF TABLES

LIST OF FIGURES

Figure

LIST OF SCHEMES

Scheme

CHAPTER 1

INTRODUCTION

> "The implications of pesticide use can not be understood without a basic understanding of pesticide chemicals and an appreciation of their benefits and risks. Ultimately, it will be up to the public - the consumers - to determine the limits of pesticide use. A better understanding of the science behind such an issue gives us a perspective that aids us in participating responsibly and fully in public policy decision-making (Parr, 1987)."

Pesticide Utility and Societal Impact

One of the primary responsibilities of any society is to support its population with an adequate supply of food. In that effort, it is estimated that nearly half of all agricultural produce is destroyed by pests, mostly during storage (Perutz, 1991). Thirty percent of the potential crop, livestock, and timber yield is believed to be lost annually to insects or other pests (Furtick, 1976; Cagliotti, 1983). Grain losses prior to harvest in developing countries of the Near East are approximately 23% with the largest losses in the production of cereal crops, especially rice (Hayes, 1991).

Advances in pesticide design over the past fifty years have significantly contributed toward increased crop yield by diminishing the population of

threatening organisms. In addition, some insecticides have been instrumental in the reduction of malaria and other insect-borne diseases in humans (Cagliotti, 1983). In addition to influencing crop yields, insecticide usage also impacts on the economy. It is estimated that without the use of pesticides, prices for fruits and vegetables would increase 50 to 100% in first world countries (Schuhman, 1976). Pesticide application for food consumption necessitates significant production; approximately 3 billion pounds of pesticides are produced in the U.S. annually, one third of which are insecticides. In addition, U.S. consumers purchase roughly 25% of all insecticides resulting in annual sales of nearly 900 million dollars (Welling, 1988).

Hazards of Pesticide Use

According to the World Health Organization (WHO), it is estimated that 3 million acute pesticide poisonings occur annually leading to 250,000 fatalities, of which 99% occur in developing countries (Stephens, 1991; Rosenstock, 1991). In Sri Lanka, nearly 13,000 people are admitted annually to hospitals for pesticide poisoning that result in approximately 1000 fatalities. It is estimated that 40,000 farmworkers of third world countries die each year as a result of pesticide intoxication. Generally, these agricultural workers are poisoned because either they cannot read, understand, or implement safety instructions, or the instructions themselves are inadequate (Perutz, 1991). Approximately 300,000 pesticide

poisonings are reported in the United States annually (Rosenstock, 1991). It is also believed that many deaths due to pesticides are unreported (Forget, 1991).

Over-exposure to insecticides is greatest for those who are directly involved in their application, including mixing concentrates and loading aircraft for aerial pesticide application (Barnes, 1976). Protective clothing for U.S. agricultural workers has been assumed to be adequate defense against exposure. In 1974, protective clothing was documented as "at least a hat or other suitable head covering, a long-sleeved shirt and long-legged trousers, or a coverall type garment, shoes and socks." Recent revisions to these recommendations by the EPA and USDA include: a liquid-proof raincoat or apron, trousers outside of boots, unlined neoprene gloves, wide-brimmed waterproof hats, unlined neoprene boots, and goggles or face shields (Stone, 1988). Other steps have been taken to prevent the occurrence of acute poisonings such as medical monitoring of agricultural workers. One such attempt has been made by California's Department of Health Services in which periodic monitoring for exposure to agrichemicals is conducted (Ames, 1989).

Despite increased protective measures for U.S. agrichemical workers, pesticide poisonings remain a continuing concern in developing countries. A significant number of poisonings seem to result from "lack of knowledge, unsafe attitudes, and dangerous practices (Forget, 1991)." A further problem relates to the state of the technology available to small farmers such as "faulty sprayers,

lack of protective equipment adapted to tropical conditions, and non-existent first-aid provisions (Forget, 1991)." It has been suggested that one of the most important factors contributing to pesticide poisonings in developing countries is a lack of information (Forget, 1991).

Because pesticides are toxic and yet help support growing populations through crop protection, several conflicts in usage have arisen. Thus, in order to justify the production and implementation of such compounds, a number of issues must be considered including: the human health risks from direct exposure and food residues, worker occupational hazards, and possible contamination of drinking water (Zilberman, 1991).

Organophosphorus (OP) Insecticides

Organophosphorus (OP) compounds are members of the insecticide arsenal that includes carbamates, chlorinated hydrocarbons, and pyrethroids. To date, more than 50,000 organophosphorus (OP) compounds have been synthesized and evaluated for their insecticidal potential (Gutmann, 1990). Among these, several OP's have been specifically stockpiled for military use as genocide-based neurotoxic agents (nerve gas) including sarin **1**, soman **2**, and tabun **3** (Figure 1; Caglioti, 1983).

The synthesis of TEPP (tetraethyl pyrophosphate **4**, Figure 1) in 1854 most likely spawned investigations of toxic OP compounds (Eto, 1974). Their

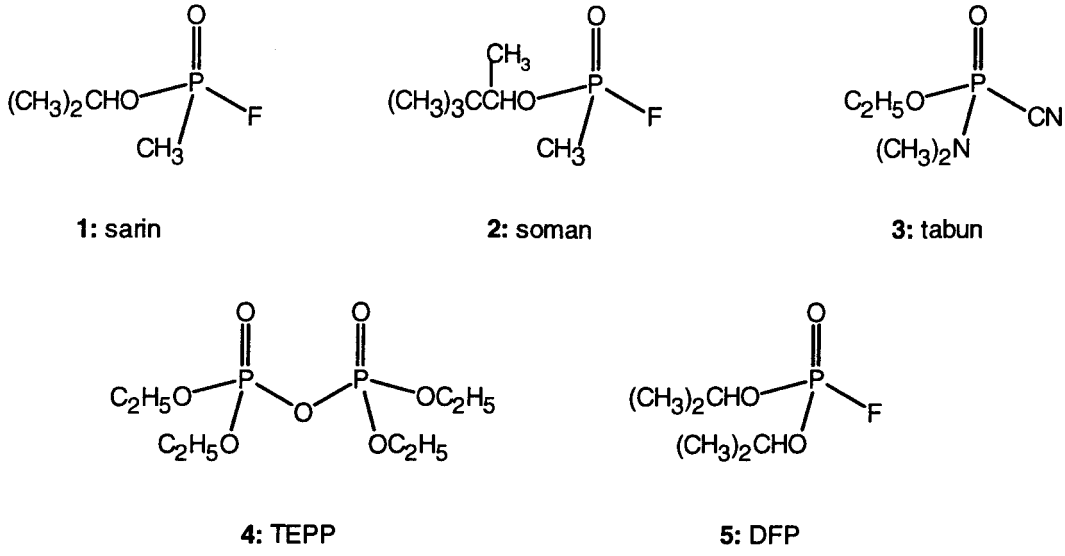

Figure 1. Neurotoxic Organophosphorus Compounds.

development was furthered by both Schrader (Germany) and Saunders (England) during WWII while searching for chemical warfare agents such as diisopropyl phosphonofluoridate (DPF **5**; Figure 1) (Eto, 1974). As an outgrowth of these studies, Schrader and coworkers identified several OP compounds that exhibited contact insecticidal activity. The first practical insecticide, Bladen, which contained the highly toxic compound TEPP, was developed by Schrader and coworkers in 1941 and was subsequently marketed in 1944 (Eto, 1974). Since the 1940's, thousands of new OP insecticides have been developed.

Because of their relatively short-lived environmental lifetime, OP's have replaced the environmentally persistent, chlorinated hydrocarbons such as DDT;

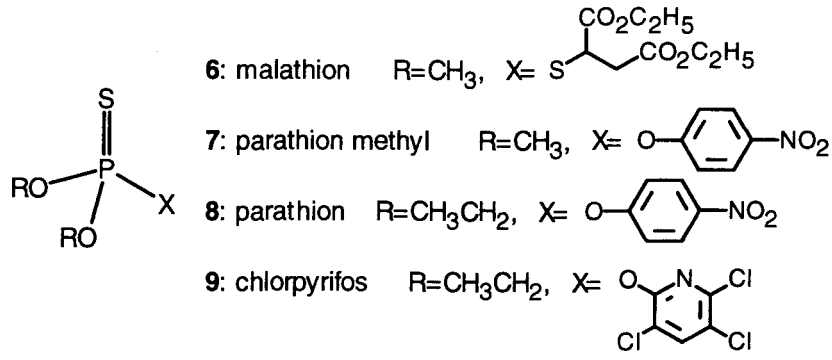

Figure 2. Common OP Insecticides.

its use was banned in the United States during the 1970's due to notable retention in body tissue and biomagnification (Matolcsy, 1988; Mahieu, 1990; Stephens, 1991). It is estimated that 31 to 48 billion pounds of the four most popular organophosphate insecticides, malathion **6**, parathion methyl **7**, parathion **8** , and chlorpyrifos **9** (Figure 2) are used each year in the United States (Stephens, 1991).

Structure and Reactivity of OP Insecticides

In order to discuss organophosphorus (OP) insecticides in detail, a brief review of nomenclature, structure, and chemical reactivity is necessary. Some general structures of OP compounds that will be discussed in this dissertation are shown in Figure 3. For insecticidal activity, one of the ligands attached to the phosphorus atom is generally required to be a good leaving group. This aspect

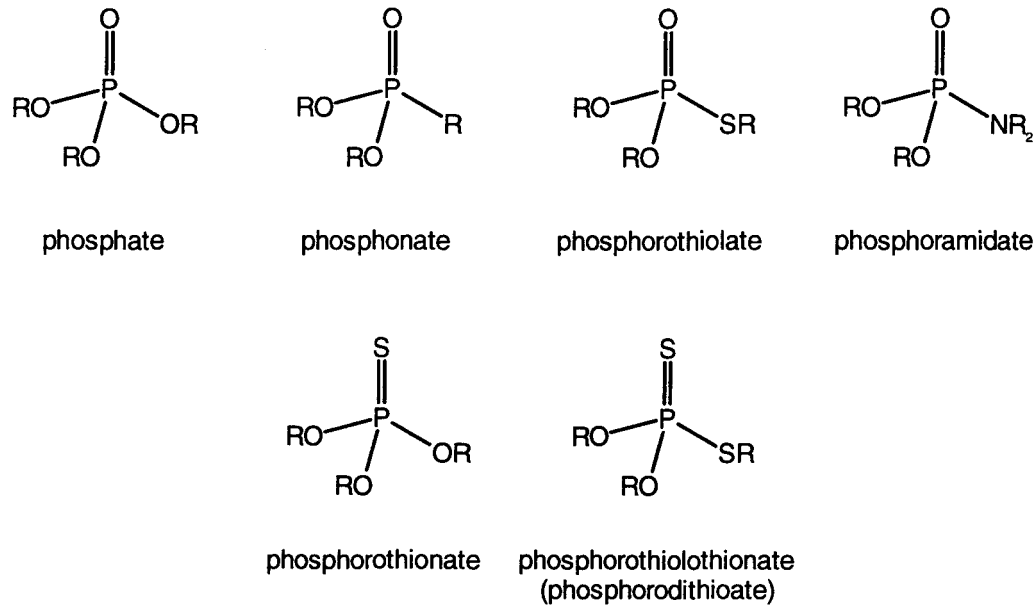

Figure 3. General Structure of OP Compounds.

of OP reactivity and its relationship to biological activity will be discussed in Section 1.8.

Most OP insecticides belong to the phosphorothionate class (P=S). Two main features of OP's that influence their chemical reactivity are: the π-atom linkage, and the σ-ligand connectivity. Two examples will serve to illustrate these points. As opposed to the sulfur of the P=S linkage, the more electronegative oxygen atom of the P=O bond imparts a greater electrophilicity at the phosphorus atom making it more susceptible to nucleophilic attack and hydrolysis (Matolcsy, 1988; Fest, 1973; Van Wazer, 1958). This feature is

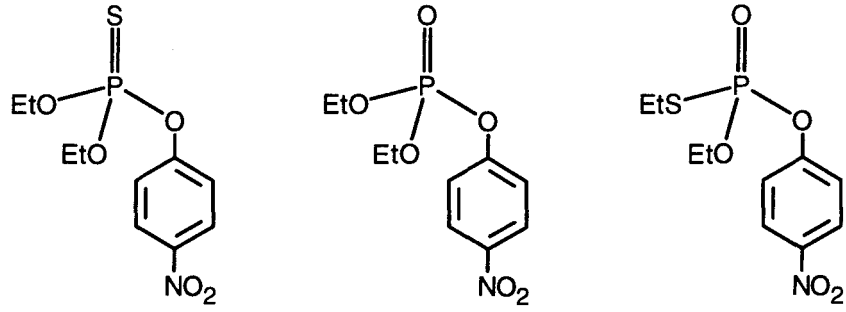

8: parathion **10:** paraoxon **11:** isoparathion

Figure 4. Parathion, Paraoxon, and Isoparathion.

exemplified by the 9-fold difference in the hydrolytic $t_{1/2}$ (pH = 8) values for parathion **8** (203,000 h) and paraoxon **10** (22,200 h) (Figure 4, O'Brien, 1967). The thiolate (P-S-R) linkage also affects the reactivity of OP's. Phosphorothiolate esters are more chemically reactive than their phosphate analogues because the sulfur atom imparts greater polarizability and decreased pπ-dπ contribution to the P-S bond due to the less efficient orbital overlap (Eto, 1974). The more rapid hydrolysis (470-fold) of isoparathion **11** compared to that of paraoxon **10** illustrates the importance of the thiolate sigma-bond contribution toward the reactivity of OP's (Heath, 1961).

Thiono-Thiolo Rearrangement

Dialkyl phosphorothionates are prone to chemical, thermal, and to a lesser

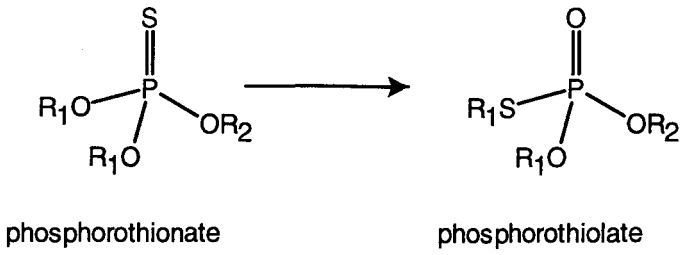

Figure 5. Thiono-Thiolo Rearrangement.

extent, photochemical induced isomerization to the corresponding S-alkyl phosphorothiolates (Figure 5). This transformation is known as the thiono-thiolo rearrangement. The rearrangement may be promoted by reaction of a phosphorothionate with an alkyl iodide to form the S-alkyl isomeride by first alkylation of the thionate followed by dealkylation (Figure 6) (Eto, 1974).

Self-isomerization, or bimolecular isomerization, occurs at elevated temperatures (80-180 ^{0}C) where one phosphorothionate is dealkylated by another

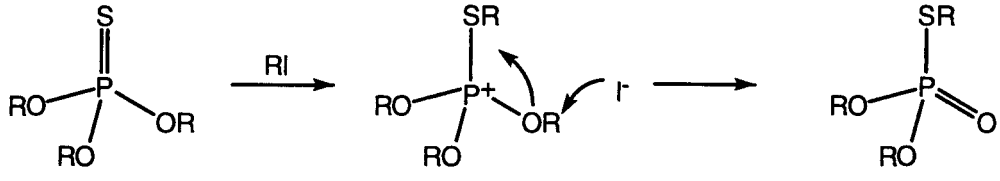

Figure 6. Alkyl Iodide Catalysis of the Thiono-Thiolo Rearrangement.

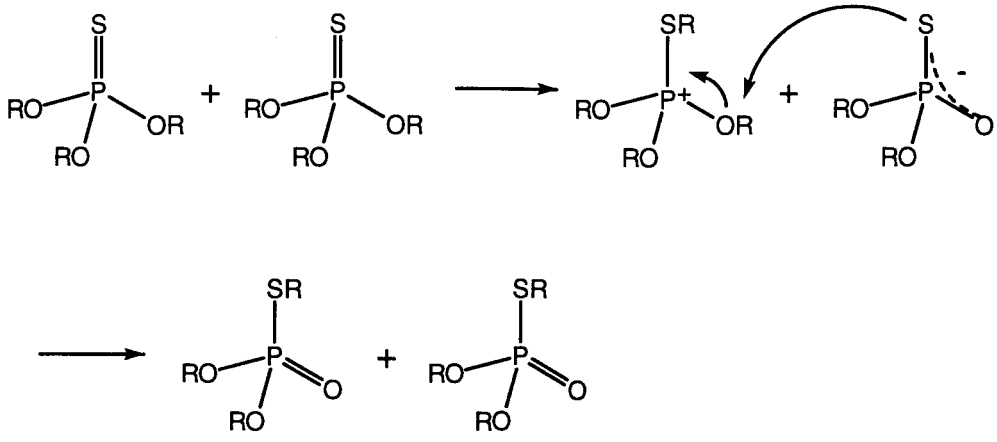

Figure 7. Self-Isomerization of Dialkyl Phosphorothionates.

to form an ambident ion pair that realkylates at the more nucleophilic sulfur atom (Figure 7) (Fest, 1973; Eto, 1974). This isomerization occurs fastest when the alkyl group transferred is methyl (Eto, 1974). Isomerization also may occur at room temperature over a long period of time when phosphorothionates are stored in polar aprotic solvents (Eto, 1974, Matolcsy, 1988).

Unfortunately, thiono-thiolo transformation may transpire during the manufacture or storage of phosphorothionate insecticides. Indeed, malathion (**6**) formulations have been found to contain as much as a 10% contamination of the thiolo isomeride, isomalathion **12** (Figure 5; R_1 = CH_3, R_2 = $SCH(CO_2Et)CH_2CO_2Et$), and it has been shown that approximately 90% of malathion **6** was isomerized to isomalathion **12** at 150 ^{0}C (Metcalf, 1953). In the

same study, parathion (Figure 5, R_1 = Et, R_2 = O-p-Ph-NO_2) was isomerized (150 ^{0}C, 24 h) to the S-ethyl thiolate in 80% yield while 90% of parathion methyl (Figure 5, R_1 = CH_3, R_2 = O-Ph-NO_2) was isomerized under the same conditions.

Mode of Action of OP's - General Aspects

Regardless of the effectiveness of OP's in insect control, numerous accidental OP poisonings of humans occur every year. The toxicity of organophosphates to mammals and insects is primarily due to their ability to inactivate the enzyme acetylcholinesterase (AChE). AChE is found in both the central and peripheral nervous system, the primary role of which is to catalyze the hydrolysis of the neurotransmitter acetylcholine (ACh, **13**; Figure 8) (Quinn, 1987). The rate at which AChE facilitates the hydrolysis of AChE **13** is on the order of 10^5 molecules per minute.

During the transmission of a nerve signal, ACh is released from presynaptic vesicles and diffuses across the synapse to bind at ACh receptors of the post-synaptic membrane, thus, completing the signal. AChE rapidly removes surplus ACh from the synapse to either terminate the neural transmission at cholinergic synapses or maintain the correct titer of ACh during enervation (Figure 9).

When an OP inactivates AChE, the result is an accumulation of ACh in the neural synapses and neuromuscular junctions promoting continued and

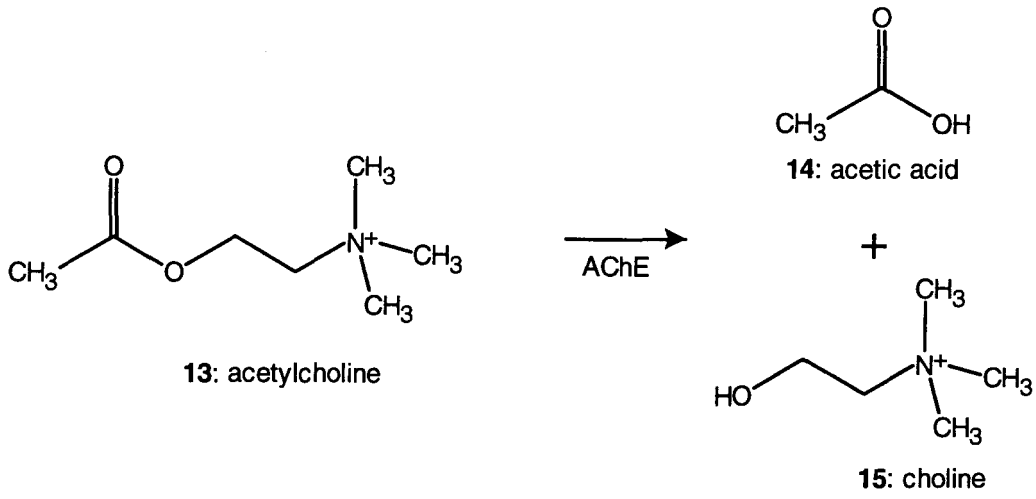

Figure 8. AChE Mediated Hydrolysis of ACh.

uncontrolled neural transmission. Inactivation of AChE is manifested in stimulation of the nicotinic and muscarinic receptors of autonomic organs and

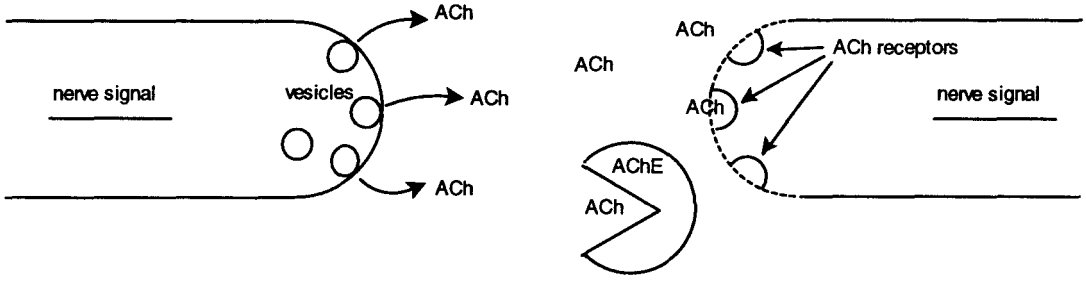

Figure 9. The Role of AChE in Neural Transmission.

skeletal muscles as well as stimulation of cholinergic receptors (predominantly muscarinic) of the CNS. General effects following OP intoxication include those outlined in Table 1 (Goodman, 1985). In severe acute poisonings, paralysis of the respiratory muscles may occur and result in death (Mahieu, 1990).

Table 1. Effects of Severe OP Intoxication on Mammals.

Muscarinic Effects	Nicotinic Effects	CNS Effects
extreme salivation	generalized weakness	confusion
involuntary defecation and urination	involuntary twitching	ataxia
sweating	fasciculations	slurred speech
lacrimation	paralysis	loss of reflexes
bradycardia		convulsions
hypotension		coma
		respiratory paralysis

The AChE Active Site

There are three important features of the active site of AChE: (1) the ester binding locus that contains a nucleophilic serine residue involved in the hydrolytic mechanism of AChE, (2) the anionic domain situated approximately 4.7 Å from the serine, which is responsible for binding the ACh quaternary ammonium group, and (3) a hydrophobic region that binds aryl-containing substrates (Figure 10; Quinn 1987).

A recent X-ray crystal structure of AChE from *Torpedo californica*

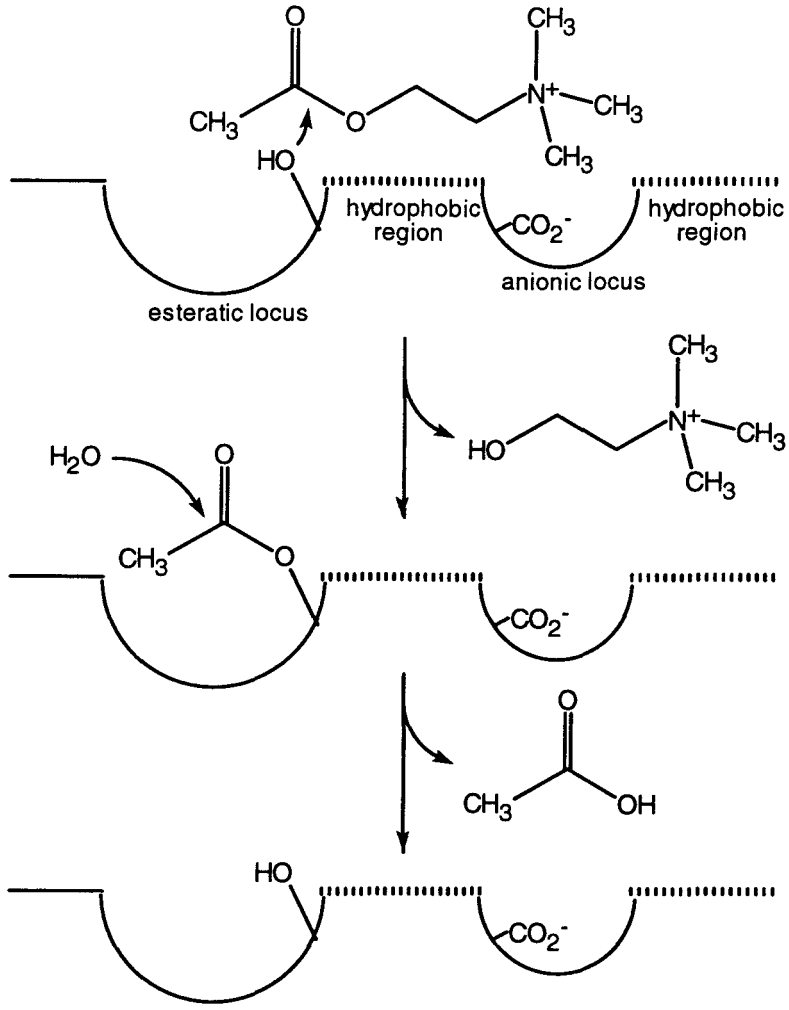

Figure 10. Salient Features of the AChE Active Site.

revealed that the active site was positioned at the bottom of a deep (approximately 20 Å) and narrow gorge penetrating halfway into the enzyme (Sussman, 1991; Maelicke, 1991). In addition, structural homology to other hydrolases such as

wheat serine carboxypeptidase-II were identified.

Mechanism and Kinetics of AChE Inactivation by OP's

OP's inactivate AChE by phosphorylation of the active site serine hydroxyl where one ligand (X) about phosphorus is displaced (Eqn. 1). The result is a covalently modified enzyme absent of any hydrolytic activity. The first step in this AChE inactivation involves the reversible formation of an enzyme-inhibitor complex and is represented by the dissociation constant, K_D (Main, 1964). K_D is generally considered a measure of the OP-inhibitor's affinity for the enzyme's active site (Fukuto, 1990). The second step of inhibition results in the irreversible

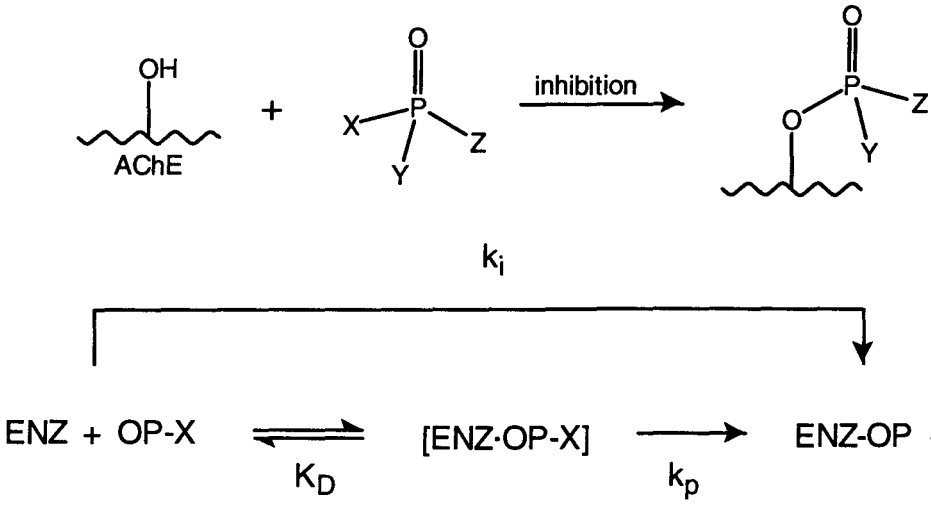

(1)

phosphorylation of AChE by an OP inhibitor. Covalent modification of the serinehydroxyl of the enzyme is responsible for the ultimate loss in the enzyme's activity (i.e. the inability to hydrolyze ACh). The phosphorylation rate constant, k_p, is considered a quantification of the reactivity of the OP inhibitor or the enzyme-inhibitor complex (Main, 1964, Fukuto, 1990).

A more useful parameter that describes the overall rate of inhibition is the bimolecular reaction (or rate) constant, k_i (Debord, 1986). This parameter is a function of both K_D and k_p ($k_i = k_p/K_D$) and a measure of the potency of an OP inhibitor. Bimolecular reaction constants (as well as K_D and k_p) for OP's are determined experimentally by the following equation:

$$1/[i] = (\Delta t / \Delta \ln v)k_i - 1/K_D \qquad (2)$$

where $[i]$ is concentration of the OP inhibitor, Δt is the time that the AChE is reacted with the inhibitor, v is the activity of AChE, and $k_i = k_p/K_D$ (Main, 1964).

Although the method described in Eqn. 2 provides useful data, most inhibitory potencies (k_i) are reported using the following equation:

$$\Delta \ln v = [i]k_i \Delta t \qquad (3)$$

where the time dependent loss of enzyme activity is monitored in the presence of a single concentration of the OP (Aldridge, 1950). Experimentally, it is more convenient to utilize Eqn. 3 than Eqn. 2 as there is one less variable. However, Eqn. 3 ignores the reversible step of the inhibition and is most valid when the K_D is several-fold greater than the inhibitor concentration (Main, 1964). In addition, the resultant k_i values obtained using this latter approach have been shown to vary inversely with inhibitor concentration, [*i*] (Main, 1964). Therefore, this determination may not be reliable for comparing the inhibitory potency of inhibitors if the concentrations used for the evaluation differ significantly.

The rate and extent of the AChE inhibition depends upon the nature of the OP-inhibitor's structure, which influences phosphorylation through the electronic environment about the phosphorus. For example, phosphates are better inhibitors than thionates. For a series of diethylaryl-substituted phenylphosphates (Figure 11), those containing more electron-withdrawing substituents were found to be more potent inhibitors of AChE. For example, the concentration of diethyl-*p*-nitrophenylphosphate (Figure 11, X = NO_2) needed to affect 50% inhibition of AChE was 10,000-fold less than diethyl-*p*-methylphenylphosphate (Figure 11, X = CH_3) (Eto, 1974).

When steric factors are considered, the rate of inhibition decreased with increasing bulkiness of the ligands that remained attached following inhibition of AChE; methoxy containing inhibitors reacted most rapidly followed by those

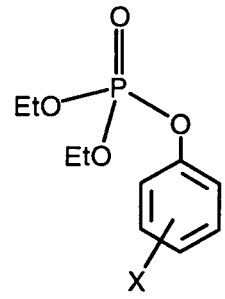

Figure 11. Diethyl Phenyl Phosphates.

bearing ethoxy, n-propoxy, and isopropoxy ligands (Gallo, 1991). Further, a rapid decrease in inhibitory activity was observed when the alkyl chain length of ethyl *p*-nitrophenyl alkylphosphonates was increased from 3 to 6 carbon atoms (Fukuto, 1990; Wallace and Herzberg, 1988).

Spontaneous Reactivation of AChE Inhibited by OP's

Following phosphorylation of AChE, the enzyme may spontaneously recover its activity as water (H_2O/OH^-) facilitates the hydrolysis of the phospho-serine linkage (Equation 4). Reactivation of AChE is analogous to the second step of the AChE-catalyzed hydrolysis of ACh (i.e., the hydrolysis of the acetoxy moiety). However, the rate of spontaneous reactivation (k_0) of AChE inhibited by an OP is far less (>10^7-fold than the turnover rate for the natural substrate, ACh) (Eto, 1974).

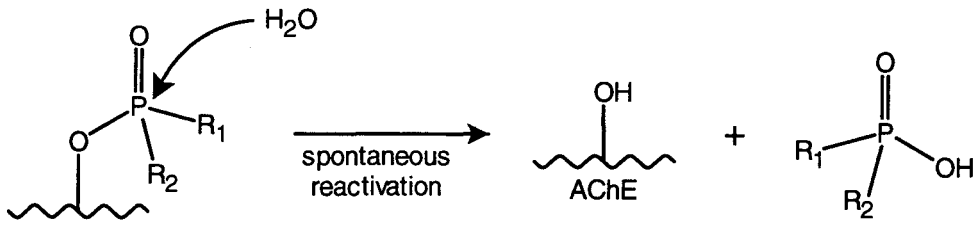

(4)

$$\text{Enz-OP(O)}R_1R_2 + H_2O \xrightarrow[k_0]{} \text{Enz-OH} + \text{HOP(O)}R_1R_2$$

Spontaneous reactivation is dependent upon not only the source of the enzyme, but upon pH, ionic strength, and temperature (Lieske, 1980; Lanks and Seleznizk, 1981; Lieske, 1990). The rate at which AChE recovers from inhibition also depends upon the nature of the appended phosphoryl group (Lieske, 1980; Clothier, 1981; Langenberg, 1988; Wallace and Herzberg, 1988, Lotti, 1991). AChE reactivates most rapidly when phosphorylated by an inhibitor with less bulky ligands (R_1 and R_2, Eqn. 4). For example, dimethoxy phosphorylated AChE ($R_1 = R_2 = -OCH_3$) reactivates at rates 15 and 30-fold faster than diethoxy and di-*n*-propoxy phosphorylated AChE, respectively (Gallo, 1991). AChE possessing a di-isopropoxy phosphate moiety is essentially recalcitrant toward reactivation (Eto, 1974).

Oxime-Induced Reactivation of AChE Inhibited by OP's

Therapeutic treatment following an OP poisoning episode usually involves

the administration of atropine (a cholinergic antagonist) in order to antagonize the effect of accumulated ACh (Goodman, 1985; Lotti, 1991). Additionally, it is also desirable to expedite the recovery process by regenerating AChE activity via facilitated displacement of the phosphoryl moiety. To this end, many therapeutic agents have been designed.

Several investigations into the design of reactivating mediators show that the nucleophilic oxime moiety is an essential feature (Miller, 1984; Bedford, 1986). Further, most potent reactivators possess a positively charged quaternary nitrogen atom that directs the reactivating species to the anionic locus of AChE in a favorable position to facilitate nucleophilic displacement of the phosphate from the enzyme (Gallo, 1991). The most commonly employed oxime used therapeutically for OP-poisoning in humans is 2-pyridine aldoxime (2-PAM, **16**) shown reacting with phosphorylated AChE in Eqn. 5 (Lotti, 1991).

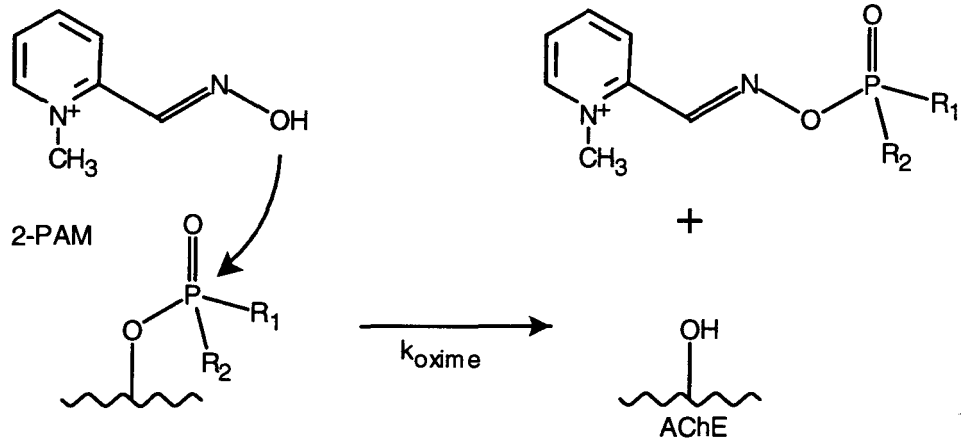

(5)

As with spontaneous reactivation, oxime-mediated displacement also is dependent upon the enzyme source (Lotti, 1991) in addition to the ligands attached to phosphorus. Phosphorylated AChE possessing less bulky ligands (such as dimethoxy) readily reactivate in the presence of oximes. For example, the reactivation rate constant, k_{oxime}, for dimethylphosphorylated ($R_1 = R_2 = OMe$) AChE is 60-fold greater than the diethyl analog (Clothier, 1981). Diethyl phosphorylated AChE undergoes oxime-promoted reactivation considerably faster than diisopropyl phosphorylated AChE (Eto, 1974).

Aging and Non-Reactivation of AChE Inhibited by OP's

AChE inhibited by an OP ester may become increasingly reluctant to reactivate as the interval of time prior to oxime administration increases. One process which explains this phenomena has been described as "aging." Aging (k_{AG}) of OP-inhibited AChE is attributed to either the dealkylation or hydrolysis of one of the two remaining phosphate ester moieties (Eqn. 6) (Eto, 1974). As a result, the charged species formed is then unsuited for the approach of

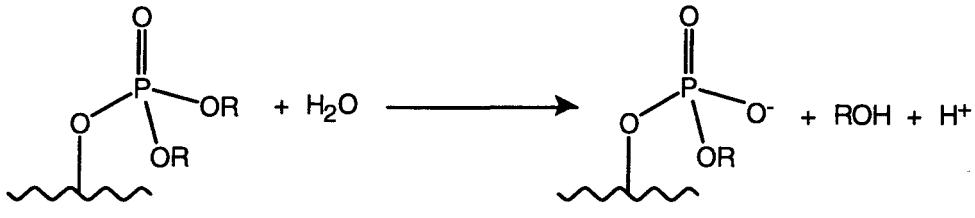

(6)

nucleophiles such as water or oximes (Gallo, 1991). An alternative explanation for time-dependent reluctance toward reactivation relies on denaturation or conformational alterations of the enzyme that make the recovery process less favorable (Thompson, 1992). AChE post-inhibitory processes may be broadly classified as those involving "non-reactivation" (k_{NR}) and accounts for the time-dependent loss of ability to reactivate regardless of process.

Non-Anticholinesterase Effects Associated with OP Exposure

Another neurotoxic effect induced by OP poisoning has been observed that is not necessarily related to anticholinesterase potency. The malady has been described as *delayed neurotoxicity*, and the effects are not seen until 8-14 days following ingestion of or exposure to certain OP's. The toxicity is manifested in weakness in the lower limbs, progressing to paralysis. In severe cases, the upper limbs may be affected with recovery slow and seldom complete (Johnson, 1980). Delayed neurotoxicity has been attributed to inhibition and aging of neuropathy target esterase (i.e., neurotoxic esterase, NTE) by a mechanism similar to that of AChE (Johnson, 1987).

Delayed toxicity following exposure to trialkylphosphorothiolates has been observed for animals where a steady decline in health was followed by death. This delayed toxicity was determined not to be the result of a neurotoxic event as discussed above, but probably due to morphological changes in the lung

(Imamura, 1983).

Stereochemical Aspects of OP Compounds

An important structural feature common to many OP inhibitors warranting discussion is stereochemistry. There are two locations where stereocenters may appear, one of which is at the carbon atom of a ligand attached to the phosphorus atom, and the other site for potential asymmetry is at the sp^3-tetracoordinated phosphorus atom when the four ligands attached are non-identical. An OP compound may contain one or both of these features, thus allowing three basic types of chiral OP compounds: phosphorus stereogenicity, carbon stereogenicity, and dual stereogenicity. Examples of OP compounds indicating the asymmetric sites* are given in Figure 12.

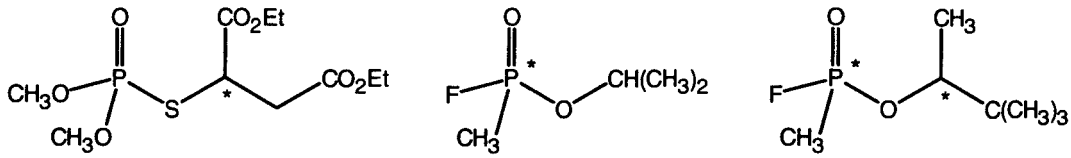

17: malaoxon

18: isopropyl methylphosphonofluoridate

2: soman

Figure 12. Three Basic Types of OP Stereogenicity.

Phosphorus Stereochemistry: Inhibition of AChE

The asymmetric phosphorus center probably most effects the inhibitory and post-inhibitory processes of AChE, the rationale being that this is the site of the molecule that is immediately involved in the covalent modification of the serine residue in the active site. This expectation is supported by a 4200-fold difference in inhibitory potency observed for the enantiomers of isopropyl methylphosphonofluoridate **18** (Figure 12) (Jarv, 1984). Several other examples exist, however, where the stereoselective inhibition is not as great (Ooms, 1965; Berman, 1989b; Hirashima, 1984; Armstrong, 1987; Eya, 1985; Lee, 1978). Noteworthy, is the observation that among the stereoisomers examined (in the preceding references), those with the *S*-configuration at phosphorus were generally more potent inhibitors of AChE.

Jarv (1984) has suggested that the stereoselective inhibition of AChE by OP-inhibitors may be due to steric limitations within binding domains of the active site. In this model, an acidic residue in the active site hydrogen bonds to the carbonyl of acetylcholine during normal ACh hydrolysis and presumably facilitates the favorable positioning of the substrate for acylation of the serine hydroxyl. It is hypothesized that this same acidic residue plays an analogous role in the inhibition of ACh by an OP (Figure 13) (Jarv, 1984).

Examination and correlation of a list of asymmetric OP's have permitted further refinements to the active site topology and suggest that there exists three binding

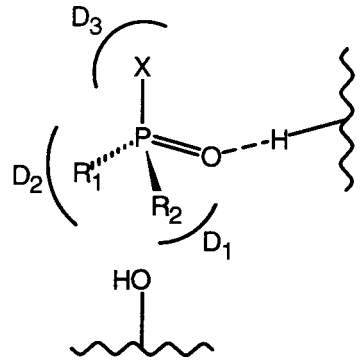

Figure 13. Proposed Binding Domains of AChE for OP Inhibitors.

domains that precisely complement the ligands about phosphorus. Structural studies suggest that domain D_3 probably accommodates the leaving group (X) of an OP inhibitor, while the binding sites D_1 and D_2 are responsible for recognizing the ligands that remain attached to phosphorus after phosphorylation (Jarv, 1984; Benschop, 1988). If the positioning of the leaving group and the phosphoryl oxygen are collectively maintained by domain D_3 and the acidic residue, and the structural match between D_1 and D_2 domains and ligands R_1 and R_2 differ sufficiently during inhibition, then binding of the inhibitor will be more favorable for one phosphorus configuration accounting for differences in inhibition rates for enantiomeric OP's (Jarv, 1984).

Phosphorus Stereochemistry: Reactivation and Aging of AChE

When an OP containing an asymmetric phosphorus atom inhibits AChE, two stereoisomeric forms of the phosphorylated enzyme are capable of forming (Figure 14) (Berman, 1989a). Therefore, any reactivation rate differences observed for AChE inhibited by enantiomeric OP's must be due solely to the phosphorus configuration as it is the only structural difference present. It has been suggested that the binding domains D_1 and D_2 described previously for stereoselective inhibition may also be involved in the stereoselective reactivation process (Jarv, 1984). The most dramatic display of stereoselective reactivation cases would occur when AChE inhibited by one OP enantiomer reactivates while the no reactivation is observed for the antipode. More commonly, OP inhibitor enantiomers show negligible to modest (2-10 fold) differences in reactivation rate (Berman, 1989a; Glickman, 1984).

Aging represents another post-inhibitory process that is influenced by the phosphorus stereochemistry. Aging differences for AChE inhibited by OP stereoisomers have indeed been observed (Berman, 1989a; Glickman, 1984); a notable case described aging of AChE inhibited by one OP stereoisomer while AChE inhibited by the other stereoisomer did not undergo this process (Berman, 1989a). The basis for this difference is assumed to be steric hinderance making the aging process less favorable for one configuration.

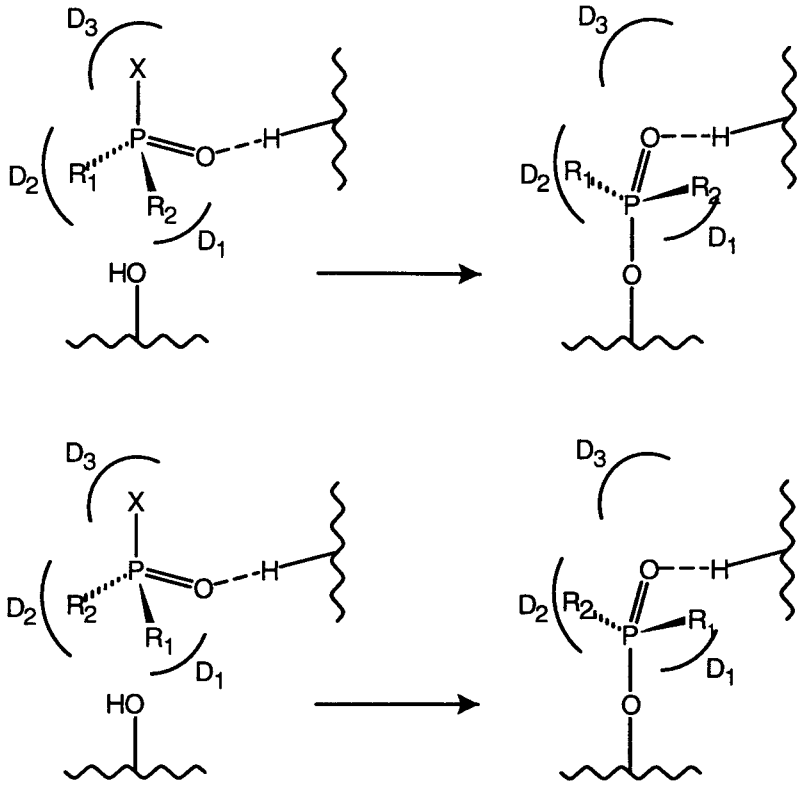

Figure 14. Stereoisomeric Forms of AChE Inhibited by an OP Possessing an Asymmetric Phosphorus Atom.

Ligand Stereochemistry: Inhibition of AChE

The stereochemistry of an OP ligand carbon atom may have its greatest effect upon inhibition of AChE in contrast to reactivation or aging (or non-reactivation) reactions because the ligand bearing the asymmetric center may be

displaced during the inhibition leaving an achiral phosphorylated enzyme. The effect of carbon chirality on the kinetic constants, k_i, K_D and k_p, will be considered.

Because enzymes are chiral molecules, it is anticipated that the association/dissociation process as defined by K_D should differ for enantiomeric inhibitors. Once the enzyme-inhibitor complex has been formed, the ligand stereochemistry may affect the subsequent phosphorylation, k_p. For example, if binding domain D_3 demands or favors a particular orientation of two moieties (R_3 and R_4) about a ligand stereocenter for enantiomeric inhibitors due to electronic or steric factors, the relative position of the reactive phosphorus center to the nucleophilic serine hydroxyl may differ due to conformational limitations (Figure

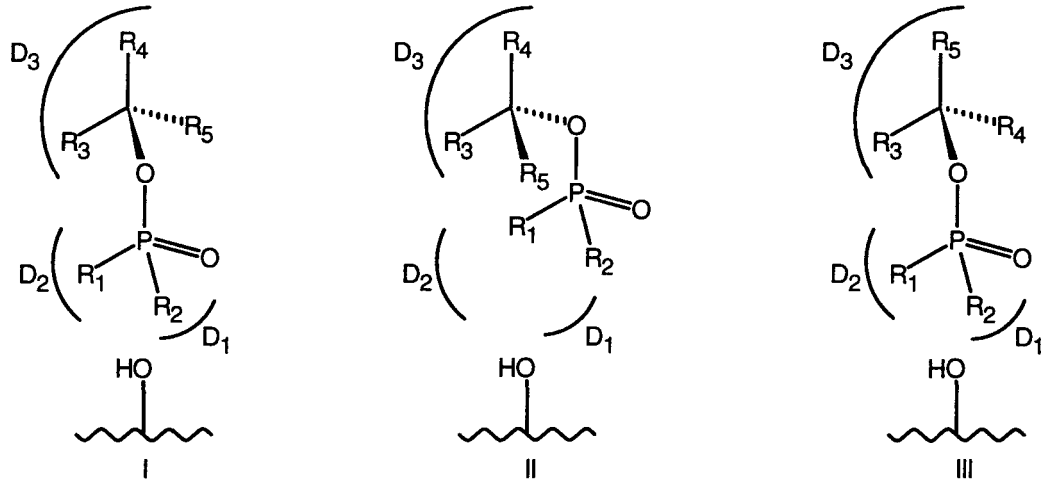

Figure 15. Influence of OP Ligand Stereochemistry upon AChE Inhibition.

15; Examples I and II). Consequently, the k_p values for enantiomeric inhibitors may differ when the phosphorus atom is not favorably situated for phosphorylation. However, if the phosphorus atom is the major positioning determinant for the OP-inhibitor and the binding domain D_3 in the active site necessitates a favorable positioning of only one moiety (R_3) about the ligand stereocenter (Figure 15, I and III), little difference in the k_p would be expected. In this case, a difference in K_D may still be observed if there is a preference to accommodate the R_4 or R_5 moiety.

Because k_i, K_D, and k_p are interrelated processes ($k_i = k_p/K_D$), the effect of ligand stereochemistry upon the overall inhibition of AChE (k_i) is dependent upon the individual effects of the kinetic parameters (previously discussed). As a consequence, enantiomeric OP inhibitors may differ in their inhibitory potency depending on the contributive differences for k_p and K_D. However, few studies have examined the effect of ligand stereochemistry upon the inhibition of AChE (Hassan, 1968; Ohkawa, 1976; Wustner, 1973; Benschop, 1988), and the specific relationship between stereochemistry upon both K_D and k_p has not been thoroughly investigated. Furthermore, the differences observed in anti-AChE potency due to ligand asymmetry (up to 5-fold) is generally less dramatic than that of enantiomeric phosphorus center OP's (2-fold to 56000-fold).

Ligand Stereochemistry: Reactivation and Aging of AChE

Ligand stereochemistry also has been shown to affect the rates of both reactivation and aging of AChE (Bucht, 1984; de Jong and Wolring, 1985; de Jong and Kossen, 1985; de Jong, 1984). AChE inhibited by soman **2** (F^- displaced upon inhibition) showed that the orientation of the pinacolyl ligand in the active site of the inhibited enzyme [sterically] governed the accessibility of the phosphorus atom by an approaching oxime. The extent of reactivation (percent recovered enzyme activity) differed between the reactivating species with the most notable difference (approximately 10-fold) in favor of the $(+_C)$-configuration (de Jong and Kossen, 1985). However, the differences observed for the rate of aging was less dependent upon the carbon configuration showing an approximate 3-fold difference (Bucht, 1984).

OP's Containing Dual Stereocenters: Inhibition of AChE

An OP with stereocenters at both carbon and phosphorus atoms may further complicate the stereoselective inhibition of AChE. To simplify this discussion, a hypothetical OP inhibitor possessing dual stereocenters (existing as four stereoisomers; R_PR_C, R_PS_C, S_PR_C, S_PS_C[1]) will be considered in which the R_PR_C stereoisomer is the strongest inhibitor (k_i) and the S_PS_C stereoisomers is the

[1]Configurational designations for an OP with stereocenters at both phosphorus and carbon are defined by the following example: R_PS_C = *R* configuration at the phosphorus atom, *S* configuration at the carbon atom.

weakest inhibitor of AChE. The inhibitory potency of the two remaining stereoisomers will depend upon the relative contributions of the phosphorus and carbon stereochemistry to the overall inhibition of AChE. For example, if the phosphorus configuration contributes more to the inhibitory strength, then it would be anticipated that the R_PS_C stereoisomer would be a stronger inhibitor than its enantiomer. Alternatively, if the carbon configuration contributes more significantly to the inhibitory profile then the S_PR_C stereoisomer is expected to show greater inhibitory potency than that of the R_PS_C stereoisomer. The specific roles of the phosphorus and carbon stereochemistries upon the inhibition of AChE may be further inferred by examining their possible effect upon K_D and k_p.

OP inhibitors that contain both carbon and phosphorus stereocenters show that phosphorus stereochemistry had a significant influence upon the stereoselective inhibitory profile with the effect of carbon atom stereochemistry, although observable, being of considerably less significance (Benschop, 1988;

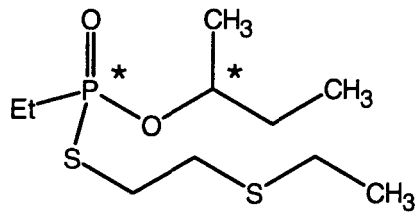

Figure 16. O-2-Butyl S-(Ethylthio)ethyl Ethylphosphonothiolate.

Wustner, 1973). This phenomenon is illustrated by the inhibitor, (O-2-butyl S-2-(ethylthio)ethyl ethylphosphonothioate (Figure 16) and the data is shown in Table 2 (Wustner, 1973).

Table 2. Inhibition of BEAChE[a] by S-2-(Ethylthio)ethyl Ethylphosphonothioate Stereoisomers.

configuration		BEAChE
P	C	k_i ($M^{-1}min^{-1}x10^{-3}$)
-	+	65.3
-	-	54.5
+	+	0.63
+	-	1.45

[a]Bovine Erythrocyte AChE.

OP's Containing Dual Stereocenters: Reactivation and Aging of AChE

When dual stereocenters are operative during the reactivation and aging of AChE, two cases must be considered. First, the displacement of the chiral ligand results in a phosphorylated enzyme that contains an asymmetric phosphorus moiety, the effects of which have already been discussed (Section 1.15). The second case involves an inhibitory pathway whereby the chiral ligand remains attached. The kinetic implications are more complicated and are discussed below.

The individual effect of ligand stereochemistry on post-inhibitory pathways has been discussed previously (Section 1.17), particularly the role of steric

hinderance on the reactivating nucleophile in the displacement of the phosphoryl moiety from the serine residue. In that instance, reactivation and aging, occurring at either phosphorus configuration, may be influenced by the ligand carbon atom stereochemistry. Further, the degree of steric hindrance imposed by one particular carbon configuration of the ligand may differ from the antipode depending upon the phosphorus configuration. These differences assume that the phosphorus configuration could sufficiently alter the orientation of the ligand in the active site. Thus, an interdependence between the phosphorus and carbon configurations in such cases may be observed or anticipated during reactivation processes.

Few reports have explored the effects of stereochemistry upon the post-inhibitory pathways of AChE inhibited by an OP possessing both carbon and phosphorus stereocenters. The effects of carbon stereochemistry alone upon post-inhibitory processes of such OP's have been examined resulting in significant differences (although considerably less than those observed for the inhibition process) and were described previously in the Section 1.17.

Summary

The phosphorylation of AChE by an OP inhibitor and the subsequent recovery of enzyme activity are intimately linked to the nature of the OP. In particular, reactivity, steric effects, and stereochemistry have all been observed to have effects upon such events. As a result, certain attributes of the AChE active

site that complement of OP characteristics can be hypothesized and probed with novel inhibitors.

CHAPTER 2

STATEMENT OF GOALS

Malathion: General

Malathion **6** [O,O-dimethyl-S-1,2-bis(ethoxycarbonyl)ethyl phosphorodithioate] is one of the world's most widely used organophosphate insecticides. Along with parathion methyl **7**, parathion **8**, chlorpyrifos **9** (Figure 2) (Eto, 1974), approximately 40,000,000,000 pounds of these four compounds are sprayed in the U.S. annually (Stephens, 1991). Malathion's broad spectrum of usage ranges from household to acreage application to control insects foraging on grains, cotton, tobacco, and fruits. Recently, it has been employed to manage the medfly problem in California (Barinaga, 1991). Malathion also has been established in veterinary medicine (Osweiler, 1984), and in public health practices as an anti-infective agent (Wester, 1989) to control insect vector-borne diseases such as malaria (*anopheles mosquito*), dengue (*aedes aegypti*), and yellow fever (*aedes*) (Caglioti, 1983).

Food safety concerns have encouraged limitations on the amount of residues for crops treated with malathion. For fruits and vegetables, the

maximum residue limit is less than 10 mg/kg while that for wheat and rye bran is 20 mg/kg (Cheminova, 1987). As with most OP insecticides, environmental persistence of malathion is low. For most fruits, vegetables and grains, the $t_{1/2}$ period is approximately two days while in soil samples and field applications the $t_{1/2}$ is 8.2 h and 2 h, respectively (Cheminova, 1987; Miles, 1991).

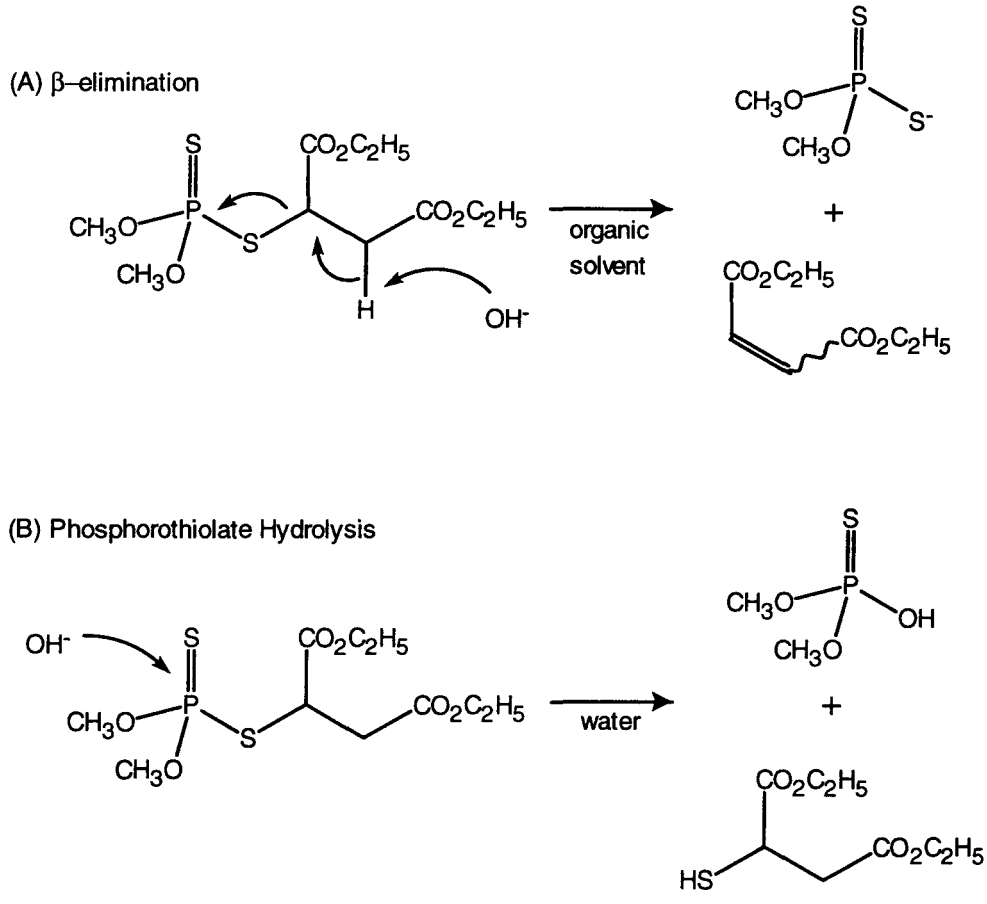

Figure 17. Hydrolysis of Malathion.

Although relatively stable to acidic aqueous conditions ($t_{1/2}$ = 6.5 days, pH2.6, 27 ^{0}C), the decomposition of malathion is catalyzed by hydroxide ($t_{1/2}$ = 2.4 h, pH 10.8, 0 ^{0}C) and depending on the type of solvent, one of two mechanisms is possible (Figure 17). While ß-elimination is favored in organic solvent (Figure 17, A), S_N2-type displacement of diethyl mercaptosuccinate predominates in aqueous conditions (above pH 9). With regard to thermostability, the malathion content after dark storage for 2 years at 40 ^{0}C decreased from 96.2% to 89.6% while the $t_{1/2}$ of malathion stored at 55 ^{0}C was 17 weeks (Cheminova, 1987).

Malathion: Mode of Action

The popularity of malathion's usage has been promoted by its relatively low mammalian toxicity (Table 3). This is primarily due to endogenous carboxylesterases that rapidly degrade malathion to the monoacids (Figure 18), which are found as urinary metabolites (O'Brien, 1967). Both the α-monoacid **20**, which is generally found in greater quantity, and the ß-monoacid **21** are virtually non-toxic to mammals (Chen, 1969; De Matteis, 1989; Ryan, 1985). Two malathion carboxylesterases responsible for this detoxication (in rats) have been identified and designated as Fraction A and B. Fraction A preferentially converts malathion to the α-monoacid **20** while the ß-monoacid **21** is the preferred product formed from hydrolysis by Fraction B (Mallipudi, 1980).

Table 3. Relative Toxicity of Biologically Active Compounds

Compound	LD_{50} mg/kg (oral, rats)
glucose	35,000
malathion	12,500
ethanol	10,000
aspirin	3,750
valium	710
caffeine	300
cocaine	17
strychnine	5

Although malathion maintains a low mammalian neurotoxicity, some experimental results suggest that it may be carcinogenic (Zimmerman, 1990). In addition, there exists uncertainties as to whether malathion is teratogenic since

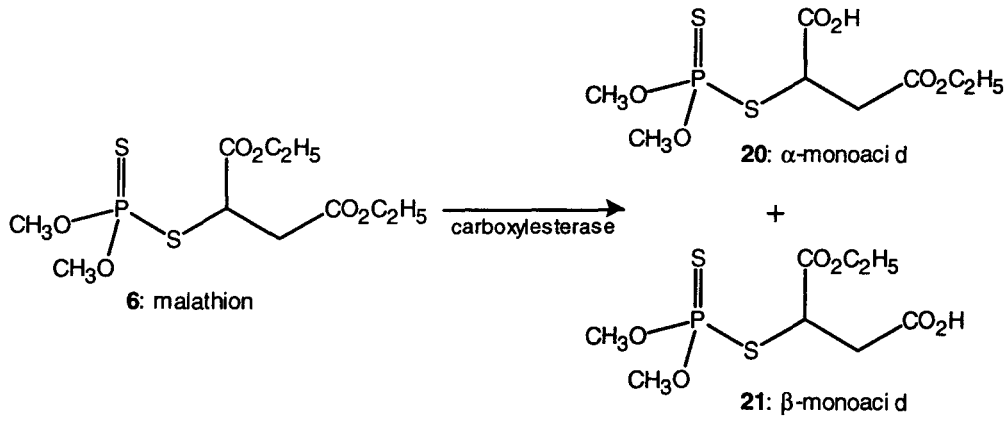

Figure 18. Hydrolysis of Malathion by Carboxylesterase.

studies have given both positive and negative results (Zimmerman, 1990). Daily doses of 1/50th the LD_{50} fed to rats resulted in reduced survival of the progeny as well as apparent growth retardation (Cheminova, 1987).

The species selectivity of malathion toward insects (and fish) is largely a result of a deficiency in detoxifying carboxylesterases by these organisms, which then permits malathion to undergo oxidation to the oxon (P=O) metabolite, malaoxon **22** [O,O-dimethyl-S-1,2-bis(ethoxycarbonyl)ethyl phosphorothionate] (Figure 19) (Cohen, 1984; Matolczy, 1988). This thionate-oxon conversion is common to the class of phosphorothionate insecticides and while phosphorothionates (P=S) are generally not effective inhibitors of AChE, bioactivation to the oxon analogues (P=O) by mixed function monooxygenases in insects (Cohen, 1984) creates more potent inhibitors of AChE (De Matteis, 1989). For example, malaoxon is a 1,000-fold stronger AChE inhibitor than malathion and nearly 80-fold more toxic *in vivo* to the rat (malathion, LD_{50} = 12,500 mg/kg; malaoxon, LD_{50} = 158 mg/kg)

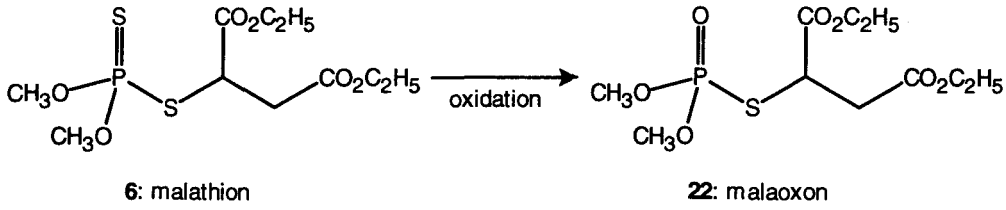

6: malathion **22**: malaoxon

Figure 19. Bioactivation of Malathion.

(Cheminova, 1987; Ryan, 1985; Umetsu, 1977).

The increased inhibitory potency of oxon analogues of phosphorothionates is primarily due to the more reactive nature of the P=O bond as discussed previously (Matolczy, 1988). It also has been hypothesized that the less electronegative sulfur atom of the P=S bond (compared to the P=O oxygen atom) may compete with small alkoxy ligands for hydrophobic binding domains of the AChE active site. In this instance, the serine hydroxyl is not positioned correctly for attack at the phosphorus atom. Thus, the absence of the P=S functionality in the oxon analogues of phosphorothionates may enhance their affinity for the active site, thereby increasing their anti-AChE potency through both reactivity and orientation. (Maxwell, 1992).

Malathion: Impurities

Whereas purified malathion is relatively innocuous to mammals, several more toxic impurities (Figure 20) result from the manufacture or storage and have been shown to potentiate or enhance the toxicity of malathion formulations (Aldridge, 1979; Lin, 1984; Toia, 1980; Mallipudi, 1980). The strongest potentiator of these impurities is isomalathion **12**. A 0.5% isomalathion contamination of malathion formulations reduced the LD_{50} from 12,500 to 4400 mg/kg (Toia, 1980, Umetsu, 1977). Isomalathion has been shown to be not only an inhibitor of AChE but also an inhibitor of the mammalian detoxifying enzyme,

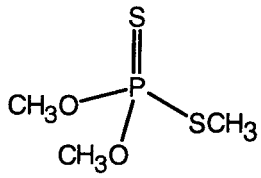

23: O,O,S-trimethylphosphorodithioate

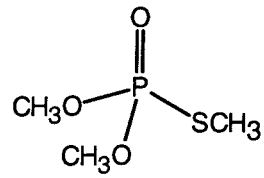

24: O,O,S-trimethylphosphorothiolate

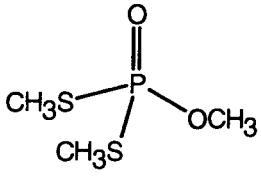

25: O,S,S-trimethylphosphorodithiolate

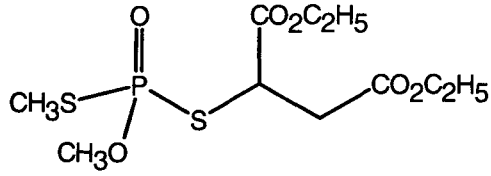

12: isomalathion

Figure 20. Impurities Found in Commercial Malathion Formulations.

carboxylesterase (Talcott, 1979; Toia, 1980; Lin, 1984; Ryan and Fukuto, 1985). When carboxylesterase is inactivated, the normal detoxication pathway is removed (Section **2.2.**), and metabolic activation **from** malathion **to** malaoxon dominates the metabolism causing the latent toxicity (anti-AChE potency) to be realized in mammals (De Matteis, 1989; Cohen, 1984).

Malathion: Stereochemistry

A structurally interesting feature of malathion is the presence of an asymmetric carbon at the succinyl ligand resulting in two enantiomers (Figure 21).

It is expected that the enantiomers of malathion would interact stereoselectively with the varying enzymes encountered *in vivo* such as cholinesterases, carboxylesterases, and oxidizing enzymes. Enantiomers of the closely related O,O-diethyl malathion **26** enantiomers (not used in agriculture) were prepared and the *S*-stereoisomer **26b** was found to be a 1.9-fold better substrate for rat liver carboxylesterase than the *R*-stereoisomer **26a** (Hassan, 1968). However, since its introduction over 40 years ago the synthesis of the malathion (O,O-dimethyl)

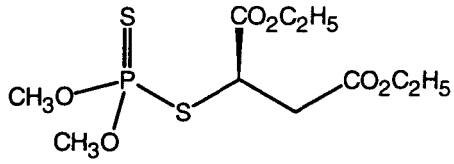

6a: (*R*)-malathion

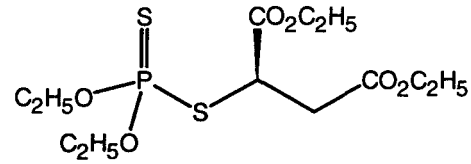

26a: (*R*)-O,O-diethyl malathion

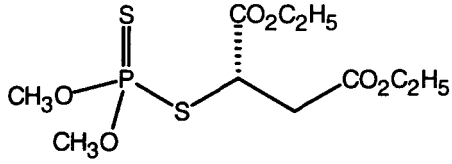

6b: (*S*)-malathion

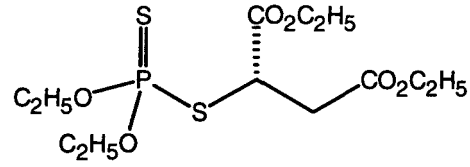

26b: (*S*)-O,O-diethyl malathion

Figure 21. Enantiomers of Malathion and O,O-Diethyl Malathion.

enantiomers has not been achieved.

Malaoxon

As discussed previously, malaoxon is the bioactivated form of malathion, responsible for its insecticidal (anti-AChE) activity. Although it has been found as a minor impurity in commercial malathion formulations, it was determined that malaoxon is not responsible for the potentiation of malathion toxicity that was

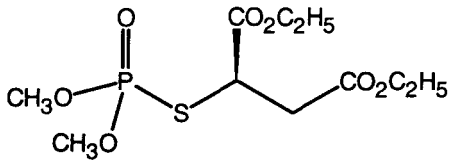

22a: (*R*)-malaoxon

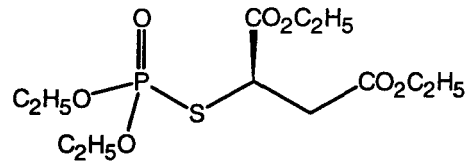

27a: (*R*)-O,O-diethyl malaoxon

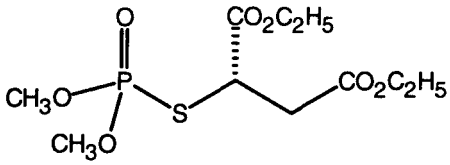

22b: (*S*)-malaoxon

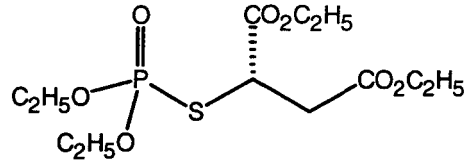

27b: (*S*)-O,O-diethyl malaoxon

Figure 22. Enantiomers of Malaoxon and O,O-Diethyl Malaoxon.

observed for other impurities (Aldridge, 1979). Although malaoxon is both an inhibitor and a substrate for mammalian carboxylesterase, hydrolysis of the carboxylic esters is the preferred metabolic pathway. (Ryan and Fukuto, 1985, Aldridge, 1979).

Like malathion, an asymmetric carbon center exists on the succinyl ligand of malaoxon allowing two enantiomers (Figure 22). Consequently, it is expected that these stereoisomers will interact stereoselectively with AChE and carboxylesterases. The O,O-diethyl analogues of the malaoxon enantiomers **27** (Figure 22) were prepared and examined for their anti-AChE and anti-carboxylesterase potency (Hassan, 1968). (*R*)-O,O-Diethyl malaoxon **27a** was a 4.4-fold stronger inhibitor of bovine erythrocyte AChE, and an 8.3-fold stronger inhibitor of rat liver carboxylesterase than its antipode **27b** (Hassan, 1968). However, O,O-dimethyl malaoxon enantiomers have not yet been prepared nor have their differential phosphorylating capabilities been examined.

Isomalathion

Isomalathion (Figure 20) is the S-methyl isomeride of malathion found in commercial formulations of the insecticide, and is formed as a result of the thiono-thiolo rearrangement (Section 1.5.). Like most S-alkyl isomerides of phosphorothionate insecticides, isomalathion shows dramatically enhanced anti-AChE potency relative to malathion for the reasons previously mentioned, i.e.

chemical reactivity of the P=O bond, and the decreased pπ-dπ contribution of the S-alkyl ligands (Fest, 1973; Thompson, 1989). Consequently, isomalathion is a 3000-fold more potent anti-AChE agent than malathion (Thompson, 1989).

Like malaoxon, isomalathion inhibits the detoxifying decarboxylesterases, but unlike malaoxon, potentiates the toxicity of malathion (Lin, 1984). Of all the impurities found in malathion formulations, isomalathion is the strongest potentiator. The isomalathion content in malathion formulations, therefore, has been a matter of considerable concern, especially since the 1976 epidemic malathion poisoning in Pakistan in which 2800 Pakistani spraymen were acutely poisoned while 5 died during a malaria control program (Baker, 1978; Iyer, 1984). The poisonings were attributed to the unusually high isomalathion content of the formulation employed (Aldridge, 1979; Iyer, 1984).

Besides the enhanced anti-AChE potency of isomalathion, another important consequence result from the isomerization of malathion to isomalathion, is the generation of a new asymmetric center at phosphorus. During the isomerization, the asymmetric carbon center of malathion on the succinyl ligand is maintained, therefore, four stereoisomers of isomalathion are produced (Figure 23). The configurational designations for the isomalathion stereoisomers is described by the following example: (*1R,3S*) = *R* configuration at the phosphorus atom, *S* configuration at the carbon stereocenter. As discussed previously for OP's possessing dual stereocenters, it is anticipated that the dual stereocenters

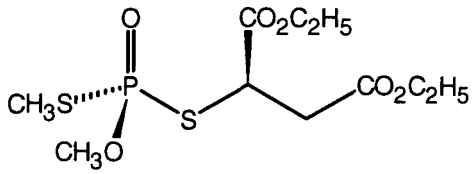

12a: (*1R,3R*)-isomalathion

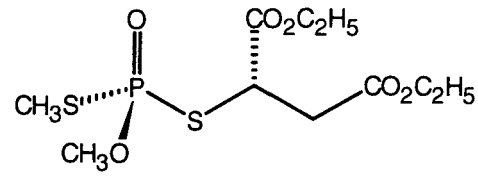

12b: (*1R,3S*)-isomalathion

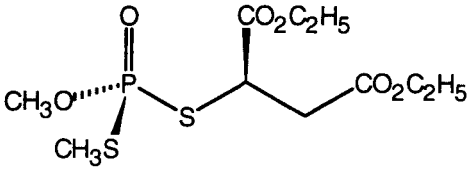

12c: (*1S,3R*)-isomalathion

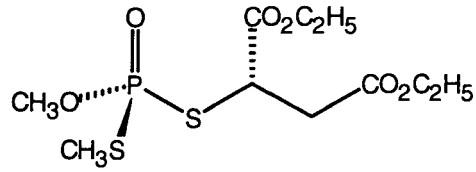

12d: (*1S,3S*)-isomalathion

Figure 23. Stereoisomers of Isomalathion.

present in isomalathion will contribute collectively toward the inhibition of AChE and possibly, reactivation and aging.

Summary

Because of the continued global application of malathion formulations, which contain various levels of the impurities malaoxon and isomalathion, it is important to fully understand the role of stereochemistry upon their modes of action. To date, however, there exists no definitive report that details the effect

of the stereochemistry of these compounds upon their interactions with varying enzymes encountered *in vivo*; i.e. carboxylesterases, oxidizing enzymes, and AChE.

The goal of this dissertation is to identify the anti-AChE profiles of the individual stereoisomers of malathion **6**, malaoxon **22**, and isomalathion **12**, and to correlate these profiles with the specific stereochemistry of these compounds. Furthermore, the effect of phosphorus and carbon stereochemistry upon the post-inhibitory fate of AChE inhibited by the individual isomalathion stereoisomers will be examined. In order to achieve the aforementioned goals, procurement of the individual stereoisomers of malathion, malaoxon, and isomalathion is necessary. However, because these enantioenriched materials were previously unavailable, a preliminary goal of this dissertation will be the first successful syntheses of these individual stereoisomers.

CHAPTER 3

SYNTHESIS OF MALATHION, MALAOXON, AND ISOMALATHION STEREOISOMERS

Synthesis of Racemic Malathion

Racemic malathion **6** was readily prepared by literature methods from the reaction of O,O-dimethyl phosphorodithioic acid and diethyl maleate **27** (Eqn. 7) (March, 1956). ^{1}H NMR analysis of the product revealed the characteristic phosphorus-proton vicinal coupling observed for O-methyl phosphorothionates, which resulted in a doublet at 3.8 ppm (Thompson, 1989; Thompson, 1992). ^{31}P NMR showed a single resonance at 96.2 ppm consistent with chemical shifts of related phosphorothionates (P=S).

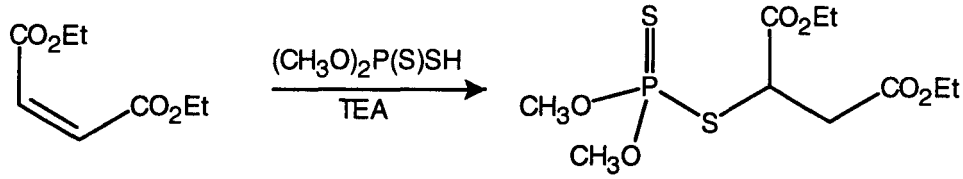

27 **6** **(7)**

Attempted Synthesis of Malathion Enantiomers from Diethyl Bromosuccinate

The report by Hassan and Dauterman (1968) described the preparation of the enantiomers of the O,O-diethyl analogues of malathion **26** (Scheme 1). Diazotization of (*S*)-aspartic acid **28a** in the presence of sodium bromide yielded (*S*)-bromo succinic acid **31a** (Holmberg, 1928), which occurred with overall retention of configuration. Formation of the ß-lactone **30a** was hypothesized to occur first with inversion, followed by ring opening of the lactone with bromide resulting in a second inversion and overall retention (Holmberg, 1928). Displacement of the bromide by potassium O,O-diethyl phosphorodithioate **33** (Scheme 1) occurred with inversion of configuration yielding (*R*)-O,O-diethyl malathion **26a** (Hassan, 1968).

Although the preparation of the malathion **6** (O,O-dimethyl) enantiomers seemed a simple extension of the above method, displacement of the bromide with O,O-dimethyl phosphorodithioate **34** under the same conditions failed. Variations in reaction conditions such as temperature, solvent, and time also were unsuccessful. Our results may, in part, explain the previous focus upon the O,O-diethyl analogues by Hassan and Dauterman (1968).

The failure of O,O-dimethyl phosphorodithioate to displace the bromide may be due to a field effect where the electron donating effect of the methoxy ligand compared to that of the ethoxy is less, thus, decreasing the nucleophilicity of the dithioate. Such field effects have been observed for phosphoric ester acids

where the acidity decreased with increasing size of the alkyl groups (Fest and Schmidt, 1973) as larger groups were less able to stabilize the conjugate base by releasing electron density into the dithioate.

Further pursuit of the approach of Scheme 1 was abandoned for two reasons: first, three opportunities for racemization at the carbon stereocenter were

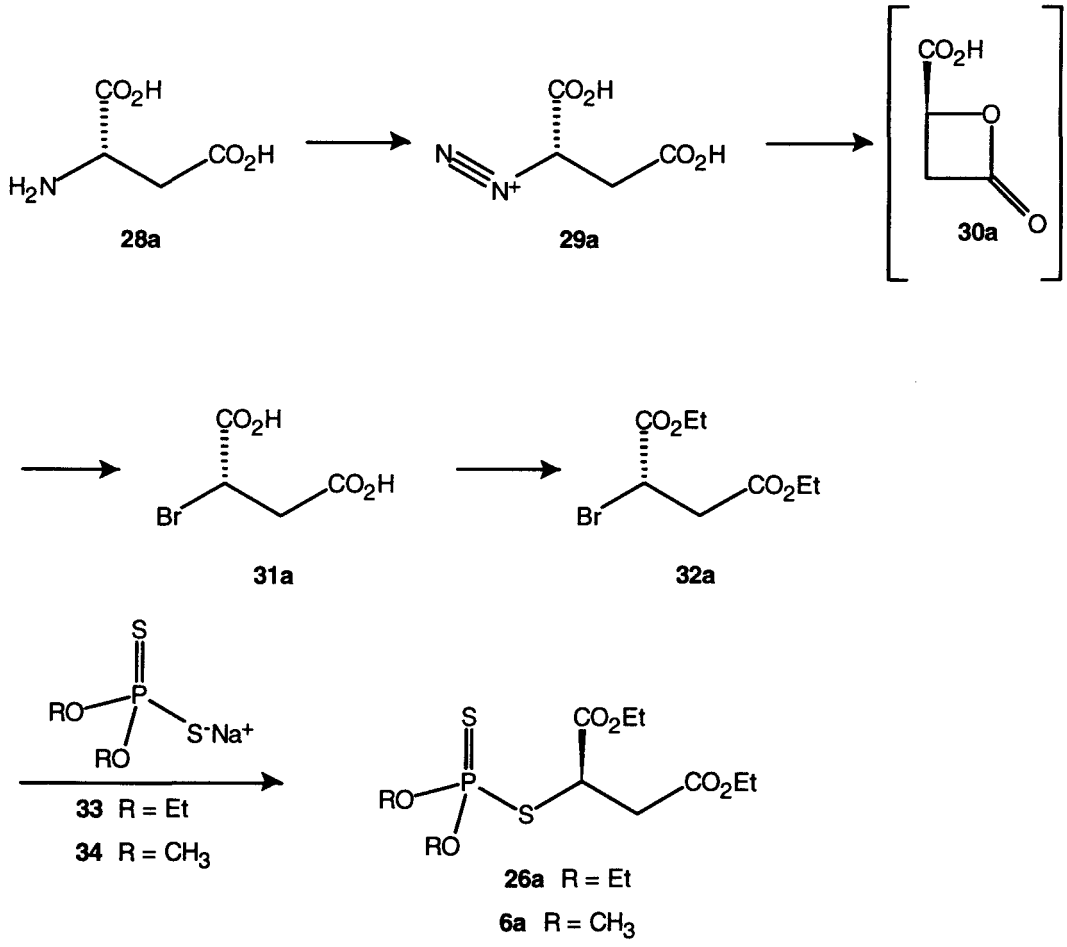

Scheme 1. Synthesis of (*R*)-O,O-Diethyl Malathion from (*S*)-Aspartic Acid.

possible and second, the simultaneous success of another method gained our attention.

Synthesis of Malathion Enantiomers from Diethyl Malate

This new strategy was designed using the same nucleophile (O,O-dimethyl phosphorodithioate potassium salt **34**) but sought to displace a better leaving group. It was believed that if the hydroxyl moiety of diethyl malate **36** could be converted to a better leaving group than bromine, it could be more easily displaced (Scheme 2). In addition, only one inversion would occur at the carbon stereocenter (Scheme 2) compared to the three reactions at the carbon stereocenter (Scheme 1).

(*S*)-Malic acid **35a** was converted to the diethyl ester **36a** (Cohen, 1984), afterwhich the hydroxyl was converted into a series of leaving groups including the tosylate, mesylate, and triflate. The (*S*)-tosylate **37a** and (*S*)-mesylate **38a** were prepared by reaction of (*S*)-diethyl malate with *p*-toluenesulfonyl chloride (tosyl chloride) or methanesulfonyl chloride (mesyl chloride), respectively. The (*S*)-triflate **39a** was prepared by reaction of trifluoromethanesulfonic anhydride (triflic anhydride) with **36a**. Identification of the tosylate, mesylate, and triflate was determined by ^{1}H and ^{13}C NMR. The ^{1}H NMR of the tosylate **37a** showed

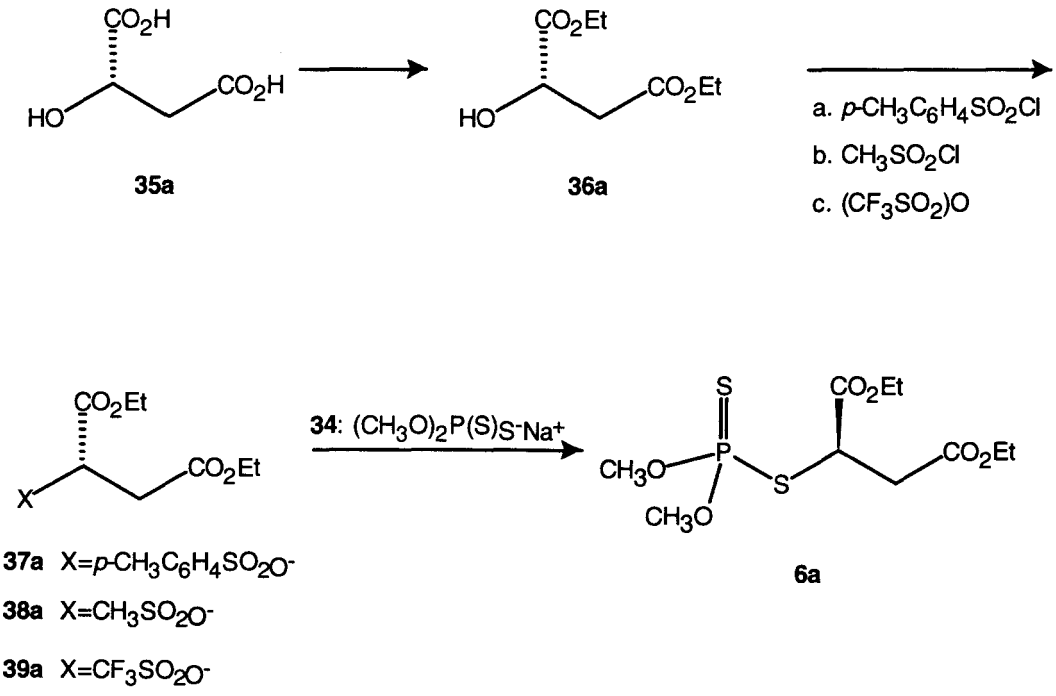

Scheme 2. Synthesis of (*R*)-Malathion from (*S*)-Malic Acid.

the *p*-substituent patterns for the aromatic resonances as well as the *p*-methyl singlet. ^{1}H NMR of the mesylate **38a** revealed an additional ^{1}H methyl singlet (3H) of the methanesulfonyl moiety to the spectrum of diethyl malate. The ^{13}C spectrum of the triflate **39a** showed the addition of a quartet corresponding to C-F coupling by the trifluoromethyl substituted carbon.

Nucleophilic substitution reactions with O,O-dimethylphosphorodithioate **34** and the hydroxyl activated compounds described above were attempted varying the time, temperature, and solvent. However, only the (*S*)-triflate **39a** entered into

the reaction with **34** (THF, 0^0C) to give *(R)*-malathion **6a** in 95% yield from diethyl malate. *(S)*-Malathion **6b** was prepared analogously starting with *(R)*-malic acid **35b**. ^{1}H, ^{13}C, and ^{31}P NMR spectra of the malathion enantiomers were identical to that of racemic material. Specific rotations of these enantiomers supported the success of this method ((*R*)-malathion **6a**, $[\alpha]^{24}_D = +79.7^0$; (*S*)-malathion **6b**, $[\alpha]^{27}_D = -80.0^0$). In an attempt to quantify enantiomeric excess, ^{1}H and ^{31}P NMR analyses of the enantiomers were conducted with a chiral shift reagent (tris-{3-[heptafluoro(hydroxy)butylidene]-(+)-camphorato}europium(III)), however, no chemical shift separation of resonances from a racemic mixture was observed.

Synthesis of Racemic and Enantioenriched Malaoxon with *m*-CPBA

The preparation of racemic malaoxon **22** from racemic malathion **6** had been reported previously using *m*-chloroperbenzoic acid (*m*-CPBA) as the oxidant (Bellet, 1974). This peracid promoted transformation is proposed to proceed via a three-membered ring intermediate (Scheme 3) (Bellet, 1974). Although the ^{1}H and ^{13}C NMR spectra of malathion and malaoxon were expectedly similar, the ^{31}P NMR phosphorus resonance of malaoxon was shifted significantly upfield (28.3 ppm) from that of malathion (96.2).

Both (*R*)- and (*S*)-malathion (**6a** and **6b**) were converted to (*R*)- and (*S*)-malaoxon (**22a** and **22b**), respectively, with *m*-CPBA in 25% yield (Scheme 3).

Specific rotations of the malaoxon enantiomers gave evidence of the success of this method ((*R*)-malaoxon, $[\alpha]^{25}_{D} = +46.7^{0}$; (*S*)-malaoxon, $[\alpha]^{27}_{D} = -43.5^{0}$).

Synthesis of Malaoxon Enantiomers by Oxidation of Malathion Enantiomers with MMPP

In order to increase the efficiency of this oxidation step, a better reagent for this transformation was sought. Hydrogen peroxide, *t*-butyl hydroperoxide, trifluoroacetic anhydride, potassium periodate all were reacted with malathion in attempts to increase the yield of malaoxon. Some of these reagents had been used successfully to effect oxidative desulfuration of phosphorothionates (Helinski, 1990; Stec, 1976). However, both peroxides resulted in extensive decomposition of the starting material while no reaction was observed with the latter two reagents. Since MMPP **46** (magnesium monoperoxyphthalate) has recently gained acceptance as a substitute for *m*-CPBA in other oxidation reactions (Brougham, 1987), it was thought that it may effect the desired transformation. Refluxing malathion overnight with MMPP in CH_2Cl_2 gave a 52% yield of the malaoxon enantiomers doubling the conversion using *m*-CPBA.

The success of this transformation prompted an investigation into the utility of MMPP for similar conversions of several other thionates (Scheme 3) to the corresponding oxons (Jackson, Berkman, and Thompson, 1992). In all cases, acceptable yields were obtained (51-72%). It also was found that the

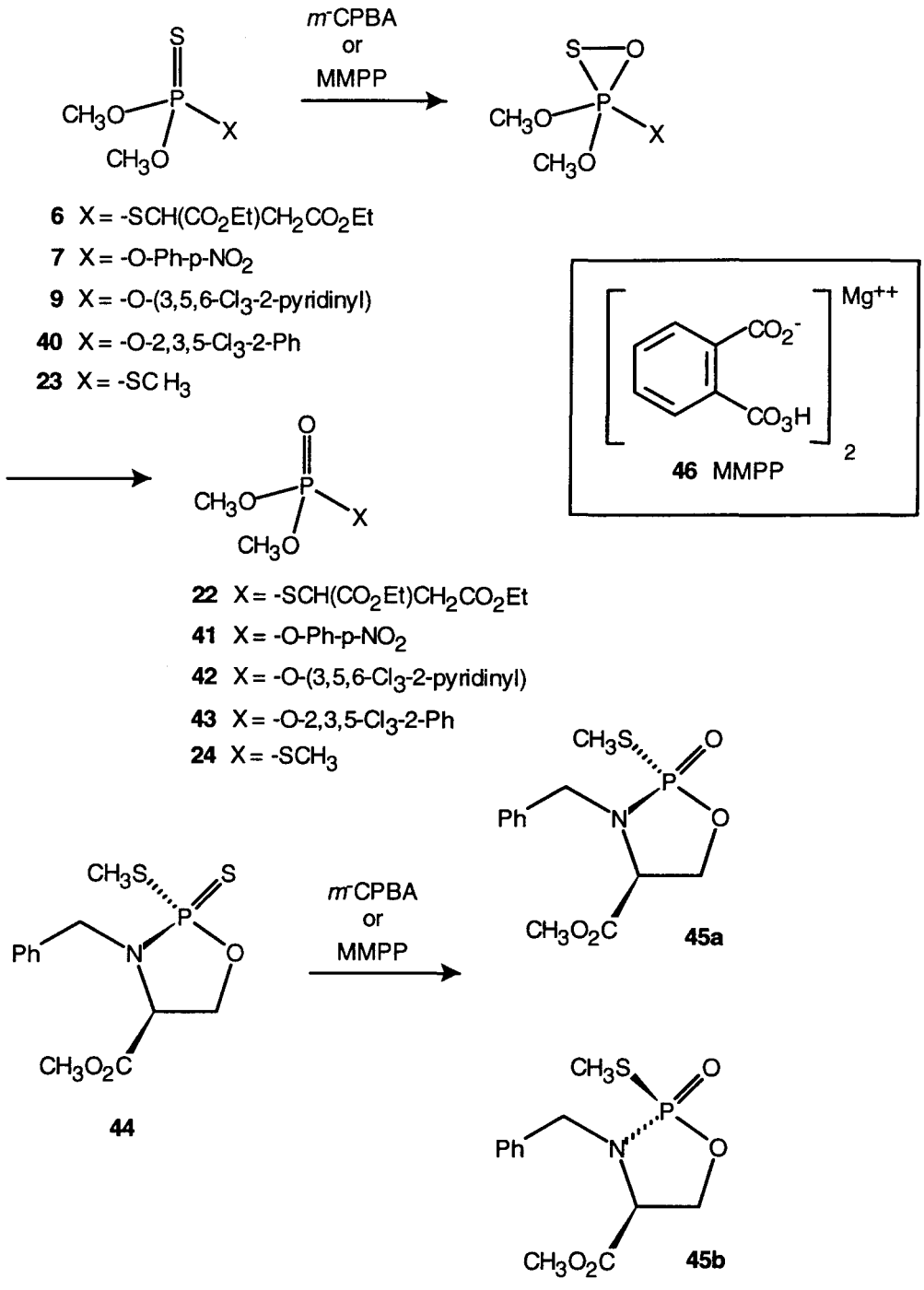

Scheme 3. Conversion of Thionates to Oxons.

stereochemical outcomes using MMPP were superior to that of *m*-CPBA. The conversion of thion **44** to oxon **45a** occurred with complete retention of phosphorus configuration while reaction with *m*-CPBA resulted in a 3.85:1 diastereomeric ratio of oxons **45a** and **45b**. The superior results obtained with MMPP was attributed to its lower reactivity than *m*-CPBA.

Synthesis of Racemic Isomalathion

The isomerization of racemic malathion **6** was conducted as previously reported (Thompson, 1989) by dealkylation with potassium ethyl xanthate (EtOCS(S)K) followed by realkylation with dimethyl sulfate (Eqn. 8). Positive identification of racemic isomalathion **12** was accomplished by comparison to known material. ^{1}H NMR revealed the presence of a new phosphorus-coupled doublet (2.4 ppm) corresponding to the S-methyl protons as a result of the isomerization. A new resonance also was observed in the ^{13}C NMR spectrum

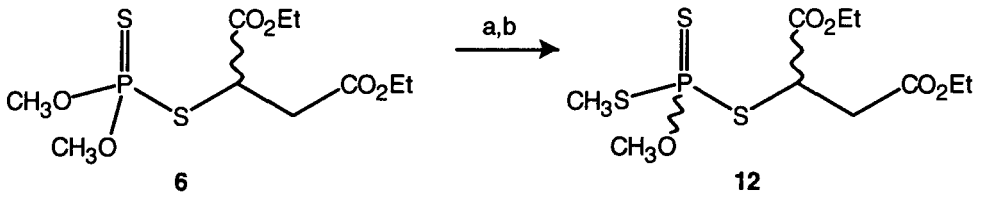

(8)

a. EtOC(S)SK b. $(CH_3O)SO_2$

(centered at 13 ppm), corresponding to the -SCH_3 moiety. Only the ^{31}P NMR spectrum identified the two diastereomers showing two resonances separated by 1.5 ppm and centered at 58 ppm.

Synthesis of ^{13}C-S-methyl Isomalathion

In an effort to aid the mechanistic evaluation of the interaction of isomalathion with AChE, ^{13}C-enriched ($^{13}CH_3S$)-isomalathion (**12'**) was desired. Using the preparative method for racemic isomalathion, ^{13}C-labeled isomalathion was obtained by substituting $(^{13}CH_3O)_2SO_2$ in the second step. ^1H NMR of the product showed considerable carbon-proton coupling of the S-methyl doublet (J = 144 Hz) while ^{13}C NMR showed the expected enhancement of the labeled S-methyl carbon.

Attempted Chromatographic Separation of Isomalathion Diastereomers

Since control over the chiral carbon center had been established using enantioenriched malic acid starting materials in the synthesis of the malathion enantiomers, the thionate-thiolate isomerization reaction would give the putative diastereomeric mixture of isomalathion (Scheme 4), which could be separated chromatographically. The dealkylation-realkylation sequence described in Equation 8 was conducted with (*R*)- and (*S*)-malathion (**6a** and **6b**) to afford either (*1RS,3R*)- or (*1RS,3S*)-isomalathion in 72% yield (Scheme 4) as a mixture

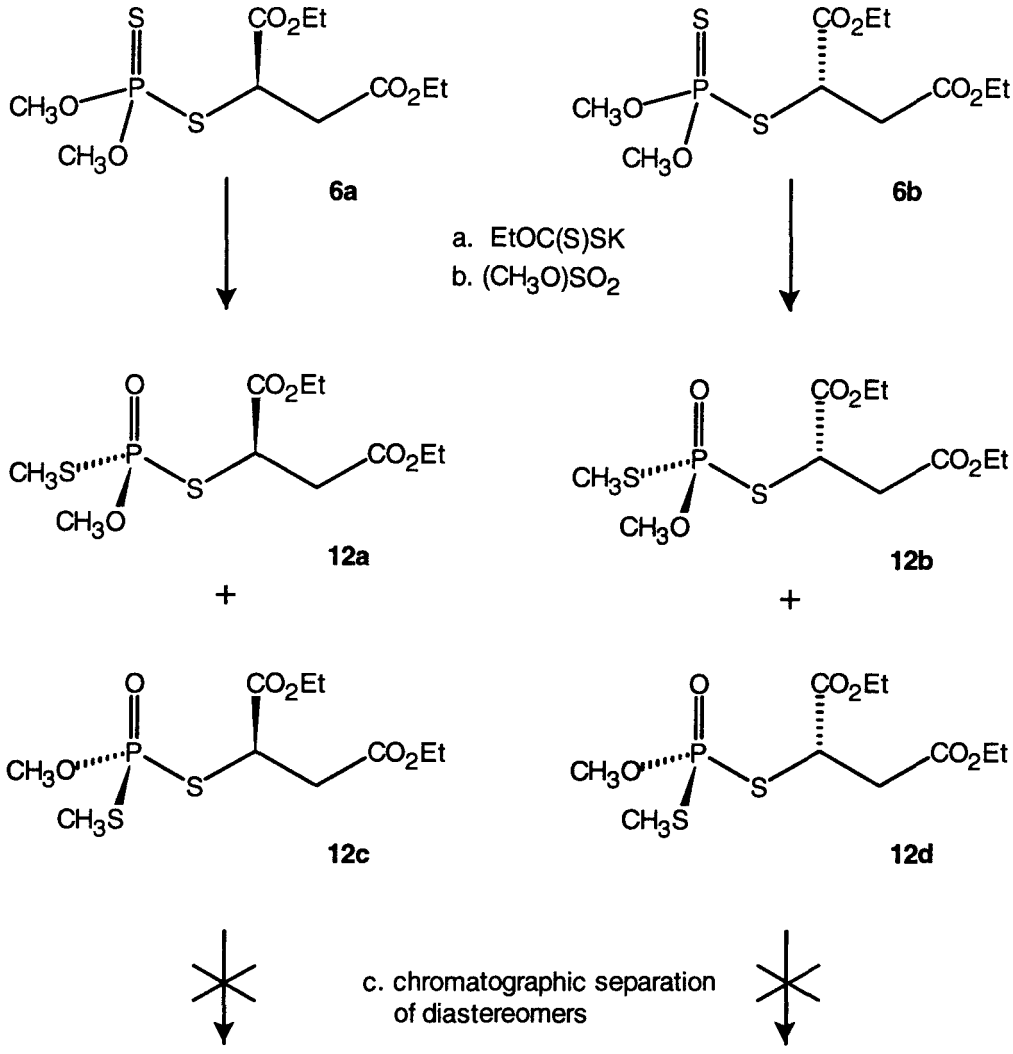

Scheme 4. Synthesis of Isomalathion Diastereomers.

of diastereomeric pairs (**12ac** and **12bd**), respectively.

As indicated in Synthesis of Racemic Malathion, isomalathion diastereomers were most readily detected by ^{31}P NMR, which provided an analytical tool to study the degree of resolution or separation of a single

stereoisomer from a diastereomeric pair. Traditional attempts at gravity silica gel chromatography were unsuccessful (numerous solvent mixtures were examined). For example gravity silica gel chromatography (petroleum ether:ethyl ether, 1:1) produced fractions enriched in the front flowing diastereomer (35% diastereomeric excess) followed first by 50/50 mixtures and later by slightly enriched mixtures of the slow band (10% diastereomeric excess). Reapplication of the front flowing enriched fractions to the column gave only 1% of the single diastereomer followed again by the elution of varying degrees of the diastereomer mixture.

Reverse phase TLC also was tried, however, only one elution band was detected. Analytical chiral HPLC (d-phenylglycine and l-leucine) could partially resolve a diastereomeric mixture but not to baseline resolution (Figure 24). Thus all chromatographic approaches failed, possibly explaining the 30 year dearth of reports on isomalathion stereoisomerism.

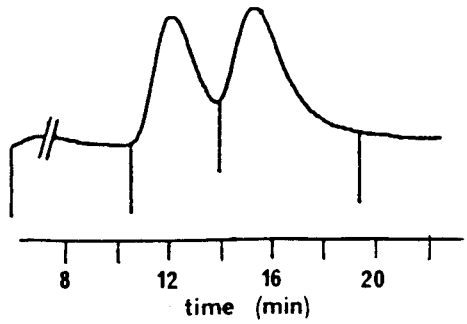

Figure 24. Partial Resolution of Isomalathion Diastereomers via Chiral HPLC.

Attempted Synthesis of Isomalathion Stereoisomers Using a Chiral Auxiliary

With the failure of the previous approach that would have allowed control over the asymmetric carbon center followed by resolution of the asymmetric phosphorus center, a convergent synthesis was planned where control of both stereocenters was achieved in separate steps, followed by the appropriate coupling of the 2 asymmetric "pieces." Previous reports indicated that resolution of certain organophosphorus compounds could be achieved by the use of chiral auxiliaries (Valentine, 1984; Koizumi, 1978). Because it had proved useful for the preparation of isoparathion methyl enantiomers **49a/49b** (Scheme 5; Ryu, 1991a), *l*-proline ethyl ester was selected as the chiral auxiliary for the resolution of isomalathion stereoisomers (Scheme 6) with anticipated success.

Thiomethyl phosphoric dichloride **47** was prepared from thiophosphoryl chloride via methanolysis followed by thermal isomerization at 100 ^{0}C. Reaction of **47** with *l*-proline ethyl ester in the presence of TEA yielded the desired chlorophosphoramidothiolate diastereomers **50**, which were resolved by column chromatography. The ^{1}H NMR spectrum showed the characteristic phosphorothiolate methyl doublet at 2.5 and 2.4 ppm for the fast and slow bands, respectively. The ethyl ester protons were also present for both diastereomers in addition to the pyrrolidine ring protons. ^{13}C NMR spectra of the diastereomers were similar but again the ^{31}P NMR spectra for the diastereomers were resolved, differing by 0.4 ppm. Specific rotations for the two stereoisomers also were

obtained (fast band, $[\alpha]_D^{24} = -52.6^0$ (c = 1.04, $CHCl_3$); slow band, $[\alpha]_D^{24} = -48.2^0$ (c = 1.15, $CHCl_3$). Thus, control over the phosphorus stereochemistry was managed.

(*S*)-diethyl mercaptosuccinate **51a** was prepared via reaction of sodium hydrogen sulfide with enantioenriched (*R*)-diethyl bromosuccinate **32b**, which had been prepared earlier (Scheme 1). Thus, with the two chiral "pieces" in hand, the stage was set for their coupling. Racemic diethyl mercaptosuccinate prepared from esterification of mercaptosuccinic acid (Ailman, 1965) was used first to study the coupling reaction to avoid unnecessary consumption of chiral materials, and was reacted with the fast-band diastereomer of the phosphoramidothiolate **50** to afford the phosphoramidodithiolate **52**. ^1H NMR showed the S-methyl doublet and the pyrolidine protons observed for **50**. The resonances for the ethyl ester methyl protons of both the prolinate and succinate moieties were superimposed and appeared as multiplets. This was also the case for the methylene protons of the ethyl esters. Two resonances at 47.52 and 48.12 ppm were observed in the ^{31}P NMR spectrum for each of the diastereomers, **52b** and **52d**, due to the use of racemic **51**.

The final stage of this method, exchange of the chiral auxiliary for a CH_3O- moiety, is normally straightforward (Ryu, 1991a). Unfortunately, both mineral acid (H^+) or Lewis acid (BF_3) promoted methanolysis were unsuccessful

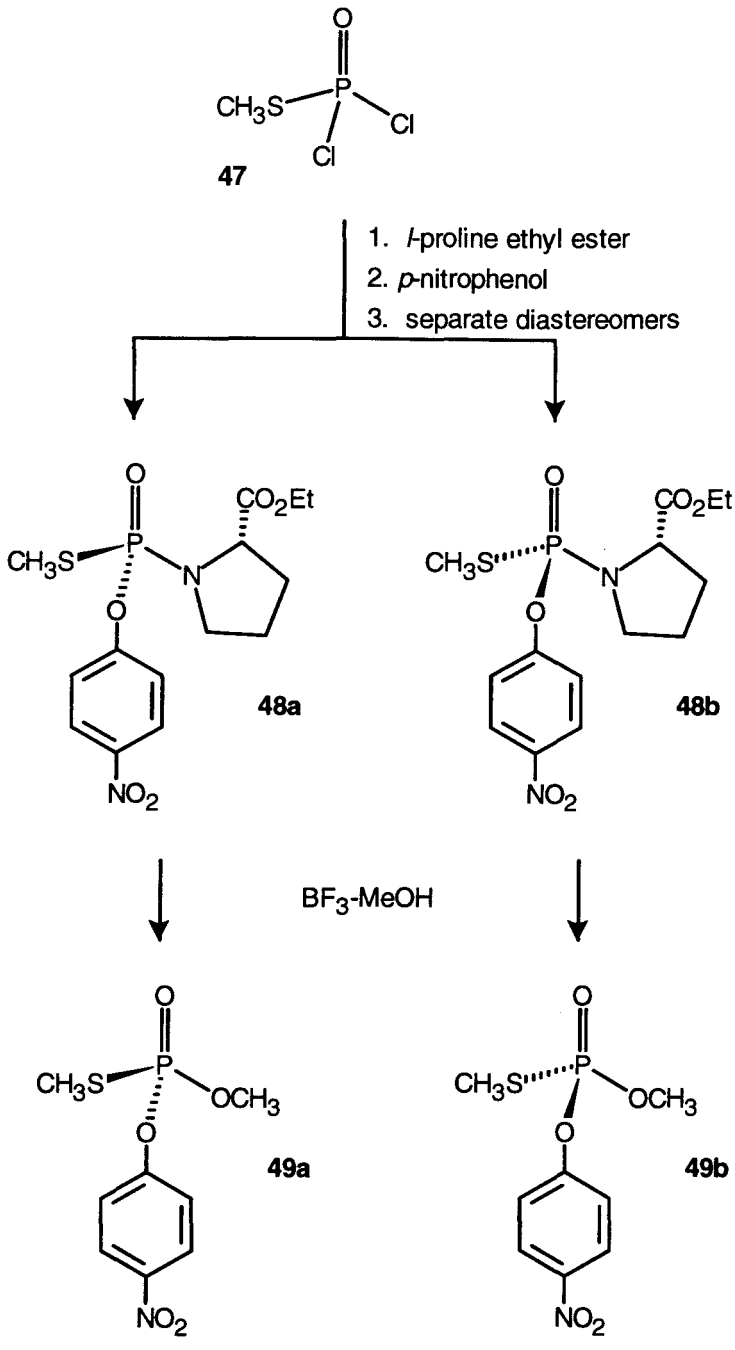

Scheme 5. Synthesis of Isoparathion Methyl Enantiomers Using a Chiral Auxiliary.

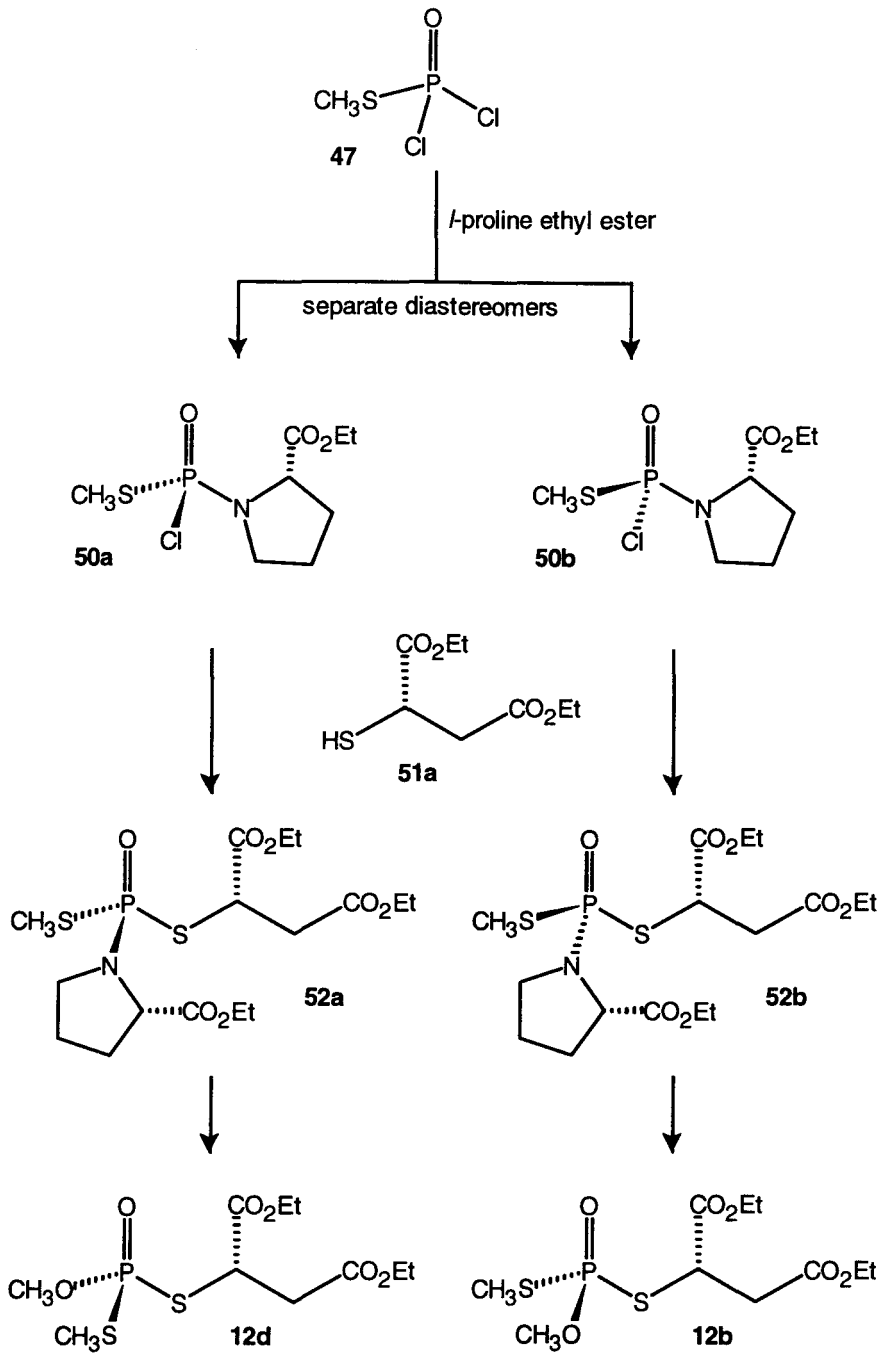

Scheme 6. Attempted Synthesis of Isomalathion Stereoisomers Using a Chiral Auxiliary.

in yielding isomalathion as indicated by TLC. One possible explanation of these results may be attributed to the presence of three electron donors connected to the phosphorus atom, which compete for the primary acid coordination site.

Attempted Synthesis of Isomalathion Stereoisomers from Isoparathion Methyl

While the stereoisomers of isoparathion methyl **49** were available through a prior study (Ryu, 1991b), an alternative to the coupling strategy was envisioned. Because *p*-nitrophenoxy is the primary leaving group of isoparathion methyl, it was thought that an S_N2-type reaction could be conducted at the asymmetric phosphorus of isoparathion methyl with optically pure diethyl mercaptosuccinate **51b** as the incoming nucleophile (Eqn 9). Again, racemic diethyl mercaptosuccinate was utilized to avoid unnecessary consumption of the chiral pool. Unfortunately, multiple variations within this strategy (varied solvents:

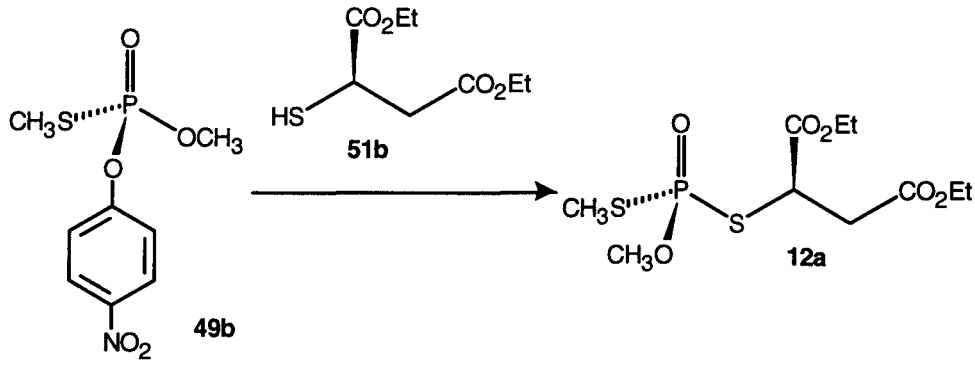

(9)

ethyl ether, THF, and DMF) with up to 5 equivalents of **51** were unsuccessful. In this instance, **51** probably acts to dealkylate the phosphorus ester rather than serve as a nucleophile.

Synthesis of Isomalathion Stereoisomers via Alkaloid Resolution

Several prior studies showed that alkaloid resolution was an effective procedure for the preparation of enantioenriched phosphoro**thiolates** (Valentine, 1984; Aaron, 1958; Aaron, 1960; Hilgetag, 1969; Hilgetag, 1959). However, there are very few examples of phosphoro**dithioate** resolution with alkaloids. The general method for this type of resolution involves either conducting an acid-base reaction with a phosphorothioic acid and the alkaloid, or dealkylating a phosphorothionate ester with the alkaloid to form the alkylated alkaloid/phosphorothioic acid salt.

Dealkylation of (*S*)-malathion **6b** with strychnine, brucine, and quinine was performed followed by attempts at fractional crystallization of the resulting alkaloid salts (Scheme 7). Fractional crystallization of phosphorothioate-alkaloid salts is commonly performed in methanol or ethanol, however, the alkaloid salts of (*S*)-malathion (**53b** and **53d**) were readily soluble in these solvents. Initial attempts dissolved the salts in methanol followed by the addition of ethyl ether to affect cloudiness. Heat was applied to affect solution, which subsequently was stored at -20^{0}C overnight. As a result, a first crop of crystals was obtained for

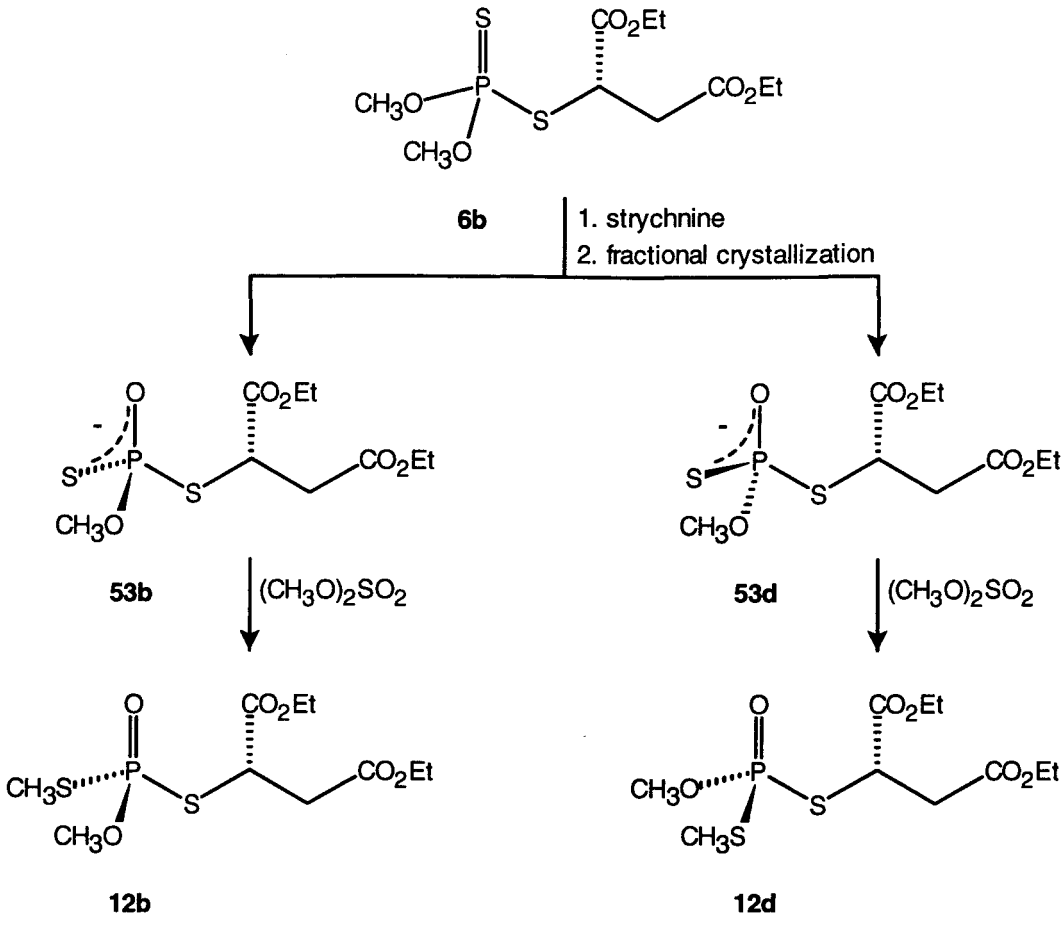

Scheme 7. Synthesis of Isomalathion Diastereomers via Alkaloid Resolution: Method I.

strychnine and brucine salts while quinine failed to produce any crystals under these conditions. These first crops were analyzed by ^{1}H, ^{13}C, and ^{31}P NMR and enrichment of one diastereomer of the (*S*)-malathion-alkaloid salt mixture was most notably and easily observed in the ^{31}P NMR spectrum as revealed by two

resonances differing by approximately 1 ppm. The most significant enrichment of the alkaloid salts was observed for the strychnine derivatives in which ^{31}P NMR revealed approximately 70% enrichment of the downfield diastereomer **53b**. Thus, preparative resolution of the isomalathion stereoisomers via strychnine salts was pursued using ^{31}P NMR as the definitive analytical tool used to determine diastereomeric purity.

Further fractional crystallization of the first strychnine salt crop (downfield diastereomer) **53b** was achieved stepwise, through repeated recrystallization in methanol-ethyl ether solutions (Figure 25). However, the [unexpected] limit of diastereomeric purity was 95%. To achieve higher resolution of the downfield (*S*)-malathion-strychnine salt **53b**, several solvent mixtures for recrystallization were examined. A mixture of ethylene glycol, absolute ethanol, and ethyl ether eventually provided the downfield alkaloid salt in 100% diastereomeric purity by ^{31}P NMR.

The mother liquor from the first crystallization of the (*S*)-malathion-strychnine salt provided no precipitated salts upon cooling (-20 ^{0}C, 5 days). The solution was concentrated to an glassy solid that showed approximately 60% enrichment of the upfield diastereomer **53d** by ^{31}P NMR. Further enrichment was first attempted by crystallization with a methanol-ethyl ether mixture as described for the downfield diastereomer. However, no further enrichment of the resulting crystals resulted. Several solvent mixtures were examined to further enhance the

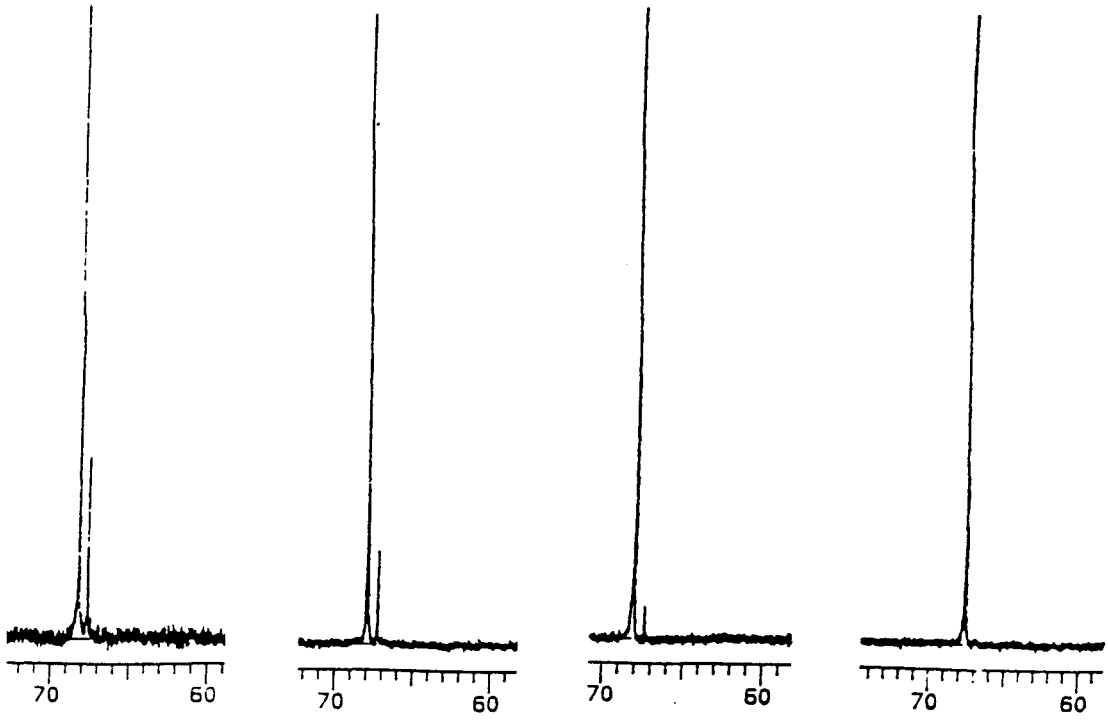

Figure 25. ^{31}P NMR Analysis of the Sequential Enrichment of Desmethyl Malathion-Strychnine Following Fractional Crystallization.

diastereomeric purity of this diastereomer (**53d**) and as a result, a mixture of methanol, ethyl acetate, and ethyl ether produced the completely resolved diastereomer after repeated recyrstallization. It was later found that if the initial crystallization was performed with this solvent mixture, the first crop of crystals produced was the downfield diastereomer **53b** in approximately 70% enrichment

while the mother liquor, upon standing at room temperature, conveniently deposited the upfield diastereomer **53d** in 100% diastereomeric purity. As a result of the above mentioned success, resolution of the diastereomeric strychnine salts of (*R*)-malathion (**53a** and **53c**) was undertaken. Initially, a methanol-ethyl ether mixture was employed for the fractional crystallization and produced a first crop with an approximate 70% enrichment of the downfield diastereomer **53c** as identified by ^{31}P NMR. Repeated recrystallization with methanol-ethyl ether ultimately produced **53c** in 100% purity. In results similar to the desmethyl-(*S*)-malathion-strychnine resolution, no crystals could be obtained using methanol-ethyl ether from the mother liquor of the first crop. Experimentation with various solvent mixtures showed that repeated recrystallization of the mother liquor with chloroform-ethyl acetate produced the completely resolved upfield diastereomer **53a**. Again, it was found that if the first crystallization was performed with this solvent mixture, the first crop that was deposited was enriched approximately 70% with **53c** while the mother liquor produced **53a** in 100% purity upon standing at room temperature.

In addition to NMR analysis of the malathion-strychnine salts **53**, specific rotations and melting points also were obtained (Table 4). The individual salts of each diastereomeric pair were identified as the levorotatory or dextrorotatory stereoisomer with respect to the phosphorus stereochemistry because the carbon configuration was known from malic acid. Similarities observed for melting

Table 4. Physical Data of the Malathion-Strychnine Salts.[a]

compound	$[\alpha]_D^{22}$	^{31}P NMR (δ)	mp (^{0}C)
53a (*1R,3R*)	+32.2 (0.25)	67.20	159-160
53b (*1R,3S*)	-45.1 (0.26)	68.12	189
53c (*1S,3R*)	+16.1 (0.31)	68.10	181-182
53d (*1S,3S*)	-61.7 (0.31)	67.18	158-159

[a]rotations performed in $CHCl_3$; concentrations in parenthesis, g/100 ml.

points and ^{31}P NMR data supported correlation of the phosphorus and carbon configurations (excluding that of strychnine) for the salts that were later confirmed through comparison to a salt analyzed by x-ray crystallography.

Assignment of Absolute Configurations of the Isomalathion Stereoisomers

In an effort to assign the absolute configuration of the carbon and phosphorus stereocenters of the resolved desmethyl malathion-strychnine salts, x-ray crystallographic analysis was desired. In order to prepare crystals for x-ray crystallography, recrystallization of the resolved salts was performed in their respective solvent mixtures at twice the dilution normally used. Recrystallization of **53c** in methanol:ether (1:5) ultimately provided crystals that were suitable for x-ray crystallographic analysis.

The crystal structure of the submitted crystal was solved and revealed a monoclinic unit cell with dimensions of 8 x 8 x 14 Å (Table 5; Berkman, 1993). Methylstrychninium cations were found in bilayer sheets that alternated with bilayer sheets of desmethyl malathion anions (Figure 26). This bilayer packing of strychnine salts had been noted previously (Gould, 1984; 1987). Ultimate determination of the structure was aided by prior knowledge of the structure and absolute configuration of strychnine (Peerdeman, 1956). As a result of this analysis, the configuration of the phosphorus stereocenter was identified as *S* (Figure 27). The carbon stereocenter configuration of **53c** was identified as *R* and was expected because this salt was initially prepared from the reaction of (*R*)-malathion strychnine. Thus, with the absolute configuration of one salt known, the configuration of the other three were assigned.

With the four alkaloid salts resolved, realkylation with dimethyl sulfate to form the respective stereoisomers of isomalathion was conducted. This step afforded the desired isomalathion stereoisomers in approximately 70% yield, which were characterized by specific rotations and ^{1}H, ^{13}C, and ^{31}P NMR. A limitation of ^{31}P NMR analysis of the isomalathion stereoismers was the inability to detect enantiomer impurities. To address this problem, a HPLC technique was developed that resolved the four individual stereoisomers (Figure 28). Compared to known racemic material, a most striking difference was the presence of a single resonance in the ^{31}P NMR spectra for each stereoisomer instead of the two

Table 5. Crystal Data for Strychnine Salt 53c.[a]

molecular formula	$C_{31}H_{41}N_2O_8PS_2$
molecular wt (amu)	664.77
d_{calcd}, g/cm^3	1.37
crystal system	monoclinic
space group	$P2_1$
Z	2
a, Å	8.3925
b, Å	8.0054
c, Å	24.3050
V, Å^3	1614.9
crystal size (mm)	0.4 x 0.24 x 0.20
total reflections	5806
unique reflections	3063
observed ($I > 2.5\sigma(I)$)	2417
final R	0.0491
final R_w	0.0463
goodness of fit	0.978

[a]from Berkman et al. *Acta Cryst.* **1993**, *C49*, 554.

observed for the diastereomeric mixtures. HPLC analysis further confirmed the successful preparation of the isomalathion stereoisomers. Both specific rotations and ^{31}P NMR data of the individual isomalathion stereoisomers confirmed the enantiomeric and diastereomeric relationships for their assigned phosphorus and carbon configurations (Table 6).

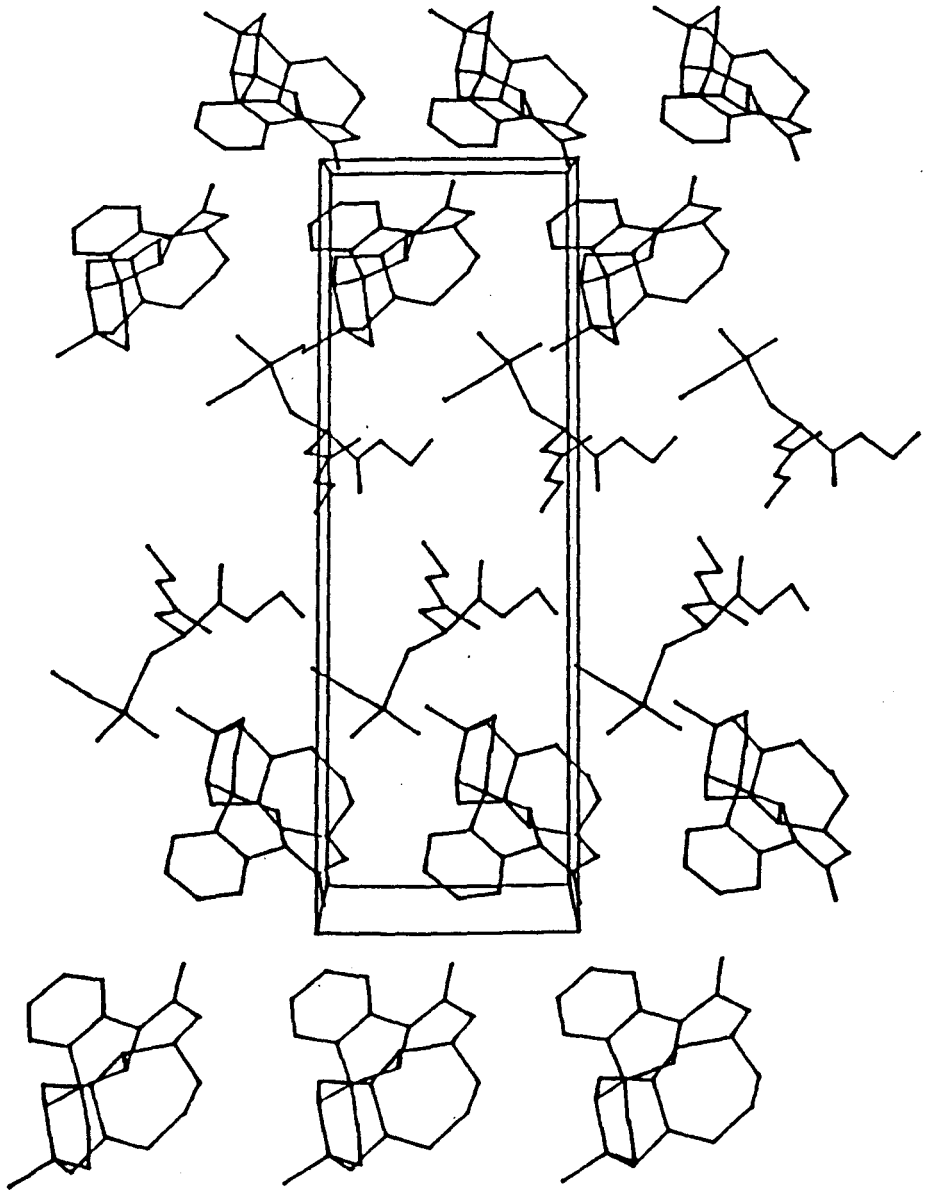

Figure 26. The Unit Cell of the Malathion-Strychnine Salt 53c.

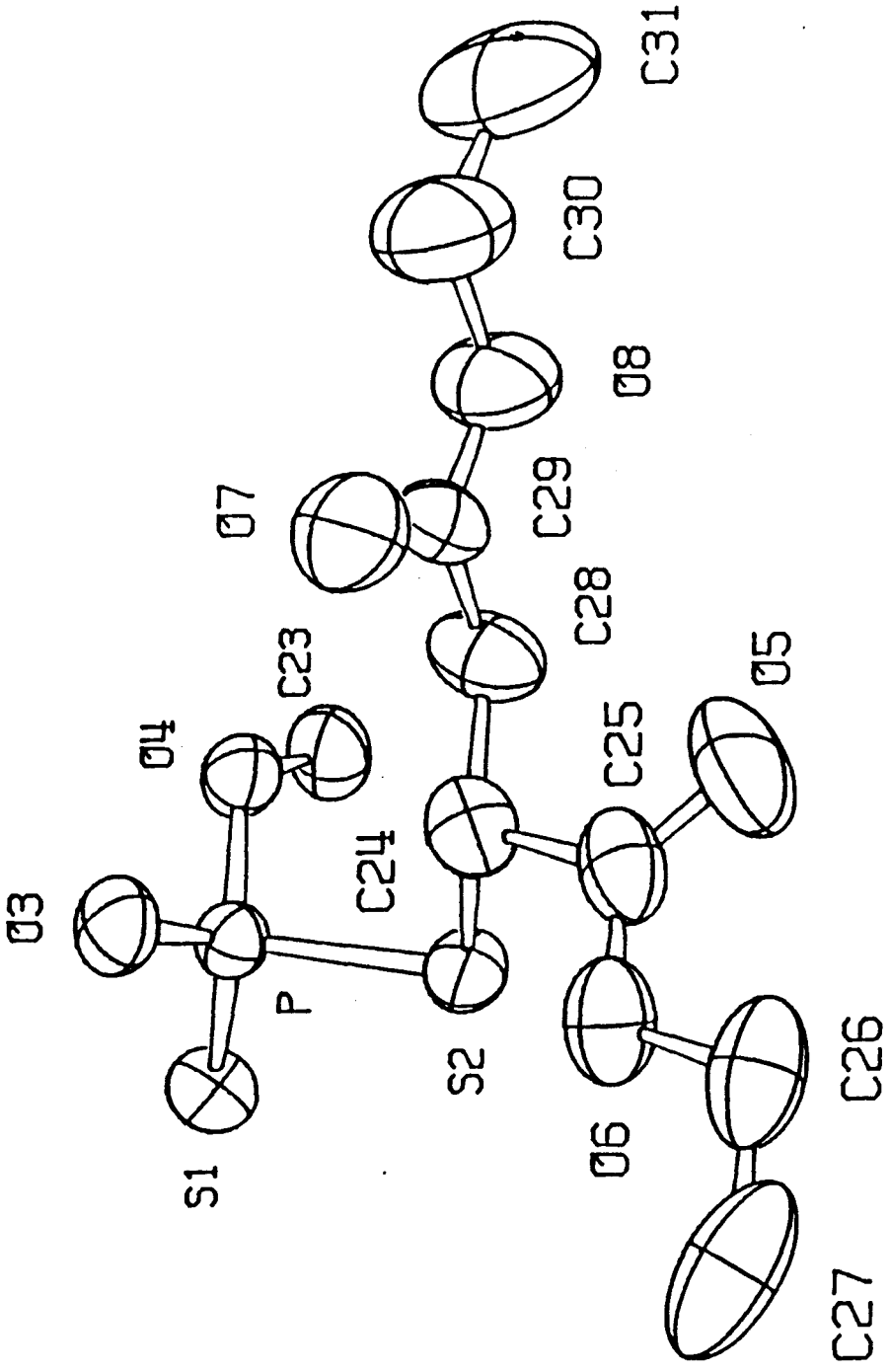

Figure 27. The structure of the 53c Anion of the Malathion-Strychnine Salt as Determined by X-ray Crystallographic Analysis.

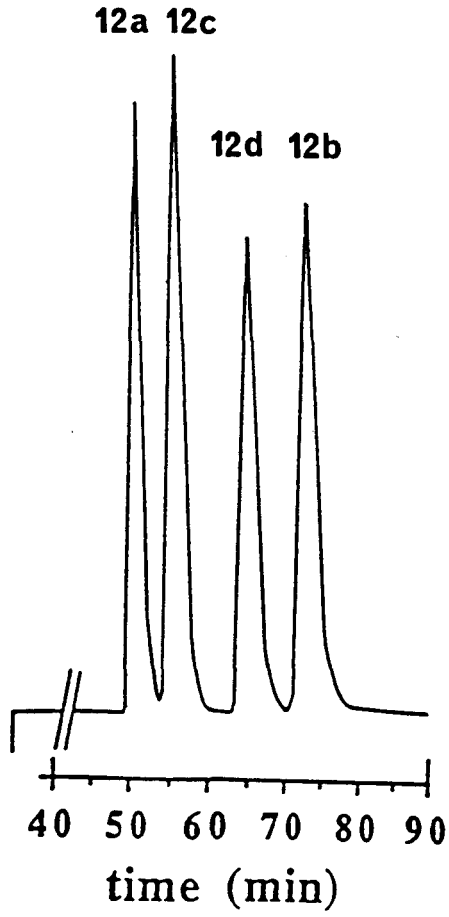

Figure 28. Chiral HPLC Resolution of Isomalathion Stereoisomers.

Competing O-alkylation to form malathion was detected by TLC in the final alkylation step (approximately 10%). This O-methylation also was observed in the dealkylation/realkylation preparation of isomalathion using KSC(S)OEt and dimethyl sulfate (Scheme 4).

Table 6. Physical Data of the Isomalathion Stereoisomers.[a]

compound	$[\alpha]_D^{22}$	^{31}P NMR (δ)
12a (*1R,3R*)	+42.3 (0.64)	58.38
12b (*1R,3S*)	-57.6 (0.50)	56.92
12c (*1S,3R*)	+58.6 (0.64)	56.92
12d (*1S,3S*)	-44.8 (0.58)	58.38

[a]rotations performed in $CHCl_3$; concentrations in parenthesis, g/100 ml.

It was assumed that the S-methylation did not disturb the phosphorus configuration, thus, allowing the absolute configurations of the resulting isomalathion stereoisomers to be known from the preceding alkaloid salts. While this method provided the four stereoisomers of isomalathion and allowed configurational assignment, there were two major disadvantages: (1) the yield of the fractional crystallization was low (20%), and (2) the process of fractional crystallization was tedious and time consuming. Consequently, an alternate method was designed.

A Simplified Synthesis of Isomalathion Stereoisomers via Alkaloid Resolution

Since the diastereomeric strychnine salts of O,O,S-trimethyl phosphorodithiolate (**54**) had been previously resolved (Hilgetag, 1969), it was

believed that these salts could be used in a reaction with the triflate of diethyl malate **39** (used in the chiral malathion synthesis) to provide the isomalathion stereoisomers **12** (Scheme 8). Using this approach, several steps could be eliminated. Again, the design was convergent attempting to couple two resolved chiral "pieces."

Resolution of the alkaloid salts **54a** and **54b** via fractional crystallization (Hilgetag, 1969) was achieved readily and in a much greater yield than that of the malathion alkaloid salts **53a**, **53b**, **53c**, and **53d**. The displacement of the triflate that followed was also successful providing the isomalathion stereoisomers **12** in an overall yield of 27% from triflate **39**, which exceeded the yield of the previous method (11% from triflate **39**).

was monitored by melting point and specific rotation. However, definitive analysis as to the stereoisomeric purity of the salts could not be conveniently determined by ^{31}P NMR as with the malathion-strychnine salts because of overlapping ^{31}P NMR resonances. Therefore, the progress of the fractional

The progress of enrichment during fractional crystallization of the two diastereomeric salts (**54a** and **54b**) crystallization steps was monitored by specific rotations and by reaction with a single enantiomer of the triflate (**39a**) followed by ^{31}P NMR analysis of the product (isomalathion, **12a** or **12c**). It was found that after three recrystallizations, a single stereoisomer of isomalathion could be

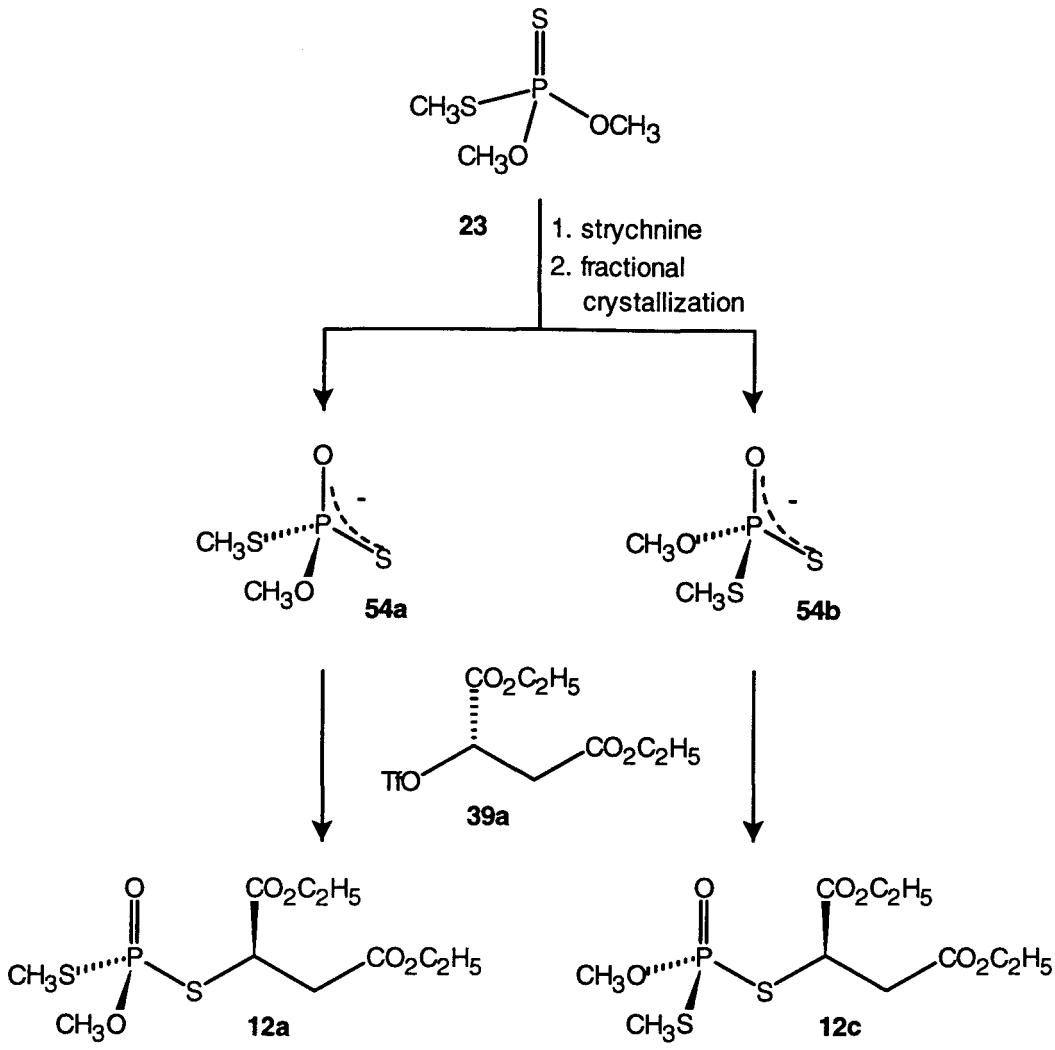

Scheme 8. Synthesis of Isomalathion Diastereomers via Alkaloid Resolution: Method II.

obtained by reaction with **39a**. The procedure was conducted with **39b** to afford the other two isomalathion stereoisomers (**12b** and **12d**).

Summary

The individual stereoisomers of malathion **6a/6b**, malaoxon **22a/22b**, and isomalathion **12a/12b/12c/12d** have been successfully prepared (>95% stereoisomeric purity by HPLC analysis) and represent the first total synthesis of these stereoisomers. The entries in Table 7 summarize salient physical data of the individual stereoisomers as well as that for critical synthetic intermediates.

With the acquisition of the individual stereoisomers of malathion, malaoxon, and isomalathion, the role of stereochemistry upon their interactions with AChE is now permitted.

Table 7. Physical Data for Malathion, Malaoxon, Isomalathion Stereoisomers, and Chiral Intermediates.

compound	$[\alpha]_D^{22}$	^{31}P NMR (δ)	mp (^{0}C)
36a (*S*)-diethyl malate	- 5.45 (1.21)		
36b (*R*)-diethyl malate	+ 5.23 (1.05)		
39a (*S*)-triflate	+ 32.6 (1.39)		
39a (*R*)-triflate	- 30.1 (1.71)		
6a (*R*)-malathion	+ 79.7 (12.5)	96.15	
6b (*S*)-malathion	- 80.0 (1.25)	96.15	
22a (*R*)-malaoxon	+ 46.7 (0.55)	28.30	
22b (*S*)-malaoxon	- 43.5 (0.75)	28.30	
53a (*1R,3R*)-salt	+ 32.2 (0.25)	67.20	159-160
53b (*1R,3S*)-salt	- 45.1 (0.26)	68.12	189
53c (*1S,3R*)-salt	+ 16.1 (0.31)	68.10	181-182
53d (*1S,3S*)-salt	- 61.7 (0.31)	67.18	158-159
54a (*R*)-salt	+ 15.8 (0.54)	78.87	202-203
54b (*S*)-salt	- 13.5 (0.63)	78.79	253
12a (*1R,3R*)-isomalathion	+ 42.3 (0.64)	58.38	
12b (*1R,3S*)-isomalathion	- 57.6 (0.50)	56.92	
12c (*1S,3R*)-isomalathion	+ 58.6 (0.64)	56.92	
12d (*1S,3S*)-isomalathion	- 44.8 (0.58)	58.38	

[a]rotations in $CHCl_3$ except **54** in MeOH; concentrations (g/100mL) in parenthesis.

CHAPTER 4

RESULTS AND DISCUSSION: The Interactions of Malathion, Malaoxon, and Isomalathion Stereoisomers with Acetylcholinesterase.

Biological Evaluation of Malathion Enantiomers

Two preparations of rat brain AChE (RBAChE; homogenized and solubilized) were selected for stereoselective inhibition studies with the malathion enantiomers (**6a** and **6b**). The rationale behind this selection was that they were observed to exhibit the greatest stereoselectivity during inhibition by isoparathion methyl enantiomers (Ryu, 1991b). Unfortunately, malathion was such a weak inhibitor of RBAChE that attempts to accurately determine the k_i of the malathion enantiomers were impeded due to the poor solubility of the compounds at the concentrations needed to affect inhibition. As a result, no reliable data was collected.

The differential toxicities of the malathion enantiomers, however, was studied in collaboration with Cheminova (Lemvig, Denmark) using several insect species. The most notable difference observed was with *Drosophila Melanogaster* where the concentration of the *R*-enantiomer **6a** needed to cause 50% mortality (LD_{50}) was 4-fold less than that of the *S*-enantiomer **6b** (Figure 29) indicating that the *R*-enantiomer **6a** is more toxic to *Drosophila Melanogaster.*

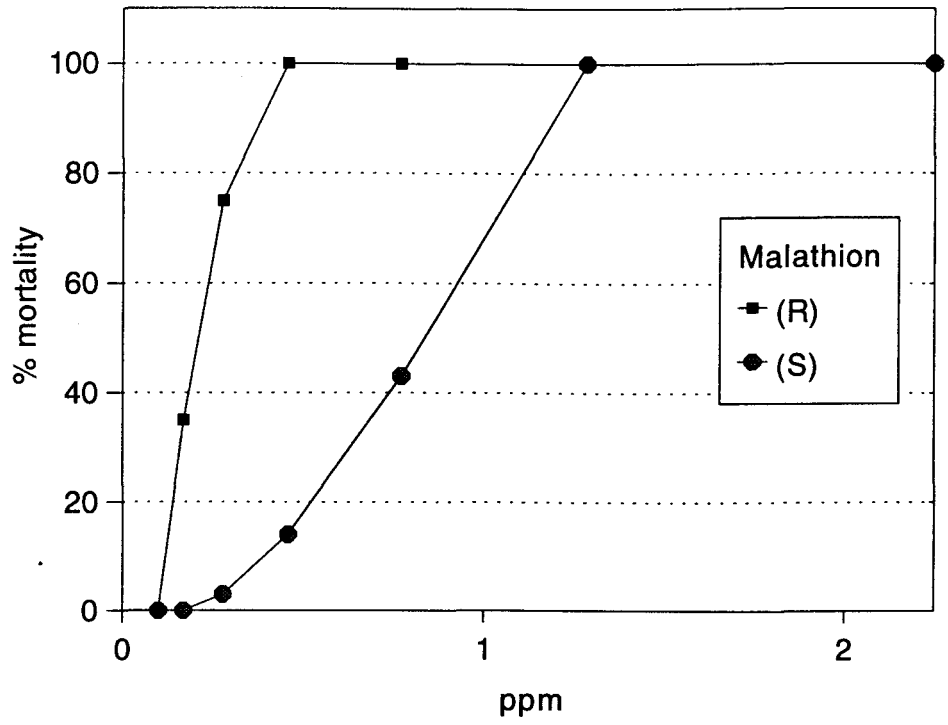

*Unpublished result from Cheminova Agro (1993).

Figure 29. Media-Test of Malathion Enantiomers with Drosophila Melanogaster.

Inhibition of AChE by Malaoxon Enantiomers

Since the O,O-diethyl malaoxon stereoisomers **27a/27b** showed a 4.4-fold difference in anticholinesterase activity (Hassan, 1968), it was presumed that similar stereoselectivity would be displayed by the O,O-dimethyl stereoisomers **22a/22b**. Results from previous investigations showed that among several sources of AChE tested against isoparathion-methyl enantiomers **49a/49b** RBAChE was

the most stereoselective while human erythrocyte AChE (HEAChE) was the least (Ryu, 1991). Thus, it was desired to examine the stereoselective inhibition profiles of these two cholinesterases against chiral malaoxon **22** to obtain an understanding of the influence of a chiral carbon ligand. In order to evaluate the inhibitory potency of the malaoxon stereoisomers and to compare them to the differences observed for the O,O-diethyl analogues (Hassan, 1968), the bimolecular rate constants, k_i, were first determined according to Eqn. 3 (Section

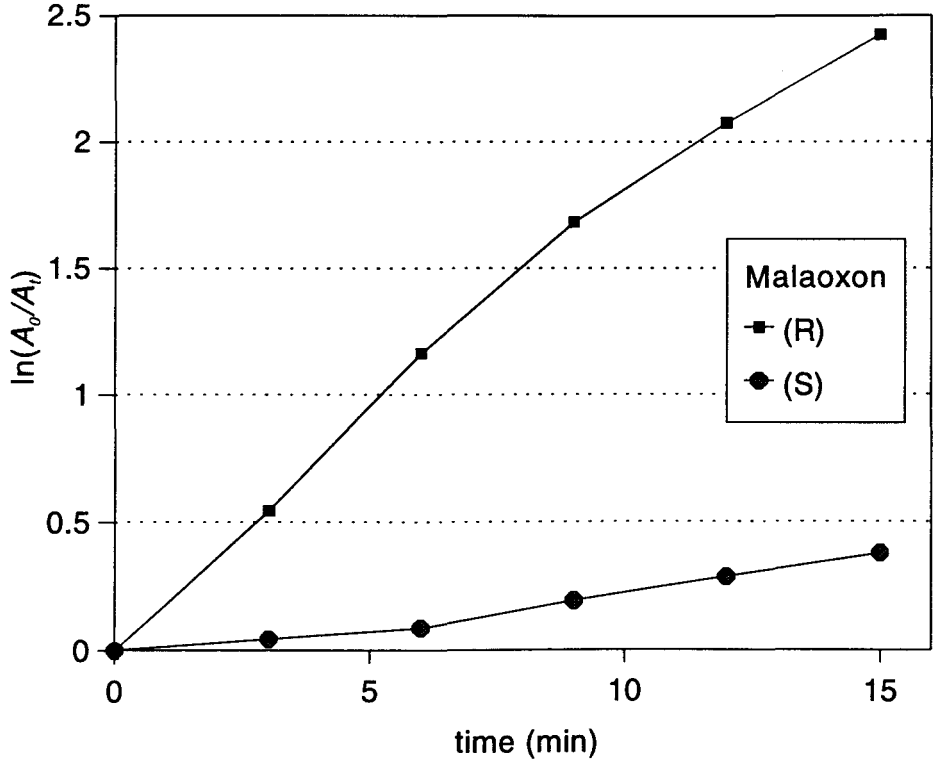

Figure 30. Inhibition of RBAChE (Homogenized) by Malaoxon Enantiomers.

1.8). Plots of $\ln(A_0/A_t)$ versus time provided curves with slopes proportional to k_i (Figure 30).

Table 8. Bimolecular Inhibition Rate Constants for Malaoxon Enantiomers.

compound	RBAChE[a] k_i $M^{-1}min^{-1}$ ($x10^3$)	HEAChE[b] k_i $M^{-1}min^{-1}$ ($x10^3$)	BEAChE[c] k_i $M^{-1}min^{-1}$ ($x10^3$)
malaoxon			
22a (*R*)	152	201	
22 (*RS*)	101	97	
22b (*S*)	30	48	
O,O-diethyl malaoxon			
27a (*R*)			28.0
27 (*RS*)			14.9
27b (*S*)			6.3

[a]homogenized, 25°C. [b]37°C. [c]bovine erythrocyte AChE (Hassan, 1968)

The k_i values showed that (*R*)-malaoxon **22a** was a 5.0-fold and a 4.2-fold stronger inhibitor than (*S*)-malaoxon **22b** of RBAChE and HEAChE, respectively (Table 8). In both cases, racemic material was found to be intermediate in inhibitory strength. The stereoisomer preference and the 4-5-fold

difference in potency is in good agreement with that reported by Hassan and Dautermann (1968) and indicates that the change from diethoxy to dimethoxy did not alter the interaction significantly.

To further understand the process of stereoselective inhibition by the malaoxon stereoisomers, the partial kinetic parameters, i.e. the dissociation constant (K_D), and the phosphorylation constant (k_p), were evaluated (Table 9) according to Eqn. 2 (Section 1.8). In order to make useful comparisons to the data obtained with chiral isoparathion methyl enantiomers (Ryu, 1991b), solubilized RBAChE was examined. Plots of $1/[i]$ versus $\Delta \ln v/\Delta t$ provided K_D as the inverse of the y-intercept while the slope of the curve is defined as k_p/K_D or k_i (Figure 31).

The data in Table 9 reveal that (*R*)-malaoxon **22a** was an 8.6-fold more potent anti-RBAChE agent (k_i, reaction constant) than (*S*)-malaoxon **22b**, which represents a more significant difference than noted previously for homogenized RBAChE. These results suggest that the stereochemistry of the succinyl carbon was indeed important in the inhibition process and comparable with the 8.3-fold inhibitory potency difference between the isoparathion methyl enantiomers **49a/49b**. The difference in inhibitory potency between the two malaoxon enantiomers is further revealed by the dissociation constant K_D where the formation of the Michaelis enzyme-inhibitor complex occurs 10-fold faster for (*R*)-malaoxon 22a. Because enzymes provide an asymmetric environment, it

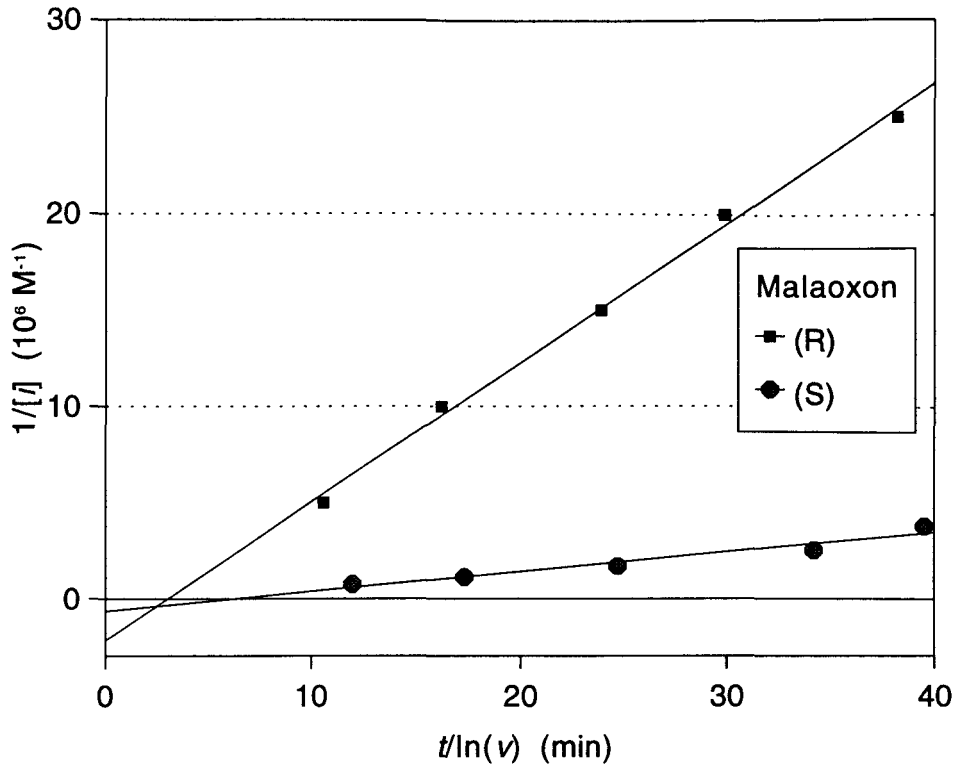

Figure 31. Inhibition of RBAChE (Solubilized) by Malaoxon Enantiomers.

is not surprising that stereoselective interactions occur with enantiomeric inhibitors. Such stereoselectivity is further anticipated since certain conformations attained by one stereoisomeric inhibitor that enhance the affinity for the active site may not be attained by an inhibitor with the opposite configuration.

The difference in the phosphorylation constants, k_p, for the malaoxon enantiomers was relatively small (1.4-fold) suggesting that the carbon stereocenter was relatively less important in the phosphorylation step as compared to the

Table 9. Kinetic Data for the Inhibition of RBAChE by Malaoxon and Isoparathion Methyl Enantiomers.[a]

compound	k_i[b] $M^{-1}min^{-1}$ ($x10^3$)	K_D mM ($x10^{-5}$)	k_p min^{-1}
malaoxon			
22a (*R*)	731 (0.07)	44	0.316
22 (*RS*)	141 (0.09)	235	0.313
22b (*S*)	85 (0.09)	387	0.327
isoparathion methyl[c]			
49a (*S*)	630 (0.08)	27	0.17
49 (*RS*)	410 (0.10)	45	0.19
49b (*R*)	78 (0.06)	273	0.21

[a]coefficient of variation in parentheses. [b]solubilized, 37 ^{0}C. [c](Ryu, 1991)

affinity for the active site (Table 9). If inhibition of AChE by malaoxon proceeds through the loss of the thiosuccinyl ligand (Scheme 9), this small difference in the k_p is not surprising.

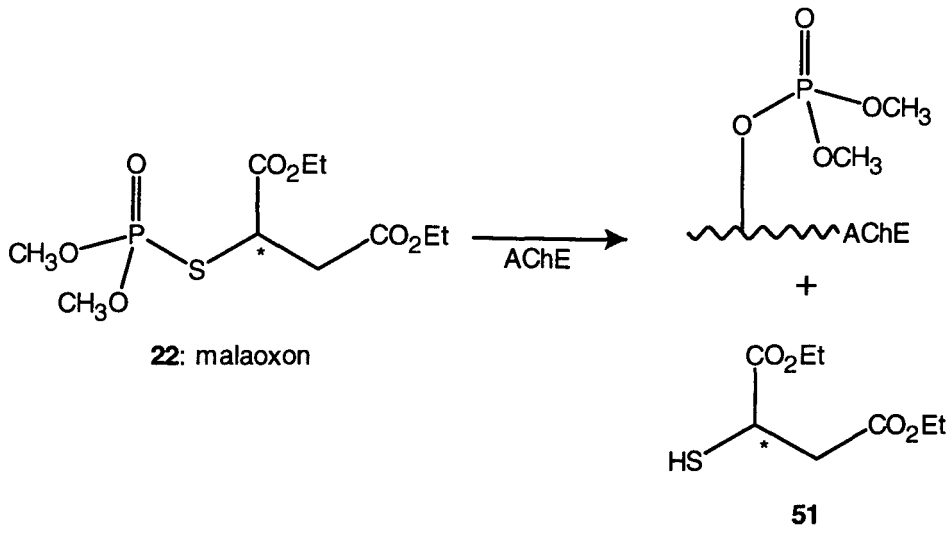

Scheme 9. Proposed Mechanism for the Inhibition of AChE by Malaoxon.

Inhibition of AChE by Isomalathion Stereoisomers

Our studies with the malaoxon enantiomers showed that the ligand stereocenter affects the inhibitor potency, and therefore prompted an inhibition study of the isomalathion stereoisomers, which also bear a phosphorus asymmetric center. Values for k_i, K_D, and k_p for the individual stereoisomers were determined against two sources of the enzyme: solubilized RBAChE and electric eel AChE (EEAChE). Solubilized RBAChE was selected in order to compare data from the malaoxon enantiomer experiments. EEAChE was examined in order to observe a possible species-dependent stereoselectivity for the isomalathion stereoisomers.

Inhibition of RBAChE by Isomalathion Stereoisomers

Initially, inhibition of RBAChE by diastereomeric mixtures of isomalathion with fixed carbon configurations (**12ac** *1RS,3R* and **12bd** *1RS,3S*; also known as semi-racemates) was conducted in order to establish the contribution of the asymmetric phosphorus toward inhibition. The kinetic parameters of inhibition (k_i, K_D, and k_p) for RBAChE were determined as described for malaoxon using Eqn 2 (Section 1.8). We found that (*1RS,3R*)-isomalathion **12ac** was only a 3.0-fold more potent inhibitor of RBAChE than (*1RS,3S*)-isomalathion **12bd** (Table 10) suggesting that either RBAChE could not distinguish the carbon configurational stereoisomers of isomalathion as well as it could with malaoxon, or that the inhibition process may be complicated due to the presence of the asymmetric phosphorus center. To more precisely address the stereoselective inhibition of RBAChE, the inhibitory profiles for the individual stereoisomers of isomalathion were determined as well (Figure 32, Table 10). In addition, an 86:14 mixture of (*1S,3S*)- and (*1R,3R*)-isomalathion obtained during the synthesis of the stereoisomers was examined to evaluate the effect a weighted mixture of inhibitors with differing potency had upon the overall inhibition profile of the mixture (Table 10).

A 29-fold difference in anti-AChE potency was found between the strongest (**12a** *1R,3R*) and weakest (**12d** *1S,3S*) inhibitor. The inhibitory potencies (k_i) of the diastereomeric mixtures (*1RS,3R*- and *1RS,3S*-isomalathion) were found

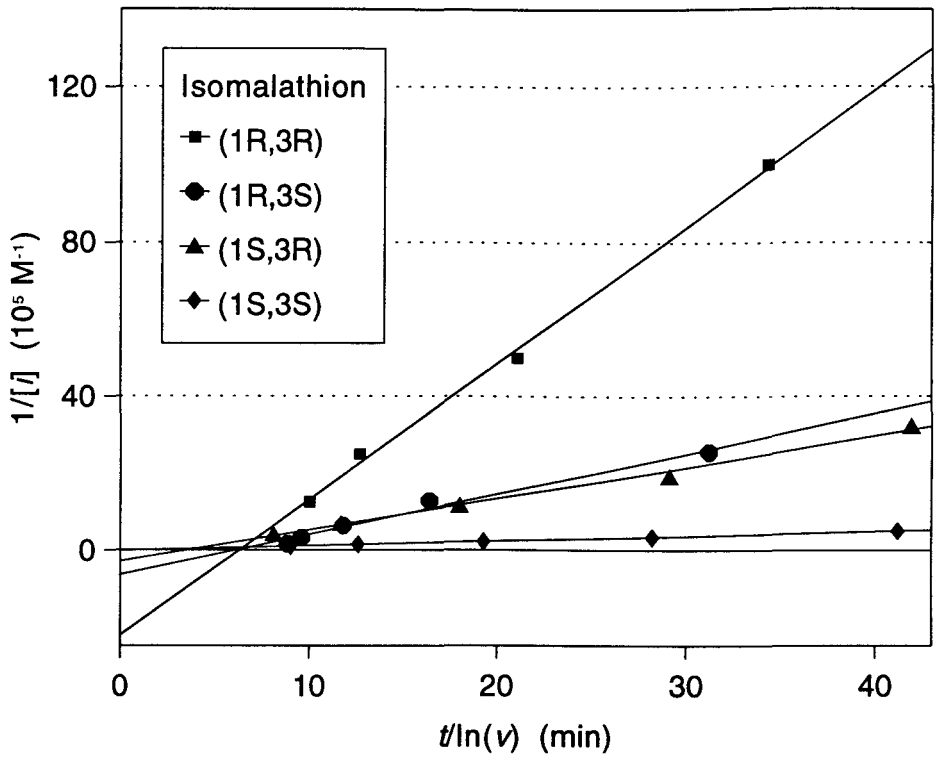

Figure 32. Inhibition of RBAChE by Isomalathion Stereoisomers.

to be midway between the respective antipodes, and the fully racemic material gave an average k_i value relative to the four stereoisomers. The 86:14 mixture of (**12d:12a**)-isomalathion reacted with RBAChE to give a k_i value that closely reflected the molar ratio of the individual stereoisomers according to the following equation: [(% stereoisomer A) x (k_i of stereoisomer A)] + [(% stereoisomer B) x (k_i of stereoisomer B)] = k_i of the AB mixture (calculated = 59 x 10^3; found = 56 x 10^3 M^{-1} min^{-1}).

Table 10. Inhibitory Kinetic Data for RBAChE Inhibited by Isomalathion Stereoisomers.[a]

stereoisomer	k_i[b] $M^{-1}min^{-1}(x10^3)$	K_D $mM(x10^{-5})$	k_p min^{-1}
12a (*1R,3R*)	347 (0.12)	55	0.192
12ac (*1RS,3R*)	260 (0.07)	66	0.170
12c (*1S,3R*)	81 (0.08)	670	0.533
12 (*1RS,3RS*)	132 (0.10)	298	0.380
12b (*1R,3S*)	105 (0.12)	188	0.189
12bd (*1RS,3S*)	86 (0.05)	414	0.353
12d (*1S,3S*)	12 (0.06)	20000	2.510
12d:12a (86:14)	56 (0.21)	440	0.233

[a]solubilized, 37 ^{0}C. [b]coefficient of variation in parentheses.

Both (*1R,3R*)- and (*1R,3S*)-isomalathion (**12a** and **12b**) were more potent inhibitors of RBAChE than the corresponding *1S*-stereoisomers; a preference for the (*R*)-configuration of the phosphorus atom was also noted for nerve gas agents and methyl phosphonates, and was ascribed to specific complementary active site features (Jarv, 1984; Benschop, 1988; Berman and Decker, 1989; Berman and Leonard, 1989). In addition, isomalathion stereoisomers with the (*3R*)-carbon configuration displayed greater inhibitory potency against RBAChE than those

with the (*3S*)-configuration at carbon. Yet, the impact on the inhibition reaction by the carbon stereocenter was further attenuated by the configuration at phosphorus. For example, the difference in inhibitory strength associated with a change in the carbon configuration from *R* to *S* was 6.8-fold when the phosphorus configuration was *S*, while the difference was only 3.3-fold when the phosphorus configuration was *R*. Likewise, the effect of the phosphorus stereocenter was leveraged by the carbon stereocenter. This effect is evidenced by a comparison of the *1S* and *1R* stereoisomers, which gave a 4.3-fold k_i difference when the carbon configuration was *R*, while the difference was 8.8-fold when the carbon configuration was *S*. Therefore, the carbon and phosphorus asymmetric centers of isomalathion act interdependently during inhibition of RBAChE.

Values for K_D and k_p were determined for the isomalathion stereoisomers (Table 10). As with the malaoxon stereoisomers, the k_i values paralleled the dissociation constants, K_D, where the isomer with the greater affinity for the active site was the stronger inhibitor. For example, (*1R,3R*)-isomalathion **12a** displayed a 3.4-fold stronger affinity for the active site than (*1R,3S*)-isomalathion **12b** (or weaker dissociation from the active site) and was a 3.3-fold stronger inhibitor. However, based solely upon the K_D values, (*1R,3S*)-isomalathion **12b** was expected to be a 100-fold stronger inhibitor than (*1S,3S*)-isomalathion **12d** rather than the observed 8.8-fold difference. The unusual magnitude of k_p (2.510) for the *1S,3S* isomer partially compensated for the poor affinity (K_D = 20,000) toward

the active site.

The k_p values obtained for inhibition of RBAChE by **12a** and **12b** were virtually identical, consistent with the results obtained with malaoxon. However, k_p values for **12c** and **12d** differed by 4.7-fold, and were significantly higher than those for **12a** and **12b**. Thus, the carbon stereochemistry significantly influenced the phosphorylation only when (*1S,3R*)- or (*1S,3S*)-isomalathion were the inhibitors, and suggested that the thiosuccinyl ligand remains attached (Scheme 10, Path B). Conversely, since there was no difference in the k_p for (*1R,3R*)- and

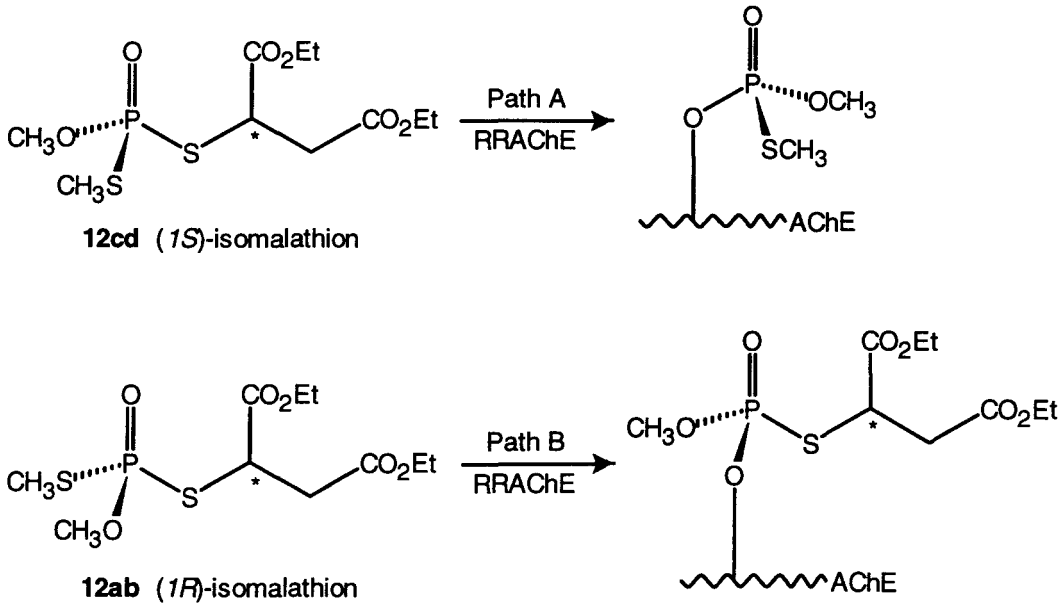

Scheme 10. Proposed Mechanism for the Inhibition of RBAChE by Isomalathion.

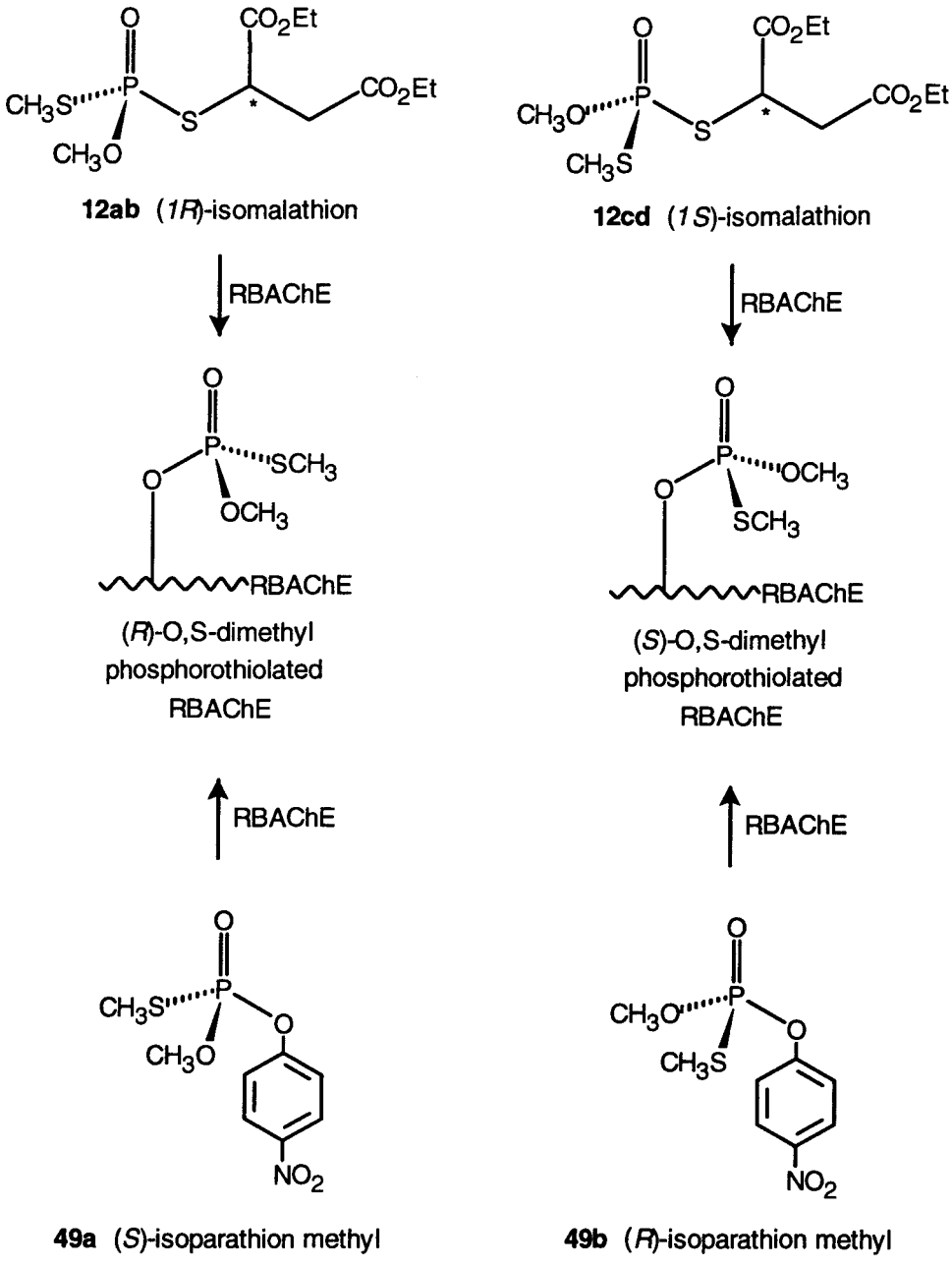

Scheme 11. Convergent Mechanisms for the Inhibition of RBAChE by Isomalathion and Isoparathion Methyl.

(*1R,3S*)-isomalathion, it is likely that the thiosuccinyl ligand is displaced and has little stereochemical influence over this step (Scheme 10, Path A). Alternatively, if RBAChE inhibition by the four isomalathion stereoisomers occurs via a common mechanism (i.e. displacement of the thiosuccinyl ligand with inversion of the phosphorus configuration (Berman and Decker, 1989) then the putative (*S*)- or (*R*)-O,S-dimethylphosphorothiolated AChE would result. Thus, the two phosphorylated enzymes resulting from inhibition by the isomalathion stereoisomers should be identical to RBAChE inhibited by (*S*)- or (*R*)-isoparathion methyl (loss of *p*-nitrophenoxy; Scheme 11).

Inhibition of EEAChE by Isomalathion Stereoisomers

In order to identify any possible species-dependent variation in the stereoselectivity (Lee, 1978; Wallace, 1991) inhibition of EEAChE by the isomalathion stereoisomers also was investigated. Further, the X-ray structure of EEAChE was recently published (Sussman, 1991), which may permit more precise calculations of active site complementarity to be conducted.

The kinetic parameters (k_i, K_D, and k_p) for the inhibition of EEAChE by isomalathion stereoisomers were determined experimentally using Eqn. 2 (Section 1.8) (Figure 33, Table 11). The results of these experiments show that differences between the weakest ((*1R,3S*)-isomalathion **12b**) and strongest ((*1S,3R*)-isomalathion **12c**) inhibitor was only 13-fold compared to the 29-fold difference

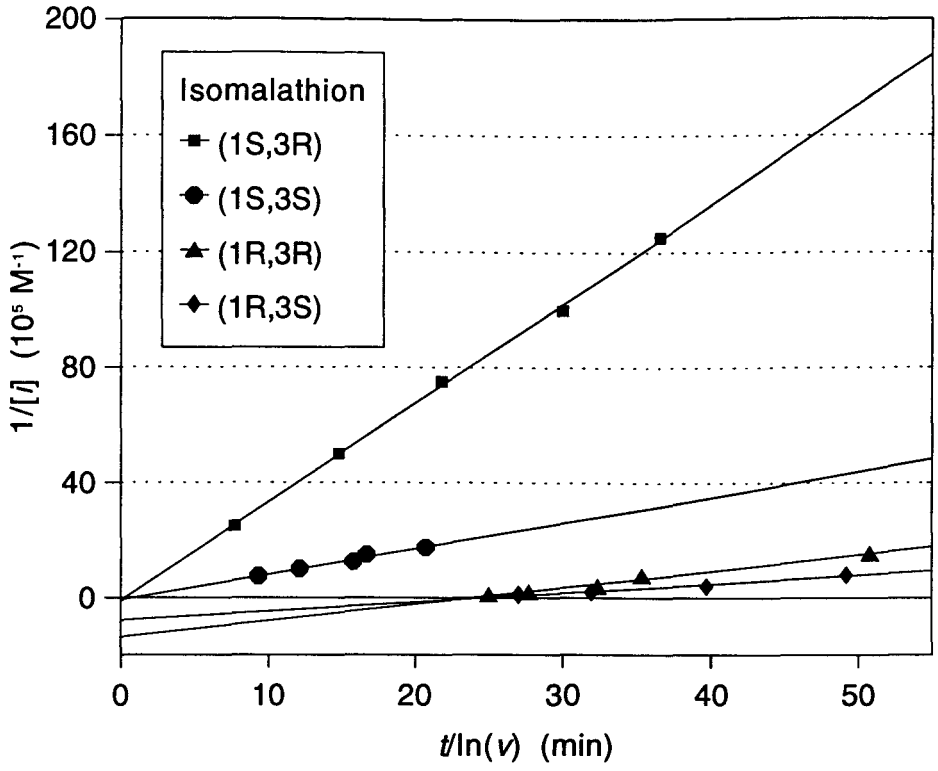

Figure 33. Inhibition of EEAChE by Isomalathion Stereoisomers.

found for RBAChE. That EEAChE discriminates less between the isomalathion stereoisomers was not unexpected since species-dependent, stereoselective inhibition against varying sources of AChE was observed for the enantiomers of fonofos oxon (Lee, 1978). For example, the fonofos oxon enantiomers are discriminated 5-fold better by mouse brain cholinesterase than EEAChE.

Isomalathion stereoisomers with the *R*-carbon configuration were stronger inhibitors of EEAChE than the isomalathion stereoisomers with the *S*

configuration, and the inhibitory strength due to the carbon configuration was again attenuated by the configuration at phosphorus but to a lesser degree than with RBAChE. For example, (*1S,3R*)-isomalathion **12c** was a 3.9-fold stronger inhibitor than (*1S,3S*)-isomalathion **12d** as compared to the 6.8-fold difference found against RBAChE. The difference in k_i between (*1R,3R*)- and (*1R,3S*)-isomalathion was only 2.3-fold compared to the 3.3-fold for RBAChE. The most striking result found for the inhibition of EEAChE was that

Table 11. Kinetic Data[a] for the Inhibition of EEAChE by Isomalathion Stereoisomers.

isomalathion	k_i $M^{-1}min^{-1}(x10^3)$	K_D $mM(x10^{-5})$	k_p min^{-1}
12a (*1R,3R*)	57 (0.04)	70	0.040
12b (*1R,3S*)	25 (0.09)	138	0.034
12c (*1S,3R*)	333 (0.07)	1330	4.590
12d (*1S,3S*)	85 (0.04)	3670	3.070

[a]coefficient of variation in parenthesis

the (*1S*)-isomalathion stereoisomers were stronger inhibitors than the (*1R*)-isomalathion stereoisomers; the inverse of the RBAChE inhibitor stereoselectivity. Thus, a species-dependent, stereoselective inhibition by isomalathion was observed for RBAChE and EEAChE not only in the extent that the enzymes

could discriminate between configurations, but also in the inhibitory strength of one configuration versus another.

Although (*1R*)-isomalathion stereoisomers had a significantly greater affinity (K_D) for the EEAChE active site by approximately 20-fold, the (*1S*)-isomalathion stereoisomers were more potent inhibitors. However, the difference in the affinity was compensated for and further dominated by the magnitude of k_p for (*1S,3R*)- and (*1S,3S*)-isomalathion, revealing another facet of the "interplay between *occupation* of the active center and *productivity* of that occupation (Berman and Leonard, 1989b)." Unlike the stereoisomers which differ only by their phosphorus configuration, those with the same phosphorus configuration show a correlation between the relative inhibitory potency (k_i) and the K_D. For example, the difference in k_i between (*1S,3R*)- and (*1S,3S*)-isomalathion was 3.9-fold while the difference in K_D was 2.8-fold. In addition, the difference in k_i between the (*1R,3R*)- and (*1R,3S*)-isomalathion was 2.3-fold while the difference in K_D was 2.0-fold.

As with RBAChE, the k_p values were identical for the *1R,3R* and *1R,3S* stereoisomers, consistent with a mechanism where the asymmetric carbon center contributes little to the phosphorylation step (Scheme 10, Path A). The EEAChE k_p values for (*1S,3R*)- and (*1S,3S*)-isomalathion differ by 1.5-fold. Since we observed that EEAChE shows less discrimination than RBAChE during inhibition by isomalathion stereoisomers, the 1.5-fold difference compared to the 4.7-fold

difference in k_p for RBAChE was not surprising. That the thiosuccinyl ligand stereochemistry is significant at all in the phosphorylation step suggests that a similar mechanistic switch to that proposed for RBAChE (Scheme 10, Path B) may also occur with EEAChE.

Reactivation of RBAChE Inhibited by Isomalathion Stereoisomers

If, indeed, the mechanisms of inhibition of RBAChE by isomalathion and isoparathion methyl are convergent as suggested in the conclusion of Section **4.4.**, then the reactivation profiles of RBAChE inhibited by these two compounds should be comparable. In an effort to clarify any mechanistic ambiguity and to distinguish the influence of stereochemistry upon the recovery processes, the rate constants of spontaneous and oxime-mediated reactivation (k_0 and k_{oxime}; Eqns. 4 and 5, Section 1.9 and 1.10) were determined.

RBAChE was inhibited by each isomalathion stereoisomer (and the 86:14 (*1S,3S/1R,3R* mixture), followed by a 40-fold dilution to halt further inhibition. The spontaneous reactivation rate constants, k_0 (Eqn. 4, Section **1.9.**) were calculated from the slope of the initial portion (0-30 min.) of the graphs plotted by *ln(100/%inhibition)* vs. *time* (Figure 34, Table 12).

Rate constants for oxime-mediated reactivation (k_{oxime}) were determined similarly. Following inhibition of RBAChE by each of the isomalathion stereoisomers and the 40-fold dilution, the enzyme was reacted with 2-pyridine

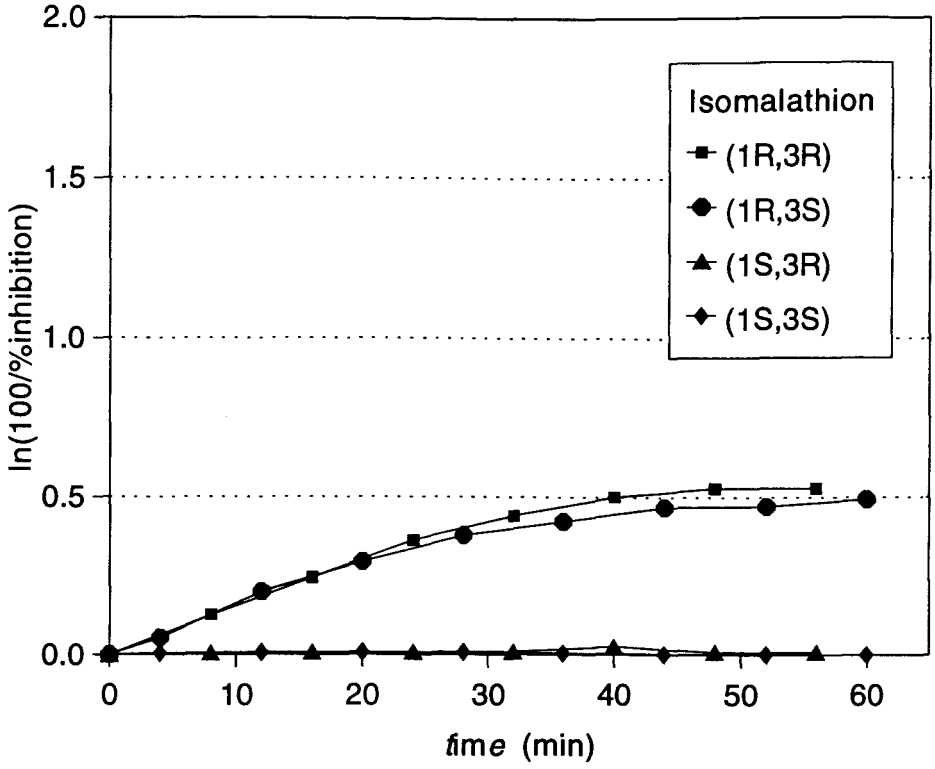

Figure 34. Spontaneous Reactivation of RBAChE Inhibited by Isomalathion Stereoisomers.

aldoxime methiodide (2-PAM). The oxime-mediated rate constants, k_{oxime} (Eqn. 5, Section **1.10.**) were calculated from the initial slope of the graphs plotted by *ln(100/%inhibition)* vs. *time* (Figure 35, Table 12).

By 60 minutes, the reactivation (spontaneous and oxime-mediated) reached a plateau and was assigned the total percent reactivation relative to uninhibited

Table 12. Reactivation Data[a] for RBAChE Inhibited by Isomalathion and Isoparathion Methyl Enantiomers.

isomer	k_0[b] $min^{-1}(x10^{-3})$	%spontaneous reactivation[c]	k_{oxime}[e] $min^{-1}(x10^{-3})$	%oxime reactivation[d]
isomalathion				
12a (*1R,3R*)	13.7 (0.03)	42 (0.13)	51.0 (0.05)	81 (0.09)
12b (*1R,3S*)	12.5 (0.03)	38 (0.05)	50.8 (0.05)	81 (0.10)
12c (*1S,3R*)	0	< 1	1.9 (0.04)	9 (0.14)
12d (*1S,3S*)	0	< 1	0	2 (0.01)
12d:12a (86:14)	8.6 (0.01)	29 (0.04)	39.3 (0.12)	66 (0.12)
isoparathion				
49a (*S*)	11.3 (0.10)[e]		50.2 (0.02)	
49 (*RS*)	10.2 (0.10)[e]			
49b (*R*)	3.5 (0.04)[e]		13.8 (0.17)	

[a]coefficient of variation in parentheses [b]correlation coefficient (c.c.) > 0.99 where applicable. [c]after 60 min. [d]c.c. > 0.99 except **12c** where c.c. = 0.49. [e] (Thompson, 1993).

enzyme (Table 12). In all instances, no additional enzyme activity returned after 120 min.

The k_{oxime} values for RBAChE inhibited by (*1R,3R*)- or (*1R,3S*)-isomalathion were 4-fold greater than the spontaneous reactivation (k_0) values. The total percent returned enzyme activity was twice that of the spontaneous

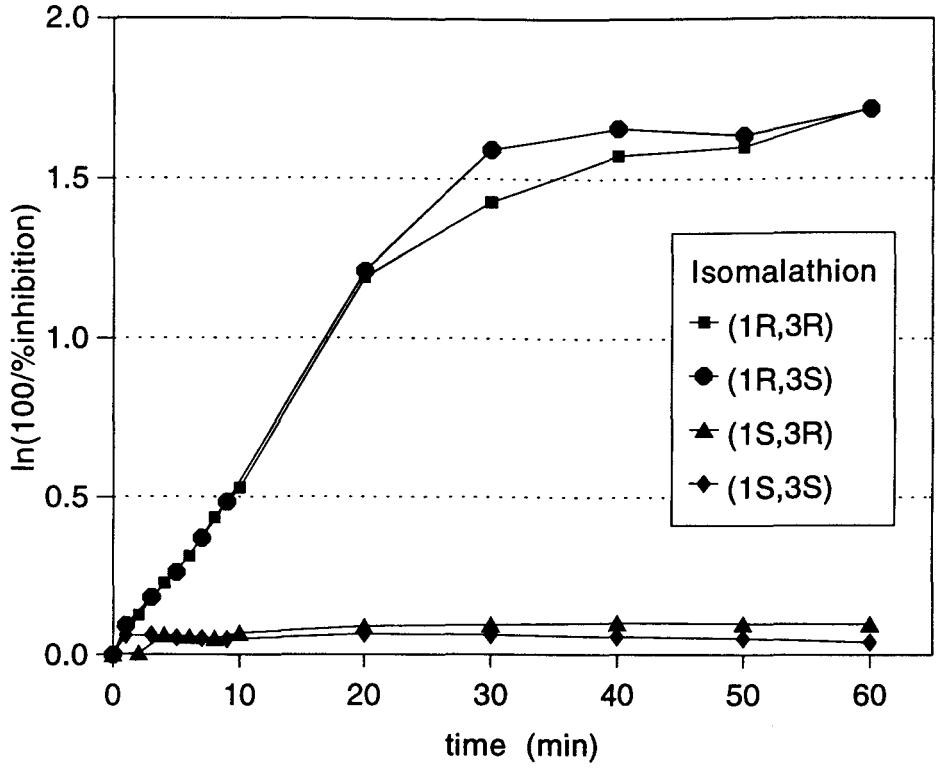

Figure 35. Oxime-Mediated Reactivation of RBAChE Inhibited by Isomalathion Stereoisomers.

process. Both the spontaneous (approximately 13 x 10^{-3} min^{-1}) and oxime-mediated reactivation (approximately 51 x 10^{-3} min^{-1}) rates for these two diastereomers were nearly identical suggesting that the resultant phosphorylated enzymes were chemically and stereochemically equivalent.

In contrast, RBAChE inhibited by (*1S,3R*)- or (*1S,3S*)-isomalathion were refractory to either spontaneous or oxime-mediated reactivation and showed only

a modest amount of total returned activity (<10%) following treatment with oxime. The minor rate of reactivation detected was probably due to background oxime based hydrolysis of acetylthiocholine (control shows 6% hydrolysis) or a 1-3% contamination by the enantiomer, which is a far superior inhibitor that can undergo reactivation.

The results of spontaneous and oxime-mediated reactivation from RBAChE by the 86:14 (**12d:12a**) enantiomer mixture strongly correlated with (*1R*)-isomalathion stereoisomer kinetics (Figure 33 and 34). From this mixture, the mole fraction of the inhibited species was calculated to be 18% inhibited by **12d** and 82% inhibited by **12a**. All reactivation observed for the mixture was attributed to RBAChE inhibited by **12a** since inhibition of RBAChE by **12d** was refractory to reactivation. The reactivation rate values were calculated from the corresponding mole fractions as 10.7 x 10^{-3}min^{-1} for k_0 and 41.6 x 10^{-3} min^{-1} for k_{oxime}, which are in excellent agreement with the observed values of 8.6 x 10^{-3} min^{-1} and 39.3 x 10^{-3} min^{-1}. Although **12a** composed only 14% of the doped mixture, it dominated the molar fraction of the inhibited enzyme owing to its greater inhibitory potency (k_i value). These results signify and augment the importance of stereoisomer purity in an evaluation of biological activity.

Some intriguing mechanistic implications can be surmised when the spontaneous and oxime-mediated reactivation rates are compared for RBAChE inhibited by isomalathion and isoparathion methyl stereoisomers (Thompson,

1993). The reactivation rates from (*1R,3R*)- and (*1R,3S*)-isomalathion (spontaneous, approximately 13 x 10^{-3} min^{-1}; oxime-mediated, approximately 51 x 10^{-3} min^{-1}), and (*S*)-isoparathion methyl (spontaneous, 11.3 x 10^{-3} min^{-1}; oxime-mediated, 50.2 x 10^{-3} min^{-1}) were comparable supporting a common mechanism of inhibition, namely, ejection of the thiosuccinyl or *p*-nitrophenoxy leaving groups, respectively, to give (*R*)-O,S-dimethyl phosphorothiolated RBAChE (Scheme 11). Although the process of phosphorylation described in Scheme 11 occurs with inversion, the phosphorus configuration remains *R* for the (*1R*)-isomalathion diastereomers.

Conversely, RBAChE inhibited by (*1S,3R*)- and (*1S,3S*)-isomalathion showed negligible reactivation compared to the slow but observable rates from (*R*)-isoparathion methyl **49b** inhibited RBAChE (spontaneous, 3.5 x 10^{-3}; oxime-mediated, 13.8 x 10^{-3} min^{-1}). One explanation for this anomaly is that inhibition of RBAChE by (*1S,3R*)- or (*1S,3S*)-isomalathion results in an inhibited enzyme that is different than the O,S-dimethylphosphorothiolated species, namely, the loss of the thiomethyl group (Scheme 10, Path B). Diminished attention was given to the possibility that the methoxide ligand was displaced during phosphorylation since the thiomethyl group was shown to be the preferred leaving group during AChE inhibition by methamidophos (Scheme 12; Thompson, 1982). It is noteworthy that this mechanistic switch is linked to the configuration at phosphorus. The hypothesis that the mechanisms of RBAChE inhibition differ

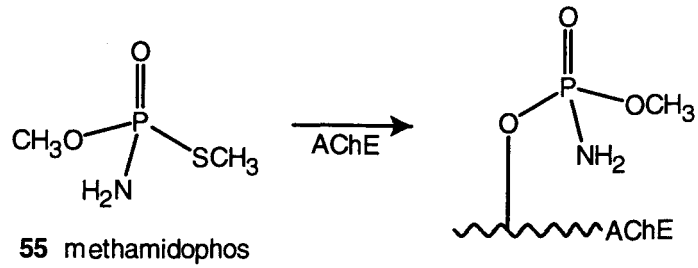

55 methamidophos

Scheme 12. Mechanism for the Inhibition of AChE by Methamidophos.

for (*1S,3R*)- and (*1S,3S*)-isomalathion from (*1R,3R*)- and (*1R,3S*)-isomalathion is unexpected since the displacement of the thiosuccinyl ligand has long been accepted as the conventional phosphorylation mechanism (Clothier, 1981). Following inhibition of RBAChE by (*1S,3R*)- or (*1S,3S*)-isomalathion, a chiral thiosuccinyl ligand was still attached to the enzyme and differences in reactivation rates (spontaneous or oxime mediated) due to the configuration of carbon were expected. Although rate differences have been observed for oxime mediated reactivation of AChE inhibited with a phosphoryl group bearing a second asymmetric center (soman) (DeJong, 1985a,b), essentially no reactivation following inhibition by either of the two (*1S*)-isomalathion diastereomers was observed, and an explanation of this phenomenon was warranted.

Several postinhibitory processes are possible following RBAChE inhibition by either of the two (*1S*)-isomalathion stereoisomers including: (a) displacement

of the thiosuccinyl ligand via a general base catalyzed mechanism (Scheme 13, Path A), (b) intramolecular phosphorylation by a second enzyme nucleophile (Scheme 13, Path B), (c) ß-elimination of diethyl fumarate or diethyl maleate (Scheme 13, Path C), or (d) reduced approach of incoming nucleophiles (H_2O, oxime) owing to steric crowding enforced by the thiosuccinyl ligand (not shown). If the succinyl thiolester-phosphorus bond is cleaved by the action of water or oxime, the remaining phosphoryl group would become charged and therefore unsuitable for reactivation by nucleophiles (Scheme 13, Path A). Diminished reactivation rates due to steric crowding has been documented in a study that

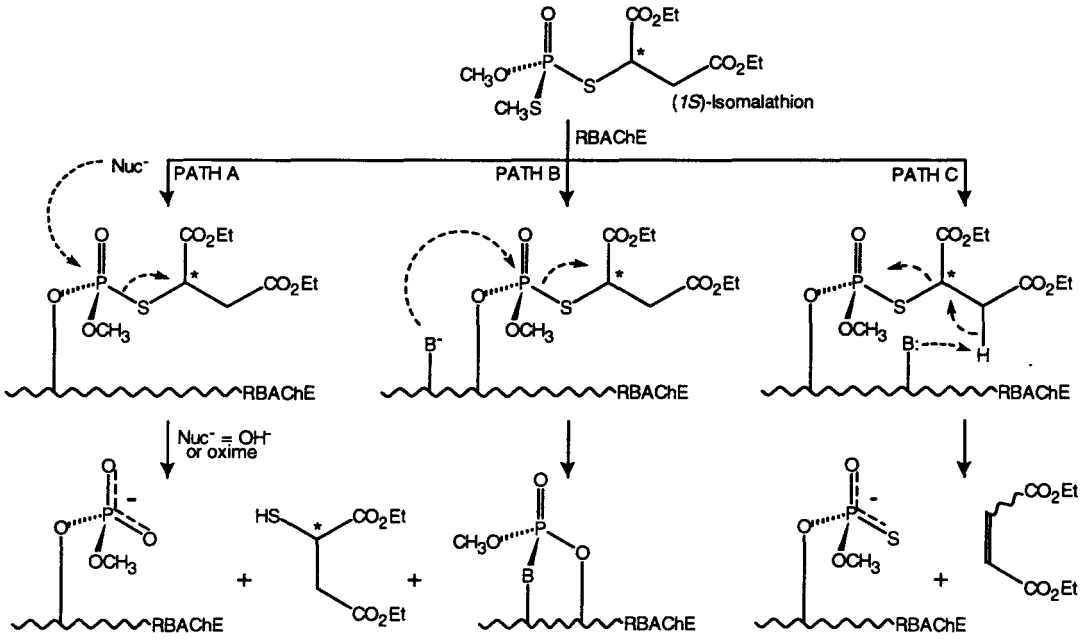

Scheme 13. Proposed Non-Reactivatable Pathway for (*1S*)-Isomalathion.

showed that the reactivation of dimethyl phosphorylated AChE was faster than diethyl phosphorylated, while diisopropyl phosphorylated AChE did not reactivate (Cassida, 1956). The ß-elimination (Scheme 13, Path C) process may occur via a general base type mechanism, which has its foundation in the methoxide-promoted ß-elimination of malathion (Bhagwat, 1974; Figure 16, Section **2.1.**). Moreover, the ejection of acrolein from hydroxylated cyclophosphamide follows a similar β-elimination mechanism (Connors, 1975).

Non-Reactivation of RBAChE Inhibited by Isoparathion Methyl Enantiomers: A Model Study

Although RBAChE inhibited by the (*1R*)-isomalathion diastereomers reactivated as expected, RBAChE inhibited by the (*1S*)-isomalathion diastereomers showed no reactivation. Thus, an examination of the significance of phosphorus (or carbon) stereochemistry upon the time dependent loss of the enzyme's ability to reactivate, i.e., non-reactivatability, is precluded by those results. If the mechanism of inhibition of RBAChE by all of the isomalathion stereoisomers occurred as initially expected (loss of the thiosuccinyl moiety, Scheme 11), then the influence of stereochemistry upon the non-reactivatability of O,S-dimethylphosphorothiolated RBAChE (provided only by the (*1R*)-diastereomers) could be examined. In an effort to obtain results for such an event, RBAChE inhibited by isoparathion methyl was examined since it would provide the putative

stereoisomers of O,S-dimethylphosphorothiolated RBAChE (Scheme 11). Furthermore, such a study would serve as a model for RBAChE inhibited by the S-methyl isomerides of other dimethyl phosphorothionate insecticides.

RBAChE was incubated with the individual stereoisomers of isoparathion methyl for 20 min to afford approximately 90% inhibition. The incubation mixtures were then diluted 40-fold to halt the inhibition and at time intervals following the dilution, 2 aliquots were withdrawn to: (1) determine the activity that returned via spontaneous reactivation and (2) to determine the total amount of activity that could be restored. The second determination was executed by reacting the aliquot with 2-PAM for 20 min. The rate constants for nonreactivatability (k_{NR}) were determined (Table 13) from slopes of graphs (Figure 36) plotted using the following equation:

$$2.3\ log[100(A_t\text{-}A_t')/(A_0\text{-}A_0')] = -k_{NR}t$$

where A_t-A_t' = (activity of the reactivated enzyme with oxime at time = t) - (activity of the inhibited enzyme without oxime at time = t) and A_0-A_0' = (activity of the reactivated enzyme with oxime at time = 0) - (activity of the inhibited enzyme without oxime at time = 0).

RBAChE inhibited by (*R*)-isoparathion methyl underwent a rate of non-reactivation approximately twice that of the (*S*)-stereoisomer confirming the

significance of phosphorus stereochemistry with regard to non-reactivation pathways. This result is not entirely surprising since RBAChE inhibited by (*R*)-isoparathion methyl reactivated approximately 3.5-fold slower than the antipode (Table 12) allowing for greater competition of non-reactivating processes. Noteworthy is the fact that RBAChE inhibited by racemic isoparathion methyl underwent non-reactivatability at a rate essentially identical to that of RBAChE

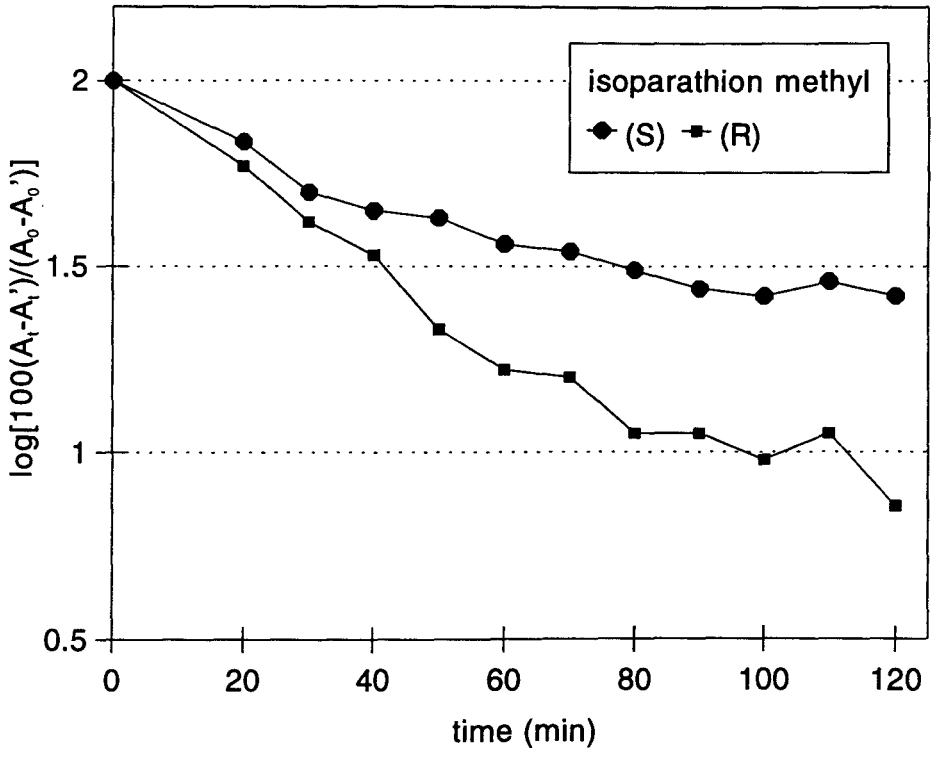

Figure 36. Non-reactivatability of RBAChE inhibited by Isoparathion Methyl Enantiomers.

inhibited by (*S*)-isoparathion. This result also was not surprising since the mole ratio of the enzyme inhibited by (*S*)-isoparathion methyl resulting from the incubation with the racemic mixture, was approximately 8-fold greater than that of enzyme inhibited by (*R*)-isoparathion methyl (Table 9). Thus, it was expected

Table 13. Non-Reactivatability of RBAChE Inhibited by Isoparathion Methyl Stereoisomers.

isoparathion methyl	k_{NR}[a] (min^{-1} x 10^{-1})
S	1.42 (0.09)
RS	1.37 (0.04)
R	3.07 (0.10)

[a]coefficient of variation in parenthesis.

that the (*S*)-stereoisomer would dominate the non-reactivatability profile of RBAChE inhibited by racemic isoparathion methyl because 8 times as much (*S*)-inhibited RBAChE was available for reactivation.

Conclusions

Malaoxon.

In conclusion, a significant stereoselective inhibition of AChE by the malaoxon enantiomers was uncovered whereby RBAChE showed greater

sensitivity to carbon asymmetry than bovine erythrocyte AChE did for O,O-diethyl malaoxon (Hassan, 1968). Furthermore, this sensitivity of RBAChE toward the carbon asymmetry of malaoxon was as great as that toward the phosphorus stereochemistry of isoparathion methyl (Ryu, 1991b).

Isomalathion.

An interdependence between both asymmetric centers (phosphorus and carbon) of the isomalathion stereoisomers was identified for the inhibition of RBAChE, and to a lesser extent, EEAChE. In addition, a species-dependent stereoselectivity was observed between RBAChE and EEAChE whereby the difference in inhibitory strength between the stereoisomers was greater for RBAChE than EEAChE. More importantly, the (*1S,3R*)- and (*1S,3S*)-isomalathion stereoisomers were weaker inhibitors of RBAChE but surprisingly stronger inhibitors of EEAChE resulting from an interdependence between stereoisomer affinity (K_D) for the EEAChE active site and the fecundity (k_p) of that affinity.

The reactivation profiles of RBAChE inhibited by the isomalathion stereoisomers along with the results from the inhibition experiments support a mechanistic switch for the inhibition of RBAChE from the expected thiosuccinyl displacement to loss of the thiomethyl ligand for (*1S,3R*)- and (*1S,3S*)-isomalathion and predicts the same for EEAChE based upon phosphorylation

constants (k_p). As a consequence, a non-reactivatable pathway is postulated for RBAChE inhibited by (*1S,3R*)- and (*1S,3S*)-isomalathion.

Although isomalathion could provide only one phosphorus configuration of O,S-dimethylphosphorothiolated RBAChE due to the mechanistic switch linked to the phosphorus stereochemistry, isoparathion methyl could furnish both configurations and thus provided a model for RBAChE inhibited by each configuration. Consequently, the results of the non-reactivation study indicated that phosphorus stereochemistry was significant (although less than for inhibition and reactivation) for post-inhibitory processes leading to non-reactivatable enzyme.

CHAPTER 5

SUMMARY

The individual stereoisomers of malathion, malaoxon, and isomalathion have been successfully prepared and as a result represent the first preparation of these stereoisomers. Two methods for the preparation of the isomalathion stereoisomers were developed, each offering distinct advantages.

Differential toxicities of the malathion enantiomers were identified for *Drosophila Melanogaster* showing (*R*)-malathion to be a 4-fold stronger insecticide. Detailed anti-AChE profiles (k_i, K_D, and k_p) for the malaoxon enantiomers were determined demonstrating that (*R*)-malaoxon was a 8-fold stronger inhibitor than its antipode. Inhibition constants (k_i, K_D, and k_p) for the isomalathion stereoisomers against RBAChE and EEAChE also were determined resulting in an apparent interdependence between both asymmetric centers (phosphorus and carbon) of the isomalathion stereoisomers for the inhibition of RBAChE, and to a lesser extent, EEAChE. Furthermore, a species-dependent stereoselectivity was observed between RBAChE and EEAChE.

The reactivation profiles (k_0 and k_p) of RBAChE inhibited by the

isomalathion stereoisomers were determined and support a mechanistic switch for the inhibition of RBAChE from the expected thiosuccinyl displacement to loss of the thiomethyl ligand for (*1S,3R*)- and (*1S,3S*)-isomalathion and predict the same for EEAChE based upon phosphorylation constants (k_p).

Results from a non-reactivation study using isoparathion methyl enantiomers to provide stereochemically opposed forms of O,S-dimethyl phosphorylated AChE, indicated that phosphorus stereochemistry was significant (although less than for inhibition and reactivation) for post-inhibitory processes leading to non-reactivatable enzyme.

CHAPTER 6

FUTURE WORK

Stereoselective Detoxication and Bioactivation of Malathion Stereoisomers

The preparation of the individual stereoisomers of malathion **6**, malaoxon **22**, and isomalathion **12** has allowed the viability of investigations concerning the role of the stereochemistry of these compounds upon the relevant metabolism and action of these compounds. For example, the stereoselectivity of malathion detoxication by mammalian carboxylesterases could be examined in an effort to identify differential *in vivo* lifetimes of the malathion enantiomers. In addition, the stereoselective activation of the malathion enantiomers to the corresponding malaoxon enantiomers by oxidizing enzymes should be examined.

Stereoselective Inhibition of Carboxylesterase by Malaoxon and Isomalathion Stereoisomers

The stereoselective inhibition of rat liver carboxylesterase by O,O-diethyl malaoxon enantiomers **27** had been previously examined (Hassan, 1968) where an 8.3-fold difference in inhibitory potency was observed for the antipodes. However, the stereoselective inhibition of the malaoxon enantiomers **22** has been

left undiscovered. Because the potentiation of malathion toxicity has been attributed to the isomalathion **12** content through inhibition of carboxylesterase, the stereoselective inhibition of this enzyme by isomalathion should be examined and the results compared to the corresponding anti-AChE potency of the individual stereoisomers. Such a study would provide a better understanding of the toxicological profiles of each stereoisomer and aid identification of the contributions of each isomalathion stereoisomer to the overall toxicity of a racemic mixture. Acquisition of malaoxon and isomalathion stereoisomers now allows such investigations to be completed.

Mechanistic Switch for (*1R*)- and (*1S*)-Isomalathion

In order to support the apparent mechanistic difference for the inhibition of RBAChE by the (*1R*)- and (*1S*)-isomalathion stereoisomers, compounds that would result in the same thiosuccinyl-linked phosphorodithiolated RBAChE such as **56b/56d** (Figure 37) could be reacted with RBAChE and the corresponding reactivation profiles determined and compared to those of RBAChE inhibited by (*1S*)-isomalathion diastereomers. The thionate analog **57** of **56** is also interesting as a potential insecticide possessing a carbethoxy portion susceptible to detoxication by carboxylesterases in addition to two potential leaving groups following bioactivation to **57**.

$^{14}CH_3S$-isomalathion stereoisomers **58** should be prepared and reacted with

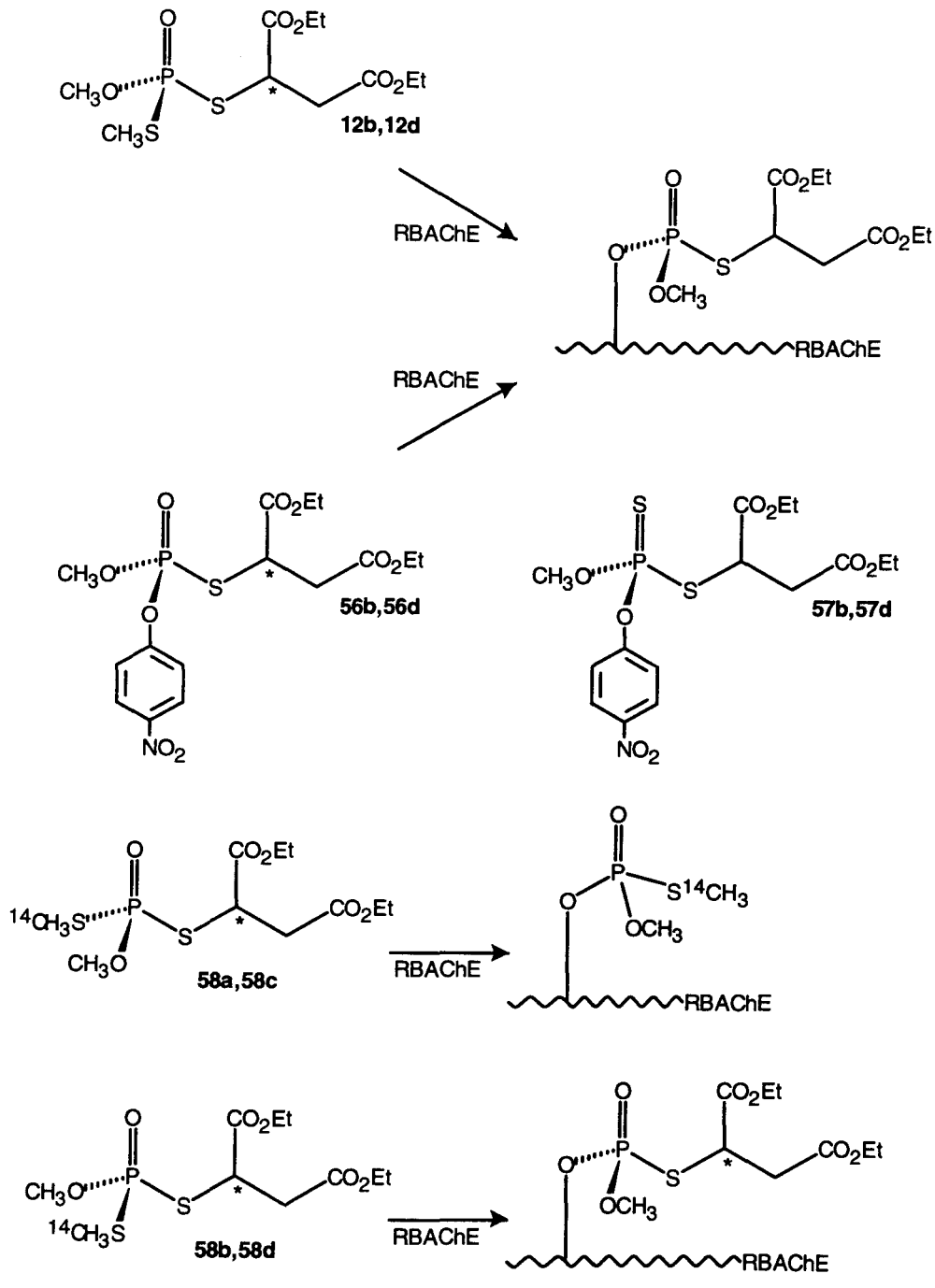

Figure 37. Mechanistic Probes for RBAChE Inhibition by Isomalathion.

RBAChE to examine the possible mechanistic switches proposed for the (*1R*)- and (*1S*)-stereoisomers. If a switch does indeed occur, then the label will remain on the enzyme for the (*1R*)-stereoisomers (**58ac**) while RBAChE inhibited by the (*1S*)-stereoisomers (**58bd**) would be devoid of the label if the S-methyl ligand was displaced.

ß-Elimination of RBAChE Inhibited by (*1S*)-Isomalathion

To further examine the ß-elimination proposed for RBAChE inhibited by the (*1S*)-isomalathion stereoisomers, inhibitors with structures prone to this elimination (Figure 38; **59**, **60**, **61**) should be devised and examined for similar reactivation profiles. Analogues that may be less prone to this type of elimination (**62**, **63**, **64**) should also be considered in an effort to examine the possibility of steric hinderance as a cause for the recalcitrant behavior toward reactivation of RBAChE inhibited by (*1S*)-isomalathion stereoisomers. In parallel chemical studies, elimination should be examined in the presence of base and compared to those rates observed for the decomposition of malathion and malaoxon (Bhagwat, 1974).

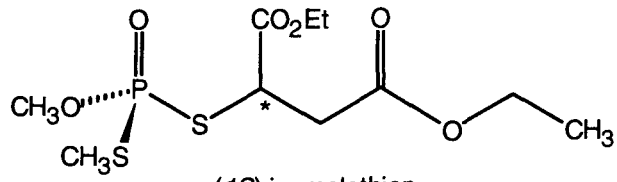

(*1S*)-isomalathion

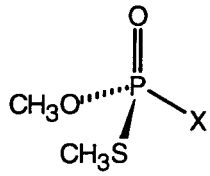

59 X=

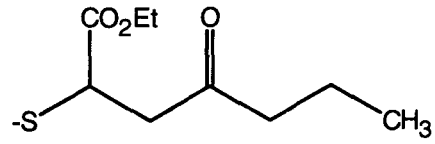

60 X=

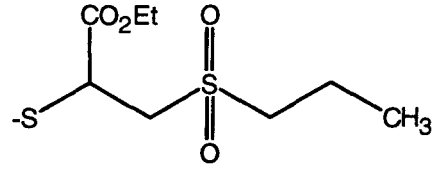

61 X=

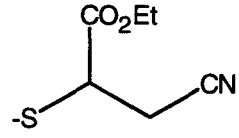

62 X=

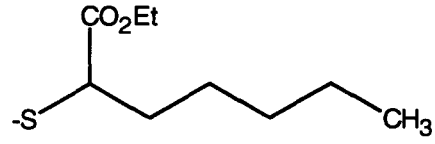

63 X=

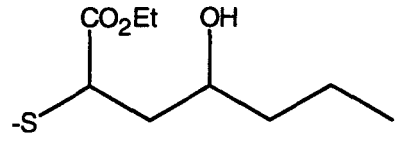

64 X=

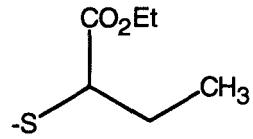

Figure 38. Possible (*1S*)-Isomalathion Analogues.

Stereoselective Inhibition and Reactivation of Other AChE's with the Isomalathion Stereoisomers

To determine possible species-dependent stereoselective inhibition of AChE by the isomalathion stereoisomers, other sources of AChE should be examined. As indicated in Section 4.5, a significant alteration of the inhibitory profile of the isomalathion stereoisomers for EEAChE compared to RBAChE has been identified. Furthermore, an examination of the reactivation profiles of EEAChE (as well as other AChE sources) inhibited by the isomalathion stereoisomers may reveal novel species-dependent reactivation or species-dependent mechanisms of isomalathion-mediated inhibition (i.e., loss of the thiosuccinyl or thiomethyl ligand).

Molecular Docking Studies

With the recent availability of the X-ray structure of EEAChE (Sussman, 1991; Maelicke, 1991), differences observed for the dissociation constants (K_D) of the isomalathion stereoisomers may be correlated with structural data of the EEAChE active site by using molecular docking studies.

Enantioenriched O,S-Dimethyl Phosphorothiolating Reagent

The resolved strychnine-dithioate salts prepared for use in the procurement of the isomalathion stereoisomers have been invaluable. Specifically, the O,S-

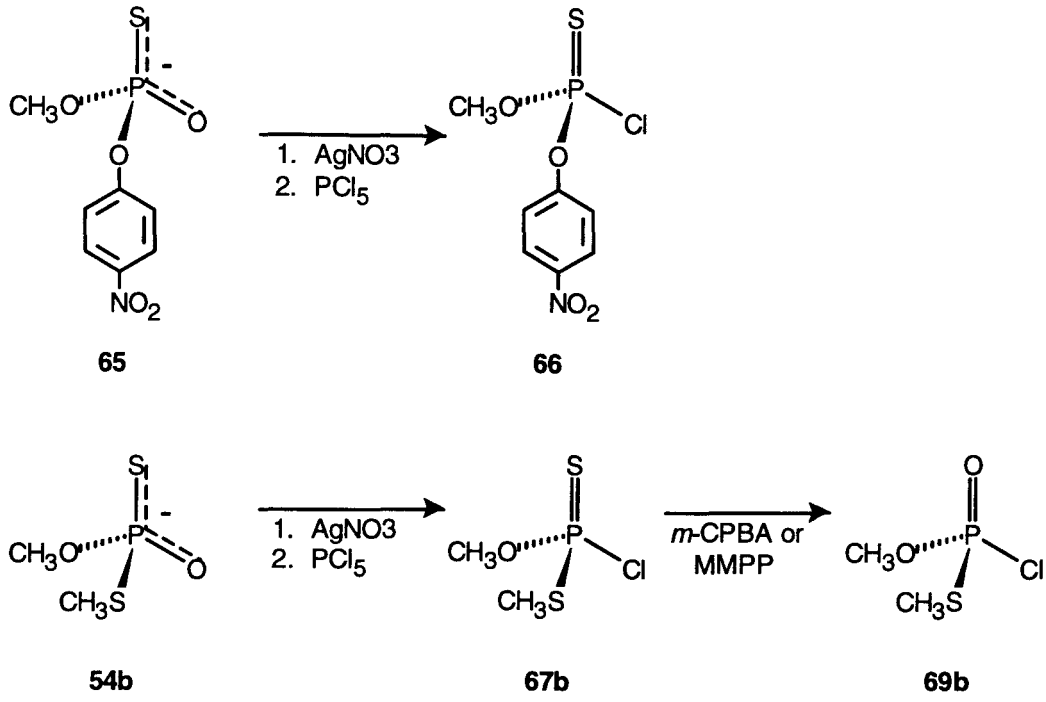

Scheme 14. Chiral Phosphorylating Agents.

dimethyl phosphorodithioate salts proved to be a convenient means to synthetically introduce the chiral O,S-dimethyl phosphorodithiolate moiety. To make this method more accessible, less toxic resolving agents may be considered such as phenethylamine, ephedrine or quinine. Furthermore, conversion of these salts to the asymmetric thiophosphoryl chloride (Scheme 14; **67**) in an analogous fashion to which the methyl *p*-nitrophenyl phosphorochloridothionate enantiomers (**66**) were prepared (Hirashima, 1983) may provide useful for introducing the enantioenriched O,S-dimethyl thiolthionophosphoryl moieties onto a nucleophilic

center. Stereoselective oxidative desulfuration of **67b** to **68b** with MMPP or m-CPBA may provide a more reactive analogue for introducing the O,S-dimethyl thiolophosphoryl moiety onto a nucleophilic center.

CHAPTER 7

EXPERIMENTAL

General

Commercially available reagents were purchased from Aldrich Chemical Co., Milwaukee, WI. All solvents and reagents were purified when necessary by standard literature methods. Melting points were determined on a Fisher-Johns melting point apparatus. Analytical thin-layer chromatography (TLC) was conducted on E. Merck aluminum-backed, 0.2 mm silica gel 60 F_{254}, TLC plates. Flash chromatography was performed with Kieselgel 60, 230-400 mesh (Merck). Elemental analyses were performed by Midwest Microlab Ltd., Indianapolis, IN.

Proton (^{1}H), carbon (^{13}C), and phosphorus (^{31}P) NMR spectra were recorded on a Varian VXR 300-NMR instrument in deuterated chloroform ($CDCl_3$) unless specified otherwise. Pertinent proton frequencies are tabulated in the following order: chemical shift (δ in ppm), multiplicity (s, singlet; d, doublet; t, triplet; q, quartet; m, multiplet), coupling constant (J in hertz), and the number of hydrogens. Proton and carbon frequencies of spectra obtained are relative to

chloroform (^{1}H, 7.24 ppm; ^{13}C, 77.0 ppm) as an internal standard unless specified otherwise. Phosphorus chemical shifts are relative to phosphoric acid (H_3PO_4) in $CDCl_3$ as an external standard.

High-performance liquid chromatography (HPLC) was performed using an ABI (Analytical Kratos Division, Ramsey, NJ) series 400 Spectroflow pump and a Spectroflow 783 programmable absorbance variable wavelength detector equipped with a flow cell of 8.0 nm in path length and 12 μL in dead volume. All results from the UV visible detector (215 nm, sensitivity range 0.1 AUFS) were recorded by a Hewlett Packard 3396A integrator (Avondale, PA). Injections were made by a Rheodyne 7125 injector (Bodman Chemical, Aston, PA) fitted with a 20 μL sample loop. Separation and purity detection were performed on a 25 cm x 4.6 mm i.d. Chiralpak AD (Regis Chemical Company, Morton Grove, IL) analytical column. Isopropyl alcohol and hexane used (mobile phase) were analytical grade and were purchased from Bodman Chemical, Aston, PA (EM Science). The mobile phase was degassed prior to use by sonication with a Bransonic Model 32 (A. Daigger Scientific, Wheeling, IL). Elution was isocratic.

Synthesis

(*S*)-Diethyl malate (36a) was prepared as described previously (Cohen, 1966) from (*S*)-malic acid. $[\alpha]_D^{24} = -5.45^0$ (c = 1.21, $CHCl_3$). ^{1}H NMR δ 1.27 (t, J = 7.2, 3H), 1.31 (t, *J* = 7.2, 3H), 2.75-2.90 (m, 2H), 4.18 (q, *J* = 7.1, 2H),

4.28 (q, J = 7.2, 2H), 4.49 (t, J = 5.3, 1H). ^{13}C NMR δ 14.02, 38.66, 60.89, 61.91, 67.23, 170.44, 173.30.

(*R*)-Diethyl malate (36b) was prepared as described previously (Cohen, 1966) from (*R*)-malic acid. $[\alpha]_D^{24} = +5.23^0$ (c = 1.05, $CHCl_3$). The NMR spectra data of this material were identical to that of **36a**.

(*S*)-O-(*p*-Toluenesulfonyl)-diethyl malate (37a) was prepared (2.96 g, 82%) as described generally in a previous report (Kabalka, 1986) starting with (*S*)-diethyl malate (2.00 g, 10.5 mmol). $[\alpha]_D^{22} = -43.4^0$ (c = 0.615, $CHCl_3$). ^1H NMR δ 1.17 (t, J = 7.1, 6H), 2.41 (s, 3H), 2.86 (d, J = 5.9, 2H), 4.05 (dq, J = 2.9, 7.1, 2H), 4.11 (q, J = 7.3, 2H), 5.19 (t, J = 5.9, 1H), 7.31 (d, J = 8.6, 2H), 7.78 (d, J = 8.4, 2H). ^{13}C NMR δ 13.9, 14.0, 21.7, 37.3, 61.2, 62.1, 73.7, 128.0, 129.6, 133.2, 144.9, 167.3, 168.0.

(*S*)-O-(Methanesulfonyl)-diethyl malate (38a). To a stirring solution of (*S*)-diethyl malate (0.200 g, 1.05 mmol) in CH_2Cl_2 (2 mL, 0^0C) under an $Ar_{(g)}$ atmosphere was added methanesulfonyl chloride (0.12 mL, 1.57 mmol) followed by the addition of TEA (0.15 mL, 1.05 mmol). After 15 min, the reaction was complete as indicated by TLC and the mixture was partitioned between 20 mL 10% HCl and 20 mL ethyl ether. The aqueous layer was extracted with 20 mL ethyl ether and the organic layers were combined, washed with 20 mL brine, dried over sodium sulfate and rotary evaporated to give a colorless oil (0.257 g, 81%. $[\alpha]_D^{22} = -23.9^0$ (c = 0.640, $CHCl_3$). ^1H NMR δ 1.24 (t, J = 7.2, 3H), 1.28

(t, J = 7.1, 3H), 2.92-2.94 (m, 2H), 3.14 (s, 3H), 4.16 (q, J = 7.1, 2H), 4.25 (dq, J = 1.9, 7.1, 2H), 5.33 (dd, J = 5.1, 6.9, 1H). ^{13}C NMR δ 14.0, 14.1, 37.0, 39.0, 61.4, 62.4, 73.9, 167.7, 168.4.

(*S*)-O-(Trifluoromethanesulfonyl)-diethyl malate (39a). Trifluoromethanesufonic anhydride (2.00 mL, 11.9 mmol) was dissolved in 10 mL CH_2Cl_2 under an $Ar_{(g)}$ and chilled to -78 ^{0}C. (*S*)-Diethylmalate (2.00 g, 10.6 mmol) was dissolved in 10 mL CH_2Cl_2 to which 2,6-lutidine (1.24 mL, 10.6 mmol) was added. This mixture was added dropwise to the anhydride over 15 min. After the addition was complete, the reaction mixture was brought to 0 ^{0}C for 1 h and then allowed to warm slowly to room temperature until TLC indicated the consumption of (*S*)-diethylmalate (2 h). The reaction mixture was concentrated to an oil followed by addition of ethyl ether to precipitate the lutidinium salt that was filtered in vacuo and washed 3 times with 50 mL ethyl ether. The filtrate was rotary concentrated to an oil (3.47 g, 100% crude yield) and used immediately in the conversion to (*R*)-malathion. $[\alpha]_D^{25}$ = +32.6^0 (c = 1.39, $CHCl_3$). ^{1}H NMRδ 1.29 (t, J = 7.2, 3H), 1.34 (t, J = 7.2, 3H), 3.06 (d, J = 5.7, 2H), 4.22 (dq, J = 2.1, 7.2, 2H), 4.33 (dq, J = 2.1, 7.2, 2H), 5.49 (t, J = 6.0, 1H). ^{13}C NMR δ 13.79, 13.92, 36.81, 61.82, 63.17, 78.80, 112.45, 116.23, 120.47, 124.70, 166.03, 167.52.

(*R*)-O-(Trifluoromethanesulfonyl)-diethyl malate (39b) was prepared as indicated above for (*S*)-O-(trifluoromethanesulfonyl)-diethylmalate starting with

(*R*)-diethylmalate. $[\alpha]_D^{25}$ = -30.1^0 (c = 1.71, $CHCl_3$). The NMR spectral data were identical to that of **39a**.

Sodium O,O-dimethylphosphorodithioate (34) was prepared from neutralizing O,O-dimethylphosphorodithioic acid with sodium carbonate in methanol. Following filtration and concentration of the solvent, crystallization was induced with ethyl ether. O,O-dimethylphosphorodithioic acid was prepared as described previously (Kabachnik, 1953; Toia, 1980). ^{1}H NMR δ 3.43 (d, *J* = 14.4). ^{13}C NMR δ 52.76, 52.85. ^{31}P NMR δ 117.6.

(*R*)-Malathion (6a). Crude (*S*)-O-(trifluoromethanesulfonyl)-diethylmalate (3.47 g) was dissolved in 20 mL THF and chilled to 0 ^{0}C under $Ar_{(g)}$ atmosphere. Sodium O,O-dimethylphosphorodithioate (2.86 g, 15.9 mmol) was dissolved in 10 mL THF and added dropwise to the triflate solution over 15 min. The reaction mixture was allowed to warm slowly to room temperature until TLC indicated the consumption of starting material (2 h). The reaction mixture was partitioned between 50 mL ethyl ether and 50 mL water. The aqueous layer was extracted with 50 mL ether, the organic layers combined, extracted with brine, dried over sodium sulfate, and rotary evaporated. Purification via flash chromatography gave a colorless oil (2.79 g, 80% yield). Rf = 0.20 (petroleum ether, ethyl ether, 1:1). $[\alpha]^{24}_D$ = +79.7^0 (c = 1.25, $CHCl_3$). ^{1}H NMR δ 1.22 (t, *J* = 7.2, 3H), 1.25 (t, *J* = 7.2, 3H), 2.84 (dd, *J* = 5.4, 17.1, 1H), 3.00 (dd, *J* = 9.0, 17.1, 1H), 3.77 (dd, *J* = 3.0, 15.3, 6H), 4.03-4.22 (m, 5H). ^{13}C NMR: δ 13.9, 14.0, 37.7, 37.8, 44.98,

45.03, 54.21, 54.27, 61.08, 62.04, 169.90, 169.99. ^{31}P NMR: δ 96.15.

(*S*)-Malathion 6b was prepared as previously described for (*R*)-malathion starting with (*R*)-O-(trifluoromethanesulfonyl)-diethylmalate. $[\alpha]^{27}_D$ = -80.0^0 (c = 1.25, $CHCl_3$). The NMR spectra data of this material was identical to that of **6a**.

(*RS*)-Malathion (6) was prepared as described previously from diethyl maleate (Mallipudi, 1980).

(*R*)-Malaoxon (22a). Method A. (*R*)-Malathion (0.200 g, 0.606 mmol) was dissolved in 3 mL CH_2Cl_2 and added to a stirring suspension of technical grade (80%) monoperoxyphthalic acid magnesium salt (MMPP, 0.187 g, 0.606 mmol) in 2 mL CH_2Cl_2. The mixture was brought to reflux for 24 h afterwhich it was concentrated and partitioned between 20 mL ethyl ether and 20 mL saturated aqueous sodium bicarbonate. The aqueous layer was extracted with 20 mL ether, the organic layers combined, extracted with brine, dried over sodium sulfate, and concentrated to an oil. Purification via flash chromatography gave a colorless oil (0.098 g, 52% yield). R_f = 0.13 (petroleum ether, ethyl ether, 1:2 volume ratio). **Method B.** (*R*)-Malathion was converted to (*R*)-malaoxon (25% yield) as described for racemic material (Bellet, 1974). $[\alpha]^{25}_D$ = +46.7^0 (c = 0.555, $CHCl_3$). ^1H NMR: δ 1.23 (t, *J* = 7.0, 3H), 1.27 (t, *J* = 7.0, 3H), 2.90 (dd, *J* = 5.4, 17.1, 1H), 3.06 (dd, *J* = 8.7, 17.1, 1H), 3.81 (dd, *J* = 4.8, 12.9, 6H), 4.08-4.24 (m, 5H). ^{13}C NMR: δ 13.91, 14.03, 38.11, 38.18, 42.38, 42.43, 54.07,

54.14, 54.22, 61.06, 62.09, 169.84, 170.00, 170.08. ^{31}P NMR: δ 28.3.

(*S*)-Malaoxon (22b) was prepared as indicated for (*R*)-malaoxon starting with (*S*)-malathion. $[\alpha]^{27}_{D}$ = -43.5^0 (c = 0.75, $CHCl_3$).

(*RS*)-Malaoxon (22) was prepared as indicated for (*R*)-malaoxon starting with (*RS*)-malathion.

(*1RS,3R*)-Isomalathion (12ac) was prepared from (*R*)-malathion via the dealkylation-realkylation sequence previously reported (Thompson, 1989). $[\alpha]^{27}_{D}$ = +41.3^0 (c = 1.25, $CHCl_3$).

(*1RS,3S*)-Isomalathion (12bd) was prepared from (*S*)-malathion via the dealkylation-realkylation sequence as previously reported (Thompson, 1989). $[\alpha]^{27}_{D}$ = -40.0^0 (c = 0.75, $CHCl_3$).

(*1RS,3RS*)-Isomalathion (12) was prepared from (*RS*)-malathion via the dealkylation-realkylation sequence as previously reported (Thompson, 1989).

($^{13}CH_3S$)-(*1RS,3RS*)-Isomalathion (12') was prepared from (*RS*)-malathion via the dealkylation-realkylation sequence as previously reported (Thompson, 1989) by substituting $(^{13}CH_3O)_2SO_2$ for $(CH_3O)_2SO_2$.

S-Methyl phosphorodichloridate (47). Thiophosphoryl chloride (21.12 g, 0.125 mol) was dissolved in 75 mL benzene (0 ^{0}C) followed by the addition of CaO (14 g), acridine (90 mg), and methanol (7.5 mL). The reaction mixture was allowed to warm slowly to room temperature, and after 3.5 h, the mixture was filtered and the product (0-methylthiophosphoryl chloride) was distilled (20

mm Hg, 45 ^{0}C). The distillate was isomerized by heating the O-methylthiophosphoryl chloride at 100 ^{0}C for 20 h as described previously (Hilgetag, 1969) after which the product, S-methyl phosphorodichloridate, was distilled *in vacuo* at 60 ^{0}C. ^{1}H NMR: δ 2.64 (d, J = 23.1).

N-(Ethyl prolinyl) S-methyl chlorophosphoramidothiolate (50). S-Methylphosphorochloridate (0.98 g, 5.94 mmol) was dissolved in 7.5 mL benzene and a solution of ethylprolinate (0.85 g, 5.94 mmol) and TEA (0.82 mL, 5.94 mmol) was added dropwise over 15 min. The reaction was stopped after 1 h. Following separation and purification by flash chromatography, colorless oils were obtained for the two diastereomers. R_f = 0.42, 0.30 (ethyl ether).

Fast Band. $[\alpha]_D^{24}$ = -52.6^0 (c = 1.04, $CHCl_3$). ^{1}H NMR: δ 1.28 (t, J = 7.1, 3H), 1.95-2.30 (m, 4H), 2.50 (d, J = 18.2, 3H), 3.38-3.46 (m, 2H), 4.19 (q, J = 7.1, 2H), 4.48 (dt, J = 3.6, 8.1, 1H). ^{31}P NMR: δ 37.71.

Slow Band. $[\alpha]_D^{24}$ = -48.2^0 (c = 1.15, $CHCl_3$). ^{1}H NMR: 1.30 (t, J = 7.2, 3H), 1.98-2.29 (m, 2H), 2.40 (d, J = 18.0, 3H), 3.51 (q, J = 6.6, 2H), 4.21 (dq, J = 1.8, 7.2, 2H), 4.35 (dt, J = 3.3, 8.5, 1H). ^{31}P NMR: δ 38.05.

(*S*)-Diethylmercaptosuccinate (51a). (*R*)-Diethyl bromosuccinate (0.5 g, 1.98 mmol), prepared as described previously (Hassan, 1968) was dissolved in 2.0 mL acetone (0 ^{0}C). Sodium hydrosulfide (0.142 g, 2.5 mmol) was dissolved in 1 mL water and diluted to 2 mL with acetone. The sodium hydrosulfide solution was added to the diethyl bromosuccinate solution, and after 2 h, the acetone was

removed by rotary evaporation and the product was extracted from the water with ethyl ether and further purified by distillation (1mm Hg, 55 ^{0}C) using a Kugelrhor apparatus to give a colorless oil (0.18 g, 44%). $[\alpha]_D^{26}$ = -19.1^0 (c = 1.6, $CHCl_3$). ^{1}H NMR: δ 1.22 (t, J = 7.1, 3H), 1.26 (t, J = 7.1, 3H), 2.16 (d, J = 9.4, 1H), 2.71 (dd, J = 6.0, 16.9, 1H), 2.96 (dd, J = 9.0, 16.9, 1H), 3.70 (dt, J = 6.0, 9.3, 1H), 4.12 (q, J = 7.1, 2H), 4.18 (q, J = 7.1, 2H). ^{13}C NMR: δ 14.08, 14.21, 36.33, 36.96, 61.02, 61.77, 170.14, 172.13.

(*RS*)-Diethyl mercaptosuccinate (51) was prepared as described for diethyl malate starting with mercaptosuccinic acid (Ailman, 1965). This material was purified as described above for (*R*)-diethyl mercaptosuccinate.

S-(1,2-Dicarbethoxy)ethyl S-methyl N-(ethyl prolinyl) phosphoramidodithiolate (52). The fast band of **50** (0.10 g, 3.68 mmol) was dissolved in 0.5 mL THF (freshly distilled) followed by the addition of diethylmercaptosuccinate (0.083 g, 4.05 mmol) and TEA (0.056 g, 4.05 mmol) and allowed to stir under an $Ar_{(g)}$ atmosphere for 20 h. The reaction mixture was filtered and purified via flash chromatography to give a colorless oil (0.056 g, 34.5%). Rf = 0.27 (ethyl ether). $[\alpha]_D^{24}$ = -48.0^0 (c = 1.24, $CHCl_3$). ^{1}H NMR: δ 1.22-1.32 (m, 9H), 1.94-2.23 (m, 4H), 2.37 (dd, J = 1.2, 15.3, 3H), 3.09-3.15 (m, 2H), 3.43-3.51 (m, 2H), 4.10-4.46 (m, 8H). ^{31}P NMR: δ 47.52, 48.12.

Strychnine-(*3R*)-isomalathion salt (53a, 53c). (*R*)-Malathion (2.0 g, 6.06 mmol) was dissolved in 30 mL methanol, strychnine (2.23 g, 6.66 mmol) was

added, and the mixture brought to reflux for 16 h. The solvent was evaporated and the waxy solid was taken up in 25 mL chloroform. Ethyl acetate (480 mL) was added followed by 70 mL ether. The solution was heated to effect solution and stored at 0 ^{0}C. After 4 days, the first crop of crystals was filtered and washed with 75 mL ethyl ether. Ethyl ether (125 mL) was added to the filtrate, which was permitted to stand at room temperature for 2 days, after which the flocculent second crop of crystals was filtered and washed with 50 mL ethyl ether. By ^{31}P NMR, the first crop (**53c**, *1S,3R*) showed 72% diastereomeric enrichment. The second crop (**53a**, *1R,3R*) showed 100% diastereomeric enrichment. The first crop was recrystallized by dissolving 1.65 g in 99 mL methanol to which 594 mL ethyl ether was added. ^{31}P NMR of the resulting crystals showed 93% enrichment. Final recrystallization of these crystals (S_PR_C) to 100% enrichment was achieved by dissolving 1.37 g in 80 mL methanol followed by the addition of 320 mL ethyl ether. Data for **53a**: mp = 159-160^{0}C. $[\alpha]_D^{24}$ = +32.2^0 (c = 0.25,$CHCl_3$). ^{1}H NMR: δ 1.18 (t, *J* = 7.1, 3H), 1.19 (t, *J* = 7.1, 3H), 1.38 (dt, *J* = 2.9, 10.5, 1H), 1.67 (d, *J* = 15.4, 1H), 2.17 (dd, *J* = 5.1, 13.3, 1H), 2.33 (dt, *J* = 6.8, 13.9, 1H), 2.68 (dd, *J* = 2.8, 17.7, 1H), 2.95-3.18 (m, 4H), 3.35 (s, 1H), 3.62 (d, *J* = 15.0, 3H), 3.84 (s, 4H), 4.00-4.17 (m, 8H), 4.21-4.35 (m, 2H), 4.43 (d, *J* = 13.1, 3H), 6.59 (s, 1H), 7.15 (t, *J* = 7.5, 1H), 7.31 (t, *J* = 7.8, 1H), 7.50 (d, *J* = 7.1, 1H), 8.07 (d, *J* = 8.0, 1H). ^{13}C NMR: δ 14.20, 14.24, 25.29, 29.75, 38.53, 39.70, 42.10, 44.43, 44.47, 47.11, 53.20, 53.39, 53.48,

55.82, 58.82, 60.65, 61.25, 61.16, 64.24, 64.32, 75.09, 116.52, 122.59, 124.82, 127.76, 130.16, 132.77, 136.67, 141.67, 166.65, 171.03, 171.42, 171.50. ^{31}P NMR: δ 67.20. Anal. Calcd for $C_{31}H_{41}N_2O_8PS_2$: C, 56.01; H, 6.22; N, 4.21. Found: C, 56.26; H, 6.23; N, 4.32. Data for **53c**: mp = 181-182^{0}C. $[\alpha]_D^{22}$ = +16.1^0 (c = 0.31, $CHCl_3$). ^{1}H NMR: δ 1.18 (t, *J* = 7.2, 3H), 1.20 (t, *J* = 7.1, 3H), 1.38 (dt, *J* = 2.8, 10.5, 1H), 1.69 (d, *J* = 16.1, 1H), 2.17 (dd, *J* = 4.6, 14.2, 1H), 2.33 (dt, *J* = 7.3, 13.6, 1H), 2.68 (dd, *J* = 2.8, 17.7, 1H), 2.95-3.18 (m, 4H), 3.34 (s, 1H), 3.62 (d, *J* = 14.9, 3H), 3.83 (s, 4H), 4.00-4.20 (m, 8H), 4.21-4.49 (m, 5H), 6.57 (s, 1H), 7.15 (t, *J* = 7.7, 1H), 7.32 (t, *J* = 7.4, 1H), 7.50 (d, *J* = 7.1, 1H), 8.08 (d, *J* = 8.0, 1H). ^{13}C NMR: δ 14.19, 14.24, 25.30, 29.76, 38.62, 38.65, 39.68, 42.11, 44.40, 44.44, 47.08, 53.22, 53.41, 53.50, 55.87, 55.91, 58.81, 60.66, 61.27, 61.84, 61.88, 64.23, 64.38, 64.42, 75.13, 116.56, 122.54, 124.87, 127.68, 130.22, 132.73, 136.74, 141.68, 168.63, 171.08, 171.66. ^{31}P NMR: δ 68.10.

Strychnine-(*3S*)-isomalathion salt (53b, 53d). (*S*)-Malathion (2.0, 6.06 mmol) was dissolved in 30 mL methanol, strychnine (2.23 g, 6.66 mmol) was added, and the mixture refluxed for 16 h. The solvent was evaporated and the waxy solid was taken up in a minimum of methanol followed by addition of 300 mL ethyl acetate and 100 mL ethyl ether. The solution was heated to reflux and allowed to cool to r.t. The first crop of crystals was filtered and washed with 120 mL ethyl ether. The filtrate was allowed to stand at room temperature and the second crop of crystals were filtered and washed with ethyl ether. By ^{31}P NMR,

the first crop (**53b**, *1R,3S*) showed 71% diastereomeric enrichment. The second crop (**53d.**, *1S,3S*) showed 100% diastereomeric enrichment. The first crop was recrystallized by dissolving 1.032 g in 62 mL methanol to which 372 mL ethyl ether was added. The resulting crystals showed 86% enrichment by ^{31}P NMR. These crystals (2.460 g) were dissolved in 150 mL of methanol followed by the addition of 750 mL ethyl ether giving crystals of 94% enrichment. Final recrystallization of these crystals to 100% enrichment was achieved by dissolving 1.100 g in 33 mL ethylene glycol and 55 mL absolute ethanol followed by the addition of 495 mL ethyl ether. Data for **53b**: mp = 189^0 C. $[\alpha]_D^{24}$ = -45.1^0 (c = 0.26, $CHCl_3$) ^1H NMR: δ 1.17 (t, *J* = 7.1, 3H), 1.19 (t, *J* = 6.9, 3H), 1.37 (d, *J* = 10.5, 1H), 1.66 (d, *J* = 15.6, 1H), 2.18 (dd, *J* = 5.5, 14.3, 1H), 2.33 (dt, *J* = 7.0, 13.9, 1H), 2.67 (dd, *J* = 2.7, 17.8, 1H), 2.94-3.17 (m, 4H), 3.34 (s, 1H), 3.60 (d, 14.9, 3H), 3.81 (s, 4H), 4.01-4.13 (m, 8H), 4.20-4.42 (m, 5H), 6.55 (s, 1H), 7.14 (t, *J* = 7.5, 1H), 7.30 (t, *J* = 7.4, 1H), 7.51 (d, *J* = 7.3, 1H), 8.06 (d, *J* = 8.0, 1H). ^{13}C NMR δ 14.17, 14.23, 25.29, 29.74, 38.60, 38.63, 39.67, 42.08, 44.39, 44.43, 47.07, 53.21, 53.39, 53.48, 55.86, 58.80, 60.66, 61.26, 61.86, 64.22, 64.38, 75.08, 116.52, 122.59, 124.85, 127.72, 130.17, 132.75, 136.69, 141.66, 168.63, 171.06, 171.63. ^{31}P NMR δ 68.12. Data for **53d**: mp = 158-159^{0}C. $[\alpha]_D^{22}$ = -61.7 (c = 0.31, $CHCl_3$). ^1H NMR δ 1.18 (t, *J* = 7.1, 6H), 1.37 (d, *J* = 10.3, 1H), 1.66 (d, *J* = 15.1, 1H), 2.16 (dd, *J* = 5.4, 13.1, 1H), 2.27-2.38 (m, 1H), 2.68 (dd, *J* = 2.7, 17.8, 1H), 2.93-3.17 (m, 4H), 3.34 (s, 1H), 3.62 (d, *J* = 15.1, 3H), 3.83

(s, 4H), 4.01-4.18 (m, 8H), 4.21-4.33 (m, 2H), 4.43 (s, 3H), 6.58 (s, 1H), 7.14 (t, J = 7.4, 1H), 7.31 (t, J = 7.8, 1H), 7.52 (d, J = 7.4, 1H), 8.07 (d, J = 7.9, 1H). ^{13}C NMR: δ 14.17, 14.23, 25.34, 29.72, 38.50, 39.67, 42.06, 44.45, 44.49, 47.10, 53.20, 53.39, 53.48, 55.78, 55.80, 58.81, 60.65, 61.28, 61.81, 64.23, 74.99, 116.48, 122.64, 124.81, 127.81, 130.12, 132.80, 136.64, 141.65, 168.66, 171.02, 171.43. ^{31}P NMR: δ 67.18.

O,O,S-trimethylphosphorodithioate (23) was prepared from as described previously (Umetsu, 1977).

Strychnine-O,O,S-trimethylphosphorodithioate Salt (54). This procedure has been reported previously (Hilgetag, 1969) but is repeated here with slight modifications. Strychnine (24.40 g, 0.0730 mol) was added to a stirring solution of O,O,S-trimethylphosphorodithioate in methanol (180 mL). The reaction mixture was brought to reflux for 24 h. Upon cooling, the first crop of crystals (**54a**, *R*) precipitated and was filtered, washed with methanol, and recrystallized twice from methanol. Data for **54a**: mp = 202-203^0 C. $[\alpha]_D^{22}$ = +15.8^0 (c = 0.545, MeOH). ^{1}H NMR: δ 1.38 (dt, J = 3.1, 10.7, 1H), 1.56 (d, J = 14.8, 1H), 1.97 (d, J = 2.8, 1H), 2.02 (d, J = 14.1, 3H), 2.14 (dt, J = 7.6, 13.7, 1H), 2.44-2.59 (m, 2H), 2.97 (dd, J = 8.2, 17.8, 1H), 3.27 (s, 3H), 3.30 (s, 1H), 3.44 (d, J = 14.6, 3H), 3.56-3.76 (m, 3H), 3.95-4.25 (m, 5H), 4.35 (dt, J = 3.2, 8.3, 1H), 6.28 (s, 1H), 7.12 (t, J = 7.6, 1H), 7.25 (t, J = 7.7, 1H), 7.37 (d, 7.6, 1H), 7.78 (d, 8.1, 1H). ^{13}C NMR: δ 13.53, 13.58, 24.18, 28.87, 38.82, 40.68,

46.03, 48.83, 52.82, 53.09, 53.18, 54.40, 58.39, 61.63, 63.78, 64.10, 74.71, 76.36, 115.82, 122.94, 125.43, 129.08, 129.93, 132.68, 135.60, 140.65, 171.32. ^{31}P NMR: δ 78.87. The mother liquor was stored at 0 ^{0}C and gave a second crop that was recrystallized in 95% ethanol. The mother liquor was concentrated *in vacuo* to a solid and recrystallized in 95% ethanol to give a third crop of crystals. The second and third crop were combined and recrystallized once more in 95% ethanol (**54b**, *S*). Data for **54b**: mp = 253^{0} C. $[\alpha]_D^{22}$ = -13.5^{0} (c = 0.63, MeOH). ^{1}H NMR: δ 1.36 (d, *J* = 10.7, 1H), 1.55 (d, *J* = 15.7, 1H), 1.91 (d, *J* = 12.2, 1H), 2.01 (d, *J* = 14.1, 3H), 2.12 (dt, *J* = 7.8, 13.7, 1H), 2.44-2.57 (m, 2H), 2.96 (dd, *J* = 8.2, 18.1, 1H), 3.27 (s, 4H), 3.44 (d, *J* = 14.5, 3H), 3.53-3.76 (m, 3H), 3.93-4.25 (m, 5H), 4.34 (dt, *J* = 3.1, 8.3, 1H), 6.28 (s, 1H), 7.12 (t, *J* = 7.6, 1H), 7.24 (t, *J* = 7.6, 1H), 7.36 (d, *J* = 7.6, 1H), 7.76 (d, *J* = 8.1, 1H). ^{13}C NMR: δ 13.56, 13.60, 24.21, 28.89, 38.84, 40.72, 46.06, 52.83, 53.11, 53.20, 54.44, 58.40, 61.63, 63.80, 64.10, 74.72, 76.36, 115.83, 122.98, 125.45, 129.09, 129.95, 132.67, 135.63, 140.66, 171.29. ^{31}P NMR: δ 78.79.

General Procedure for the Stereoisomers of Isomalathion (12) from Strychnine-isomalathion Salt (53). To a 0.12 M stirring solution of **12** in methanol:acetone (1:3), 1 equiv of dimethyl sulfate was added and the solution was brought to reflux for 3 h, afterwhich 3 mL ethyl ether was added to precipitate the sulfate salt. The reaction mixture was filtered, concentrated to an oil and purified via flash chromatography (petroleum ether:ethyl ether; 1:2) to

give a colorless oil.

General Procedure for the Preparation of Isomalathion Stereoisomers (12a,12b,12c,12d) from Strychnine-O,O,S-trimethylphosphorodithioate salt (54). To a 0.2 M stirring suspension of **54** in CH_3CN was added 1 equiv of a 0.78 M solution of **39** in CH_3CN dropwise over 5 min. After 1 h, the solution was diluted two fold with ethyl ether to precipitate the strychninium triflate salt and the mixture was filtered *in vacuo*. The filtrate was concentrated *in vacuo* to an oil and purified by gravity chromatography (petroleum ether:ethyl ether; 1:1) to give the respective stereoisomer of **12** as a colorless oil.

***(1R,3R)*-Isomalathion (12a).** Prepared from **53a** (0.313 g, 0.471 mmol) to give **12a** (0.098 g, 63%). $[\alpha]_D^{22} = +43.6^0$ (c 0.55, $CHCl_3$). Prepared from **54b** (1.10 g, 2.17 mmol) and **39a** (0.700 g, 0.217 mmol) to give **12a** (0.220 g, 31%). $[\alpha]_D^{22} = 42.3^0$ (c 0.64, $CHCl_3$). ^{1}H NMR: δ 1.23 (t, *J* = 7.1, 3H), 1.27 (t, *J* = 7.1, 3H), 2.36 (d, *J* = 16.9, 3H), 2.97 (dd, *J* = 5.2, 17.2, 1H), 3.08 (dd, *J* = 8.9, 17.1, 1H), 3.84 (d, *J* = 13.6, 3H), 4.08-4.25 (m, 5H). ^{13}C NMR: δ 13.38, 13.43, 13.98, 14.08, 38.16, 38.21, 43.24, 43.27, 53.83, 53.93, 61.12, 62.18, 169.93, 170.01. ^{31}P NMR: δ 58.38.

***(1R,3S)*-Isomalathion (12b).** Prepared from **53b** (0.200 g, 0.301 mmol) to give **12b** (0.066 g, 66%). $[\alpha]_D^{22} = -64.3^0$ (c 0.59, $CHCl_3$). Prepared from **54b** (1.57 g, 3.11 mmol) and **39b** (1.00 g, 3.11 mmol) to give **12b** (0.612 g, 60%). $[\alpha]_D^{22} = -57.6^0$ (c 0.50, $CHCl_3$). ^{1}H NMR: δ 1.23 (t, *J* = 7.1, 3H), 1.27 (t, *J* =

7.1, 3H), 2.37 (d, J = 16.8, 3H), 2.94 (dd, J = 5.2, 17.1, 1H), 3.08 (dd, J = 8.8, 17.1, 1H), 3.85 (d, J = 13.7, 3H), 4.09-4.26 (m, 5H). ^{13}C NMR: δ 13.13, 13.17, 13.96, 14.07, 37.97, 38.02, 43.35, 43.40, 54.00, 54.11, 61.11, 62.18, 169.89. ^{31}P NMR: δ 56.92.

(*1S,3R*)-Isomalathion (12c). Prepared from **53c** (0.313, 0.471 mmol) to give **12c** (0.122 g, 79%). $[\alpha]_D^{22}$ = +57.5^0 (c 0.57, $CHCl_3$). Prepared from **54a** (1.10 g, 2.17 mmol) and **39a** (0.700 g, 2.17 mmol) to give **54a** (0.178 g, 25%). $[\alpha]_D^{22}$ = +58.6^0 (c 0.64, $CHCl_3$). The NMR spectral data of this material was identical to that of **12b**.

(*1S,3S*)-isomalathion (12d). Prepared from **53d** (0.300 g, 0.452 mmol) to give **12d** (0.107 g, 72%). $[\alpha]_D^{22}$ = -34.2 (c 0.59, $CHCl_3$). Prepared from **54a** (1.57 g, 3.11 mmol) and **39b** (1.0 g, 3.11 mmol) to give **12d** (0.523 g, 51%). $[\alpha]_D^{22}$ = -44.8 (c 0.58, $CHCl_3$). The NMR spectral data of this material was identical to that of **12a**.

Assay of Anti-cholinesterase Potency

Determination of k_i (time dependent).

Of an appropriately diluted solubilized rat brain AChE (approximating an acetylthiocholine hydrolysis rate of 0.100 Abs. units/min), 1.09 mL was withdrawn and placed in a test tube and transferred to a Forma-Scientific constant temperature shaker bath set at 37 ^{0}C. To each of six cuvettes was added 2.5 mL

of DTNB solution (3.33 x 10^{-3} M 5,5'-dithiobis(2-nitrobenzoic acid (DTNB) and 5.9 x 10^{-4} M sodium bicarbonate in pH 7.6 phosphate buffer) and 0.020 mL acetylthiocholine iodide (ATCh-I) solution (7.5 x 10^{-3} M in pH 7.6 phosphate buffer) and these cuvettes were placed in a Beckman DU-40 spectrophotometer equipped with a kinetic Soft-Pac module. From the test tube of AChE solution, 0.10 mL was withdrawn and added to cuvette 1 to serve as a control. To the remaining 0.990 mL in the test tube, 0.100 mL of an inhibitor solution was added and the enzyme solution vortexed. At 3, 6, 9, 12, and 15 min, 0.100 mL of the enzyme-inhibitor solution was added to cuvettes 2, 3, 4, 5, and 6, respectively. The rate of hydrolysis was monitored at 412 nm at 30-s intervals for 15 min from the addition of the enzyme. The bimolecular inhibition rate constant (k_i) was determined (in triplicate) using the following equation as defined previously (Aldridge, 1950):

$$\ln (A_0/A_t) = [\mathrm{i}]k_i t$$

where A_0 represents the initial activity of the enzyme (time $t = 0$), A_t represents the depressed enzyme activity at time = t following the addition of the inhibitor [i].

Determination of k_i, K_D, and k_p (concentration dependence).

Five of test tubes containing suitably diluted AChE solution (0.490 mL) were each treated with 0.010 mL of a progression of inhibitor concentrations. A sixth test tube was treated with 0.010 mL of methanol to serve as control. The inhibition was permitted to progress for 20 min, and the remaining enzyme activity was determined as described above (**A**) over a period of 15 min (30-s intervals). The bimolecular reaction constant (k_i), dissociation constant (K_D), and phosphorylation constant (k_p) were determined using the following equation as defined previously (Main, 1964):

$$1/[i] = (\Delta t / \Delta \ln v)k_i - 1/K_D$$

where Δt = 20 min, $\Delta \ln v = \ln(A_0/A_{20})$, and $k_i = k_p/K_D$. Assays involving solubilized rat brain AChE and electric eel AChE were performed similarly except that the solutions were made with pH 7.6 and pH 8.0 phosphate buffer, respectively.

Spontaneous Reactivation

Solubilized rat brain AChE (0.20 mL) and 0.80 mL of 0.1 M phosphate buffer (pH 7.6) were added to each of two test tubes. A 0.010-mL inhibitor solution that caused 90% inhibition was added to the first tube and incubated in a shaker bath at 37 ^{0}C for 20 min. Synchronously, MeOH (0.010 mL) was added

to the second tube as a control and placed in the bath for 20 min. Following inhibition, the first tube was further diluted with 40 mL of phosphate buffer (pH 7.6) to halt inhibition (t = 0 min), and 1 mL was withdrawn and placed in a cuvette containing 1.5 mL of 5,5'-dithiobis(2-nitrobenzoic acid) (DTNB) solution (3.33×10^{-4} M DTNB and 5.9×10^{-4} M $NaHCO_3$ in pH 7.6 phosphate buffer) and 0.020 mL of acetylthiocholine iodide (ATCh-I) solution (7.5×10^{-3} M in pH 7.6 phosphate buffer) to determine the remaining enzyme activity (A_0) while the remainder of the solution was returned to the bath. The second tube was diluted with 40 mL of phosphate buffer (pH 7.6), and 1 mL of the diluted solution was placed in a second cuvette containing the solutions described above to determine the initial enzyme activity (A, control). At subsequent 4-min intervals, 1 mL was withdrawn from the remaining diluted solution of tube 1 and the enzyme activity (A_t) determined. The rate constant for spontaneous reactivation (k_0) was calculated from the linear portion of the graph (0-32 min) using the following equation:

$$\ln (100/ \% \text{ inhibition}) = k_0 t$$

where % inhibition = $100[(A - A_t)/(A - A_0)]$.

Oxime-Mediated Reactivation

Solubilized rat brain AChE (0.20 mL) and 0.80 mL of phosphate buffer (pH 7.6) were placed in each of two test tubes, and the identical procedure to spontaneous reactivation was followed. Following dilution with 40 mL of phosphate buffer (pH 7.6), 1 mL was withdrawn from the first tube and the remaining enzyme activity determined (A_0). Immediately following, 2-pyridine aldoxime methiodide (2-PAM; 0.20 mL; 1.0 x 10^{-2} M) was added to the diluted solution and the enzyme mixture returned to the water bath. The point at which oxime was added was considered reactivation time $t = 0$. The second tube was diluted with 40 mL of buffer and assayed for activity (A_t). The rate constant for oxime-mediated reactivation (k_{oxime}) was calculated from the linear portion of the graph (0-10 min) using the following equation:

$$\ln (100/ \% \text{ inhibition}) = k_{oxime}t$$

where % inhibition = $100[(A - A_t)/(A - A_0)]$.

After 10 min had elapsed, the enzyme was assayed at 10-min intervals to determine the returned enzyme activity and the total % reactivation after 60 min. Total % reactivation was calculated using the following equation:

total % reactivation = 100 - (% inhibition at 60 min).

Non-Reactivatability

Rat brain AChE stock solution (0.20 mL) was diluted to 1.0 mL with phosphate buffer (pH 7.6) and incubated for 20 min with inhibitor to produce approximately 10-15% residual activity. Following the inhibition, the sample was diluted with 40 mL of phosphate buffer (t = 0), and at regular time intervals, 1-mL aliquots were withdrawn and added to a 1.52-mL solution containing DTNB and ATCh-I as noted previously to determine the enzyme activity that returned via spontaneous reactivation over the time course of this experiment. Concurrently, 2-mL aliquots were withdrawn and reacted with 1,1'-trimethylenebis(4-formylpyridinium bromide) dioxime (TMB-4) (0.010 mL; 2.0 x 10^{-3} M) or 2-PAM for 20 min. The enzyme activity was evaluated as described above to determine the amount of returned activity from oxime-mediated reactivation. The rate constants of non-reactivatability (k_{NR}) were calculated from the linear portion of the graphs (20-60 min) according to the following equation:

$$2.3 \log [(A_t - A_t')/(A_0 - A_0')] = -k_{NR}t$$

where $A_t - A_t'$ = (activity of the reactivated enzyme with oxime at time = t) -

(activity of the inhibited enzyme without oxime at time = t) and A_0 - A_0' = (activity of reactivated enzyme with oxime at time = 0) - (activity of inhibited enzyme without oxime at time = 0).

APPENDIX A

ENZYME INHIBITION ANALYSIS PROGRAM

```
1000 '  KI .... AN ENZYME INHIBITION ANALYSIS PROGRAM
1100 '  Determination of Bimolecular Inhibition Rate Constants "ki"
1200 '            Written by Clifford E. Berkman  8/24/90Í
1300 '         This program was written using equations from:
1400 ' INTRODUCTION TO BIOSTATISTICS   by   Sokal and Rohlf
1500 '                          { pages 237, 247 272 }
1600 'For GWBASIC
1700 '*******   ENTER TIME POINTS following Time = 0  *******
1800 '
1900 CLS: PRINT  "DETERMINATION OF ki"
1950 DIM X(100): DIM Y(100): DIM A(100)
2000 PRINT: INPUT: "Name of inhibitor compound: ",INHIB$
2100 PRINT: INPUT: "Inhibitor concentration (M): ",INHIBCONC
2200 PRINT: INPUT: "This is Run #: ",R: CLS
2250 PRINT: INPUT:  "Number of cuvettes = ",N
2300 PRINT  "Cuvette # 1 :": PRINT  "Time (min) = ";0
2400 INPUT  "Activity (rate) =  ",A0: PRINT
2500 FOR C=1 to N-1
2600        PRINT  "Cuvette #";C+1;":": INPUT  "Time (min) = ",X(C)
2700        INPUT  "Activity (rate) =  ",A(C): PRINT
2800        Y(C)=LOG(A0/A(C))
2900        SUMX=SUMX + X(C)
3000        SUMY=SUMY + Y(C)
3100        SUMXY=SUMXY + X(C)*Y(C)
3200 NEXT C
3300 XMEAN=SUMX/(N-1)
3400 YMEAN=SUMY/(N-1)
3500 SUMPRODXY=SUMXY-SUMX*SUMY/(N-1)
3600 FOR C=1 TO N-1
3700        SUMSQRX=SUMSQRX + (X(C)-XMEAN)^2
3800        SUMSQRY=SUMSQRY + (Y(C)-YMEAN)^2
3900 NEXT C
4000 SLOPE=SUMPRODXY/SUMSQRX
4100 INTERCEPT=YMEAN - SLOPE*XMEAN
4200 CORRELCOEFF=SUMPRODXY/(SUMSQRX*SUMSQRY)^.5
4300 STDDEVSLOPE=(((SUMSQRY-SUMPRODXY^2/SUMSQRX)/3)
     /SUMSQRX)^.5
4400 KI=SLOPE/INHIBCONC
4500 CLS: LPRINT: LPRINT: LPRINT
4600 LPRINT TAB(10); "Bimolecular Inhibition Rate Constant Determination:
     'ki'"
```

```
4700  PRINT TAB(10); "Bimolecular Inhibition Rate Constant Determination:
      'ki'"
4800  LPRINT:  LPRINT:  LPRINT
4900  LPRINT:  LPRINT "Inhibitor Compound:  " TAB(40) INHIB$: LPRINT
5000   PRINT:   PRINT "Inhibitor Compound:  " TAB(40) INHIB$:  PRINT
5100  LPRINT "Inhibitor Concentration:  " TAB(40) INHIBCONC; " M": LPRINT
5200   PRINT "Inhibitor Concentration:  " TAB(40) INHIBCONC; " M": PRINT
5300  LPRINT "Time","ln(A0/At)" TAB(40) "Run #";R: LPRINT
5400   PRINT "Time","ln(A0/At)" TAB(40) "Run #";R:  PRINT
5500  FOR C=1 TO N-1
5600        LPRINT X(C),Y(C): PRINT X(C),Y(C)
5700  NEXT C
5800  LPRINT: PRINT
5900  LPRINT "Equation for the Line:" TAB(40) "Y= "; SLOPE; " X +
      ";INTERCEPT
6000   PRINT "Equation for the Line:" TAB(40) "Y= "; SLOPE; " X +
      ";INTERCEPT
6100  LPRINT: LPRINT "Correlation Coefficient:  " TAB(40) CORRELCOEFF:
      LPRINT
6200   PRINT:  PRINT "Correlation Coefficient:  " TAB(40) CORRELCOEFF:
       PRINT
6300  LPRINT "Standard Deviation of the Slope:  "; TAB(40) STDDEVSLOPE:
      LPRINT
6400   PRINT "Standard Deviation of the Slope:  "; TAB(40) STDDEVSLOPE:
       PRINT
6500  LPRINT "::::::::::::::::::::::::::::::>>>>>"; TAB(40) "ki = " KI
6600   PRINT "::::::::::::::::::::::::::::::>>>>>"; TAB(40) "ki = " KI
6700  LPRINT CHR$(12)          'Epson Printer Form Feed
6800  END
```

APPENDIX B

SAMPLE DATA AND CALCULATION OF RATE CONSTANTS

Bimolecular Rate Constant

Sample Data and Calculation of k_i according to Eqn. 3 for the inhibition of RBAChE by (*R*)-malaoxon (Figure 30, Table 8) are shown.

$$\ln(A_0/A_t) = [i]k_i t$$

$[i] = 1.00 \times 10^{-6}$ M

t (min)	A_t (Abs_{412nm}/min)	$\ln(A_0/A_t)$
0	0.1005	-----
3	0.0583	0.544
6	0.0314	1.16
9	0.0187	1.68
12	0.0126	2.07
15	0.0089	2.42

$k_i = 1.56 \times 10^5$ ($M^{-1}min^{-1}$) r = 0.993

Bimolecular Reaction, Dissociation, and Phosphorylation Constants

Sample Data and Calculation of k_i, K_D, and k_p according to Eqn. 2 for the inhibition of RBAChE by (*1R,3R*)-isomalathion (Figure 32, Table 10).

$$1/[i] = (\Delta t/\Delta \ln A)k_i - 1/K_D$$

$$k_i = k_p/K_D$$

Δt = 20 min

$\Delta \ln A = \ln(A_{0\ min}/A_{20\ min})$

A_0 = 0.0952 ($Abs_{412\ nm}$ /min)

$[i]$ (M)	$1/[i]$ (M^{-1})	A_{20} (Abs_{412nm} /min)	$\Delta t/\ln(A_0/A_{20})$
2.50×10^{-6}	20.0×10^{6}	0.0703	66.0
5.00×10^{-6}	10.0×10^{6}	0.0531	34.3
10.0×10^{-6}	5.00×10^{6}	0.0369	21.1
20.0×10^{-6}	2.50×10^{6}	0.0198	12.7
40.0×10^{-6}	1.25×10^{6}	0.0129	10.0

$k_i = 3.34 \times 10^{5}$ ($M^{-1}min^{-1}$) r = 0.991

$K_D = 5.34 \times 10^{-7}$ (M)

k_p = 0.178

Spontaneous Reactivation

Sample Data and Calculation of k_0 according to Eqn. 4 for the spontaneous reactivation of RBAChE inhibited by (*1R,3R*)-isomalathion (Figure 34, Table 12).

$$\ln(100/\%\text{inhibition}) = k_0 t$$

$$\%\text{inhibition} = (A - A_t)/(A - A_0)$$

A = 0.0475 ($Abs_{412\ nm}$/min)

t (min)	A_t (Abs_{412}/min)	%inhibition	ln(100/%inhibition)
0	0.0077	100.0	0.000
4	0.0093	96.0	0.041
8	0.0123	88.4	0.123
12	0.0145	82.9	0.187
16	0.0164	78.1	0.247
20	0.0170	76.6	0.266
24	0.0198	69.6	0.362
28	0.0207	67.3	0.396
32	0.0214	65.6	0.422
36	0.0217	64.8	0.433
40	0.0227	62.3	0.473
44	0.0262	53.5	0.625
48	0.0236	60.1	0.510
52	0.0243	58.3	0.540
56	0.0202	68.6	0.377
60	0.0217	64.8	0.434

k_0 = 0.0136 (min^{-1}) r = 0.990

Oxime-Mediated Reactivation

Sample Data and Calculation of k_{oxime} according to Eqn. 4 for the spontaneous reactivation of RBAChE inhibited by (*1R,3R*)-isomalathion (Figure 34, Table 12).

$$\ln(100/\%\text{inhibition}) = k_{oxime}t$$

$$\%\text{inhibition} = (A - A_t)/(A - A_0)$$

A = 0.0671 (Abs_{412nm}/min)

t (min)	A_t (Abs_{412}/min)	%inhibition	ln(100/%inhibition)
0	0.0084	100.0	0.000
1	0.0127	92.7	0.076
2	0.0146	89.4	0.112
3	0.0177	84.2	0.172
4	0.0203	79.7	0.227
5	0.0222	76.5	0.268
6	0.0240	73.4	0.309
7	0.0276	67.3	0.396
8	0.0293	64.4	0.440
9	0.0299	63.4	0.456
10	0.0324	59.1	0.526

k_0 = 0.050.6 (min^{-1}) r = 0.997

APPENDIX C

SAMPLE SPECTRA

(*S*)-Diethyl malate (36a)

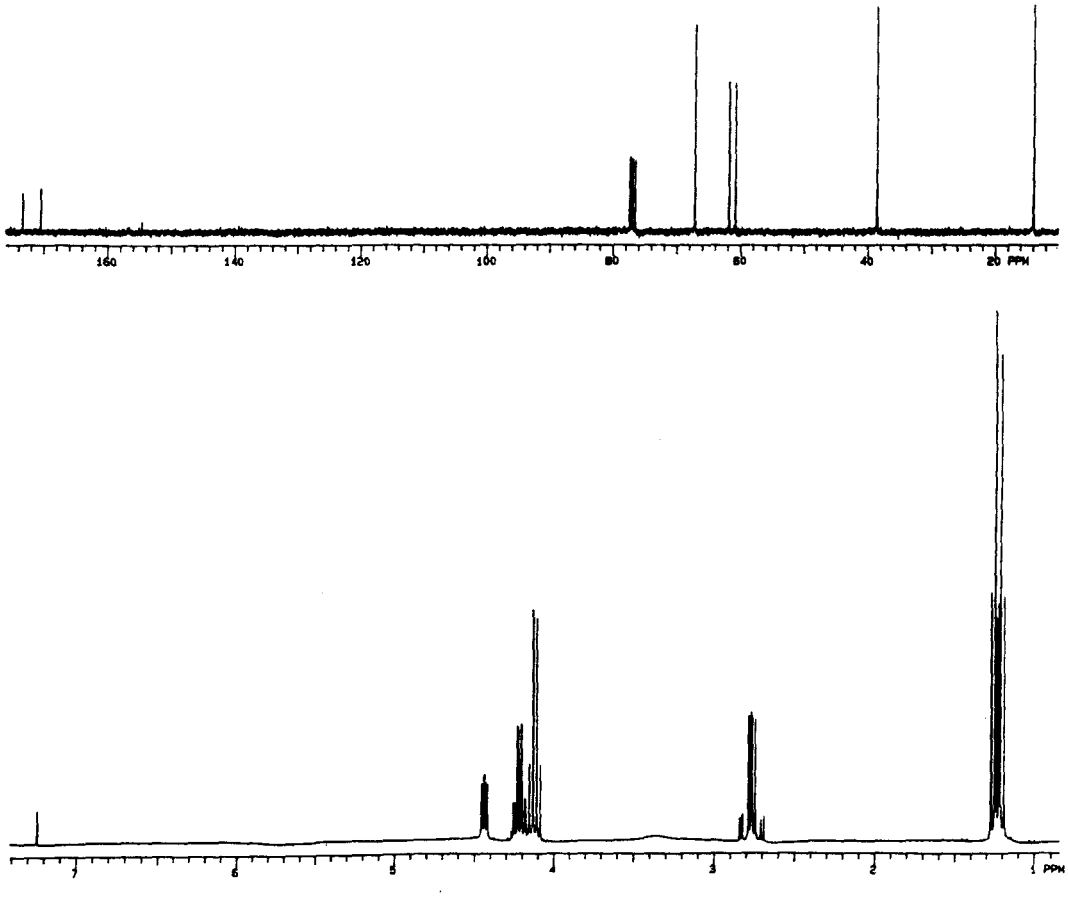

(*S*)-O-(Trifluoromethanesulfonyl)-diethyl malate (39a)

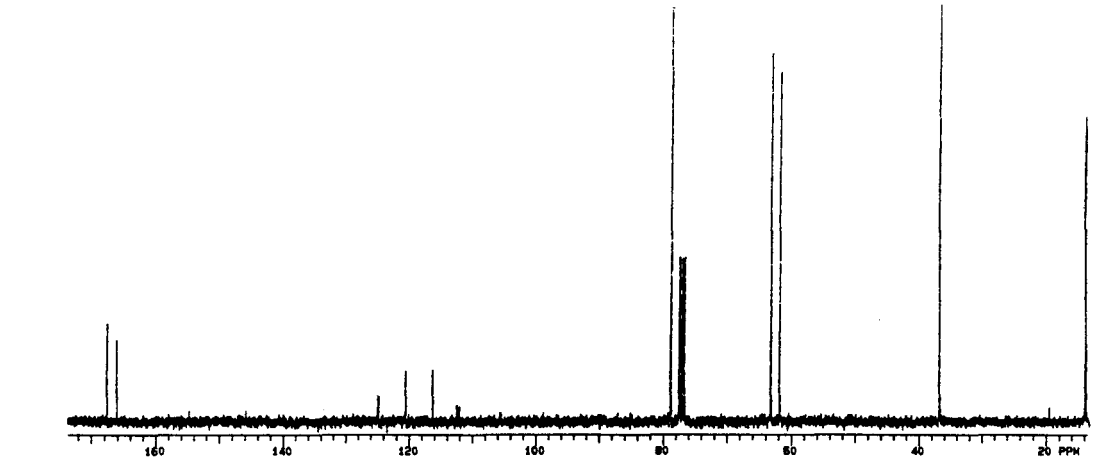

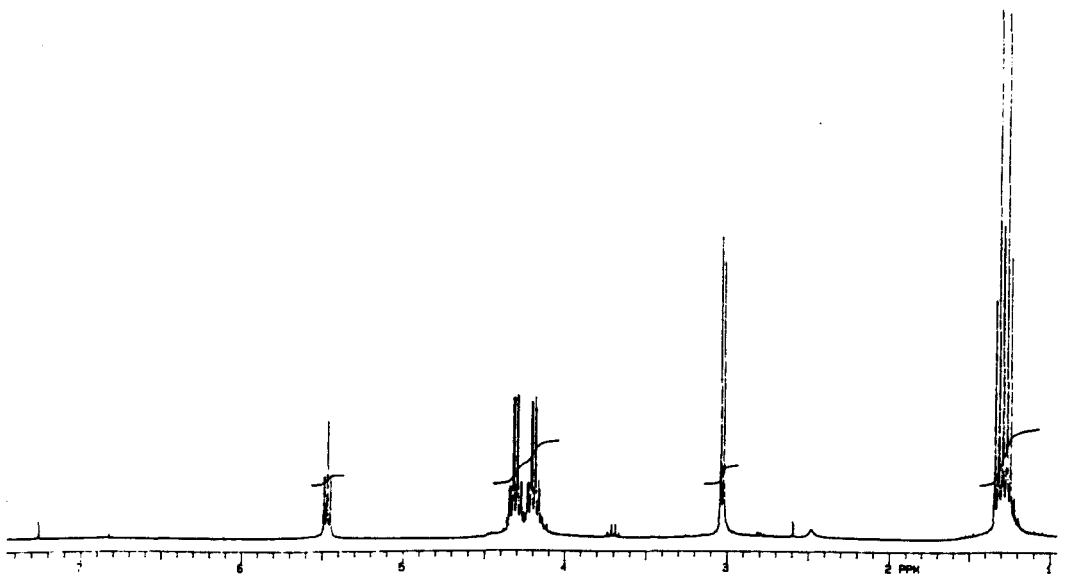

(*R*)-Malathion (6a)

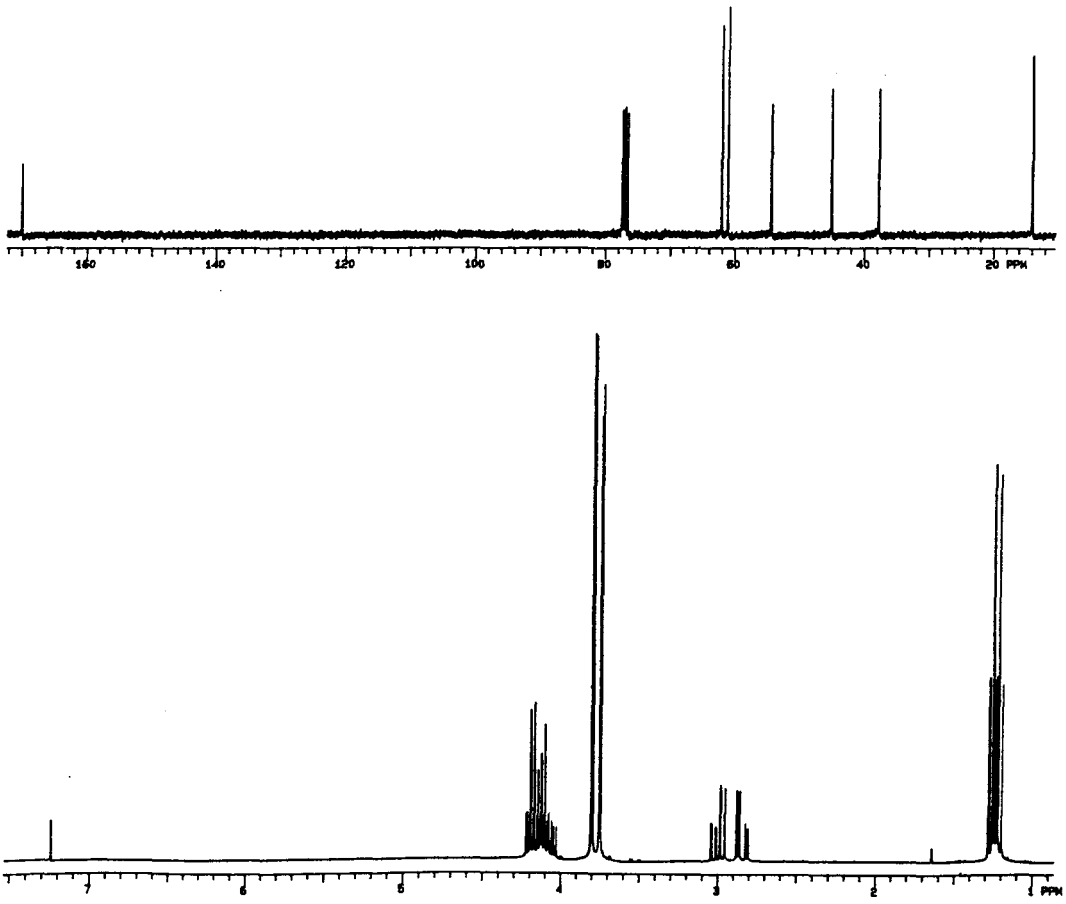

(*R*)-Malaoxon (22a)

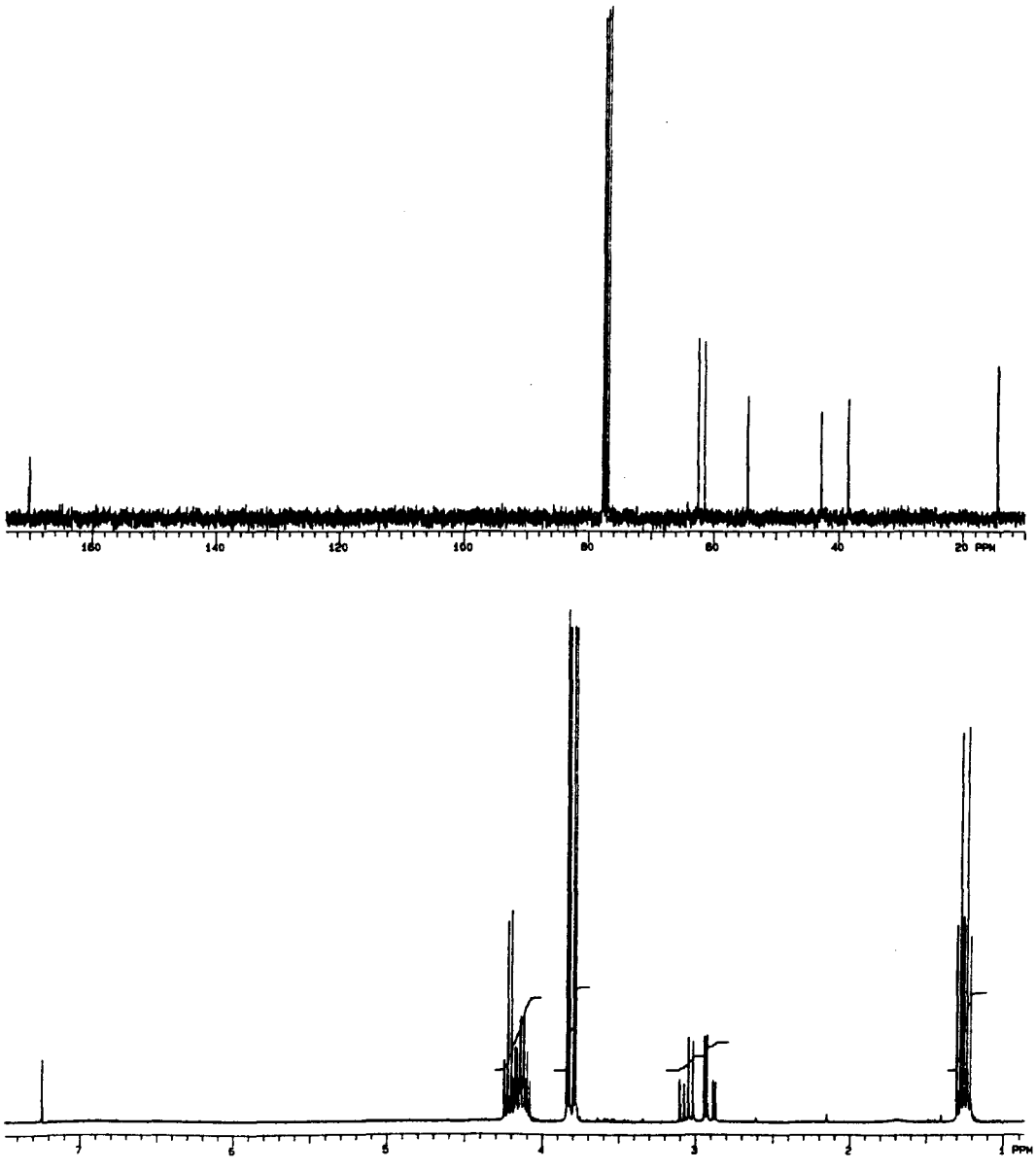

N-(Ethyl prolinyl) S-methyl chlorophosphoramidothiolate (50; Fast Band)

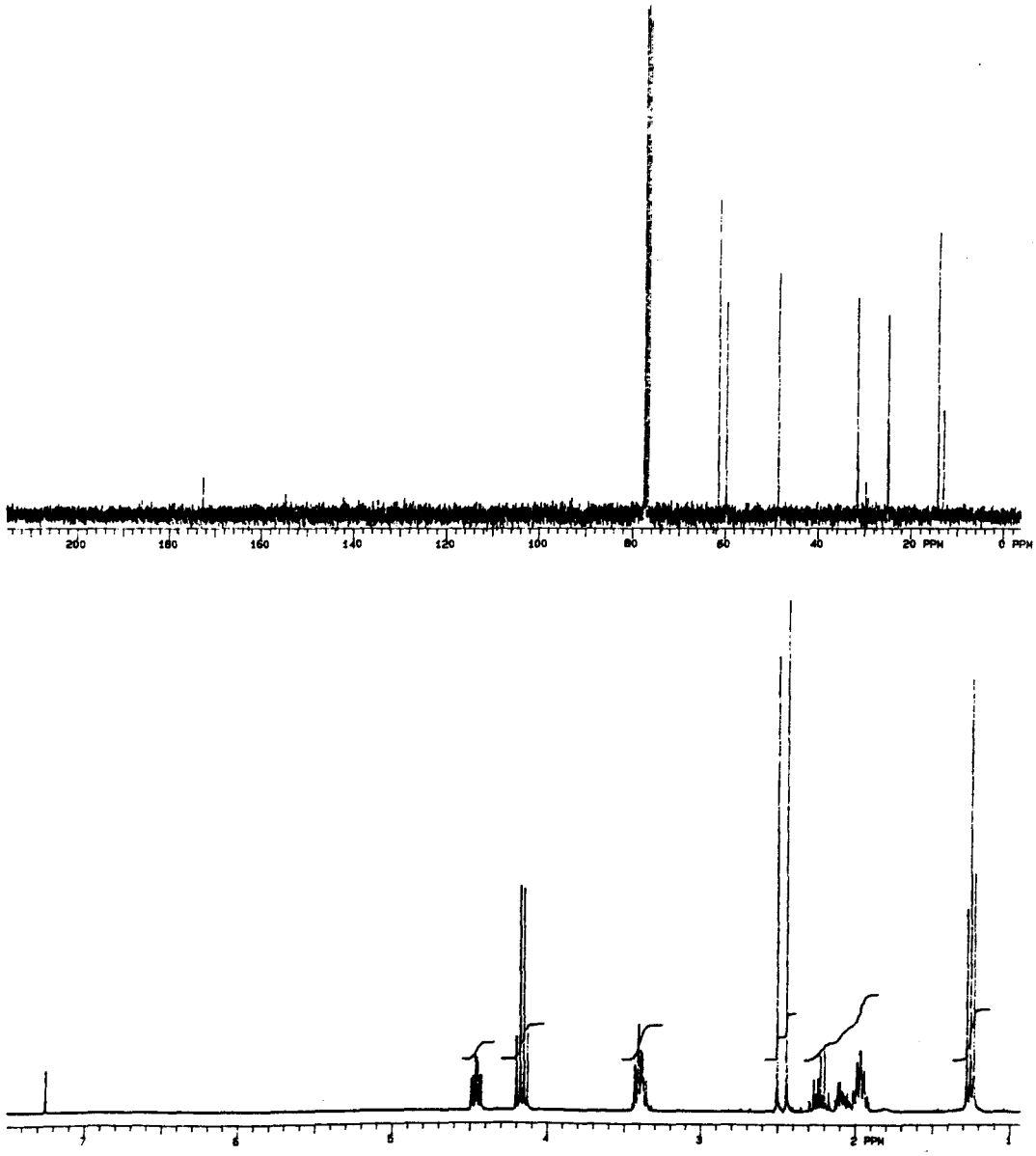

N-(Ethyl prolinyl) S-methyl chlorophosphoramidothiolate (50; Slow Band)

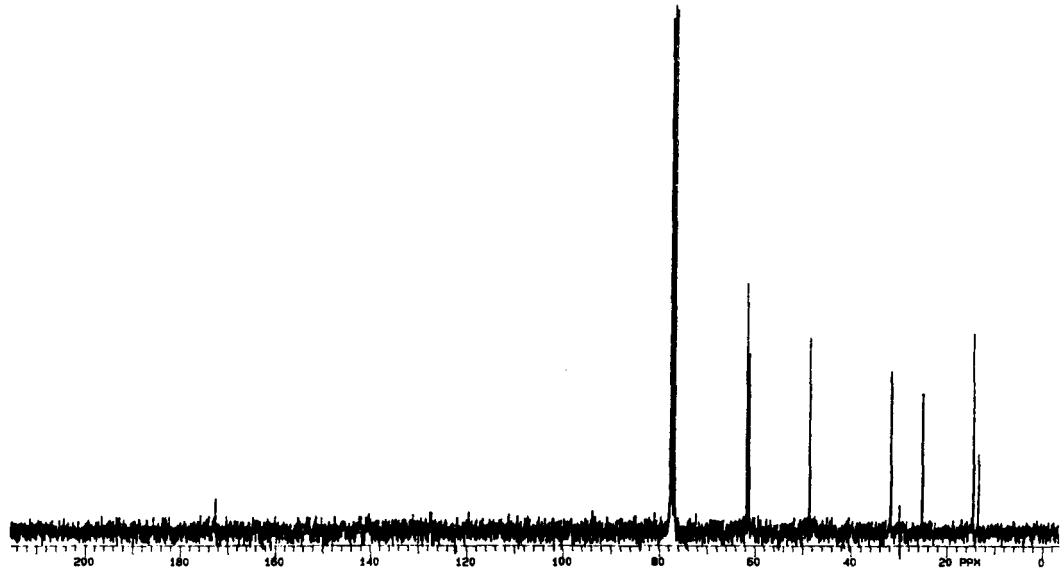

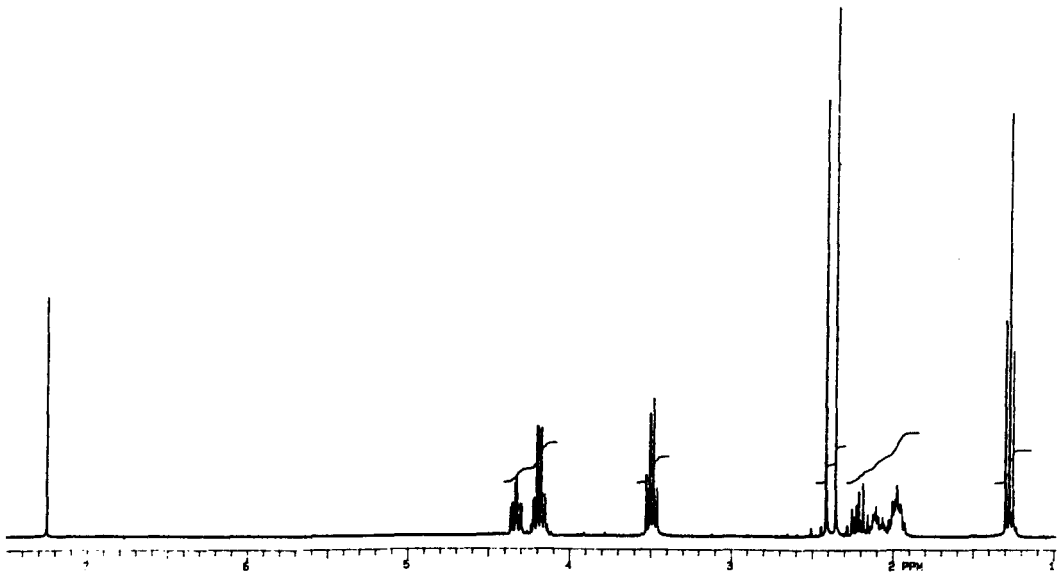

Strychnine-(*3R*)-isomalathion salt (53a)

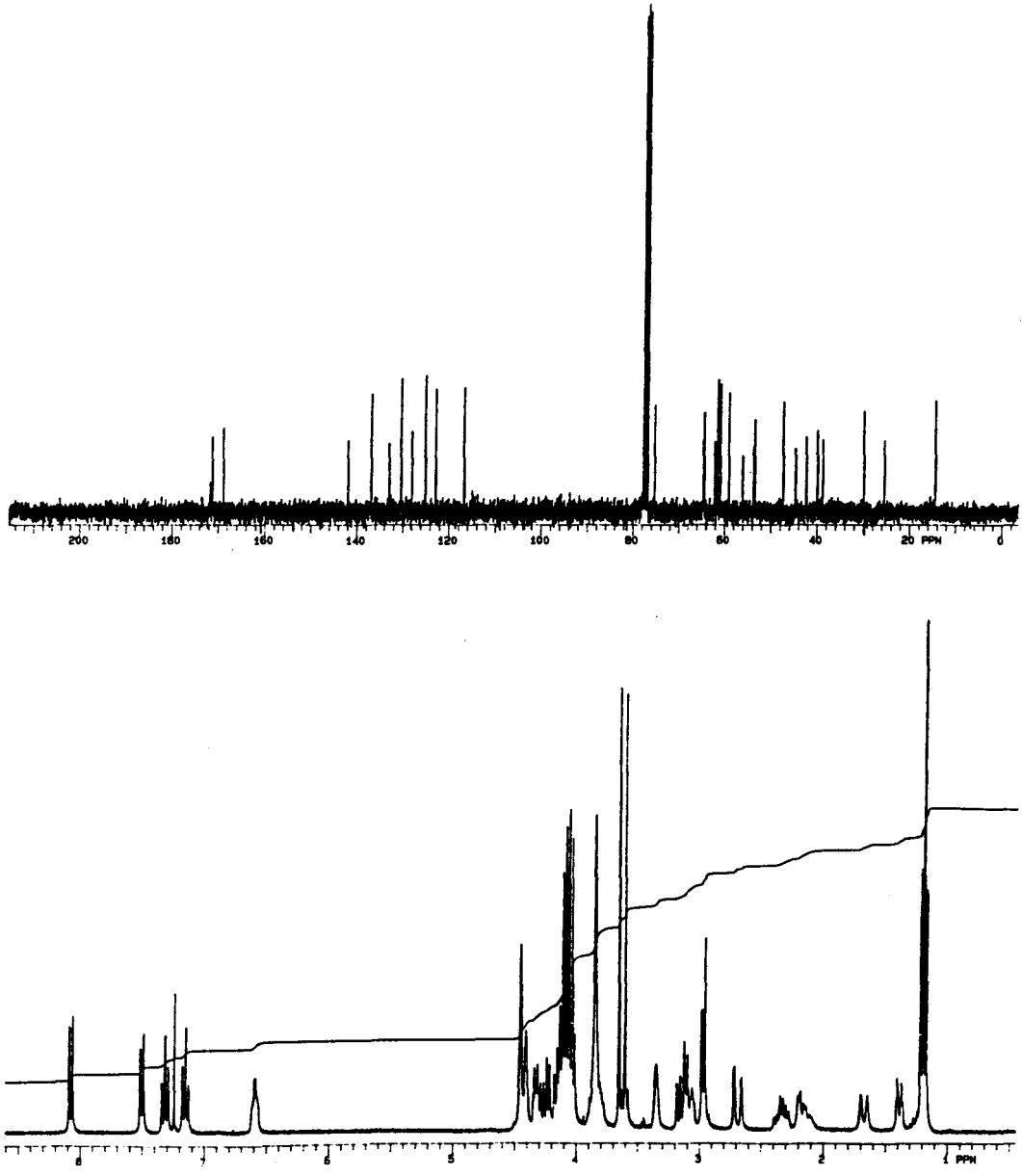

Strychnine-(*3R*)-isomalathion salt (53b)

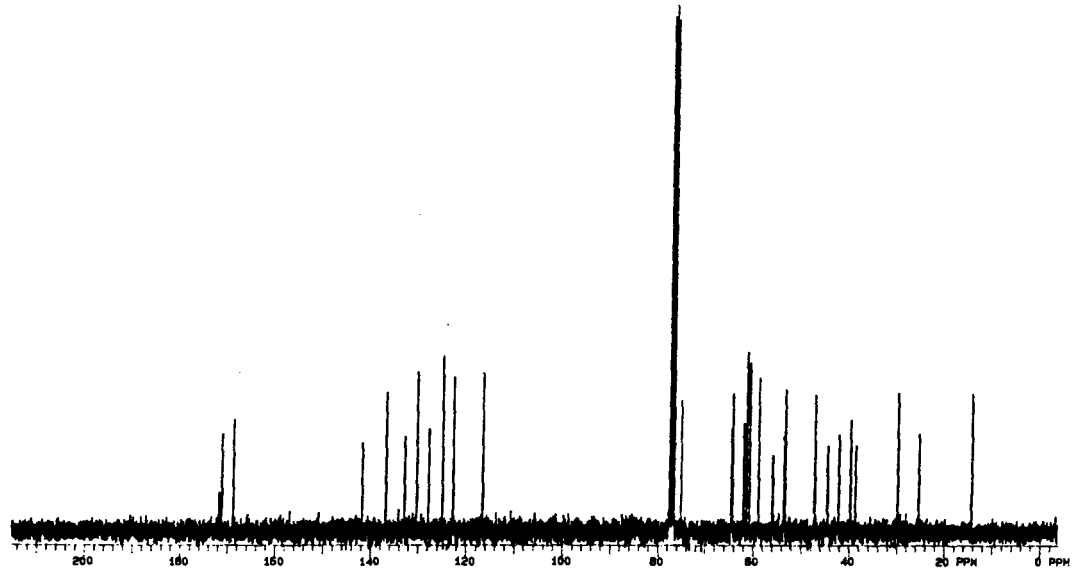

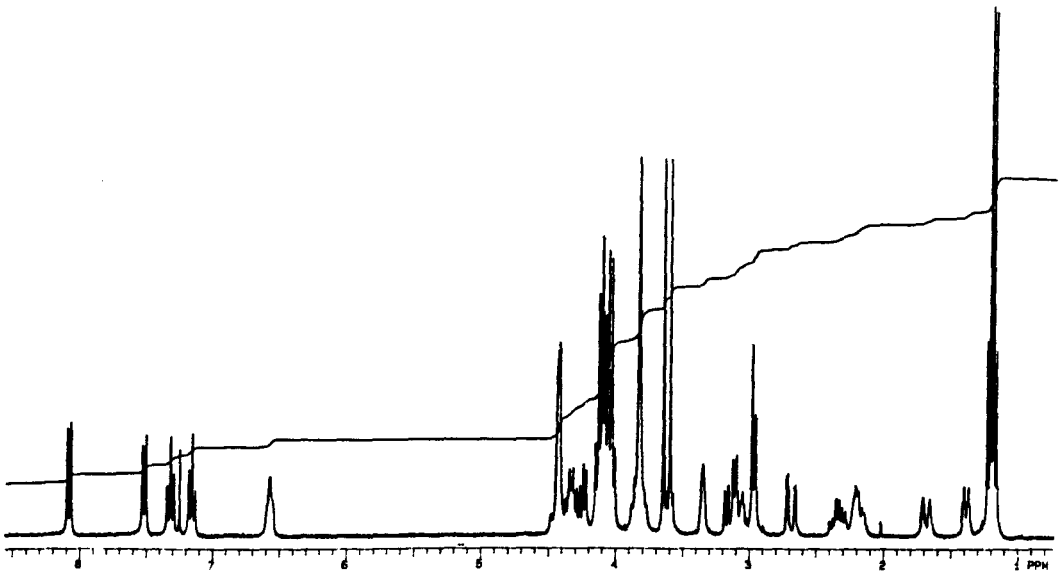

Strychnine-(*3R*)-isomalathion salt (53c)

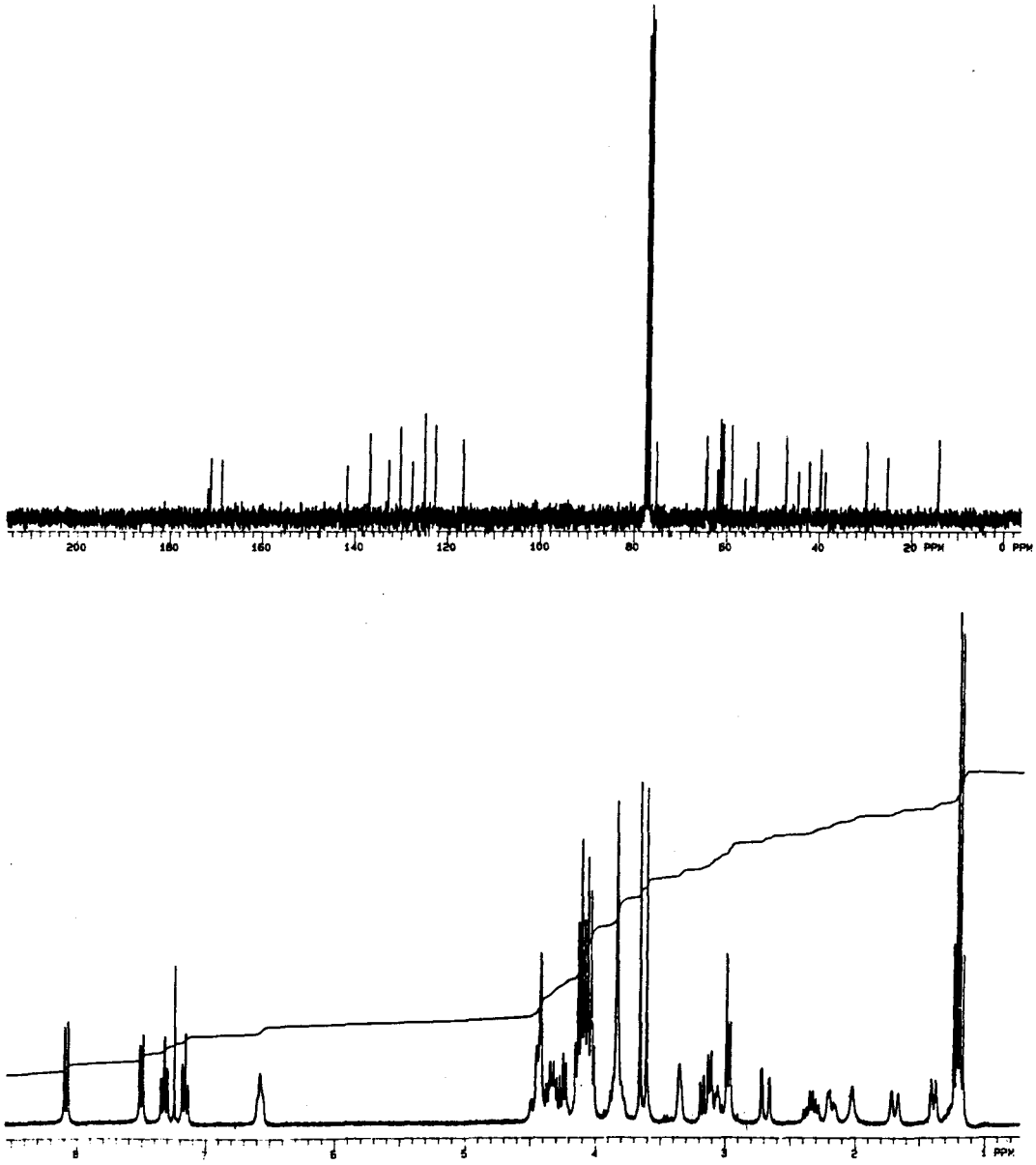

Strychnine-(*3R*)-isomalathion salt (53d)

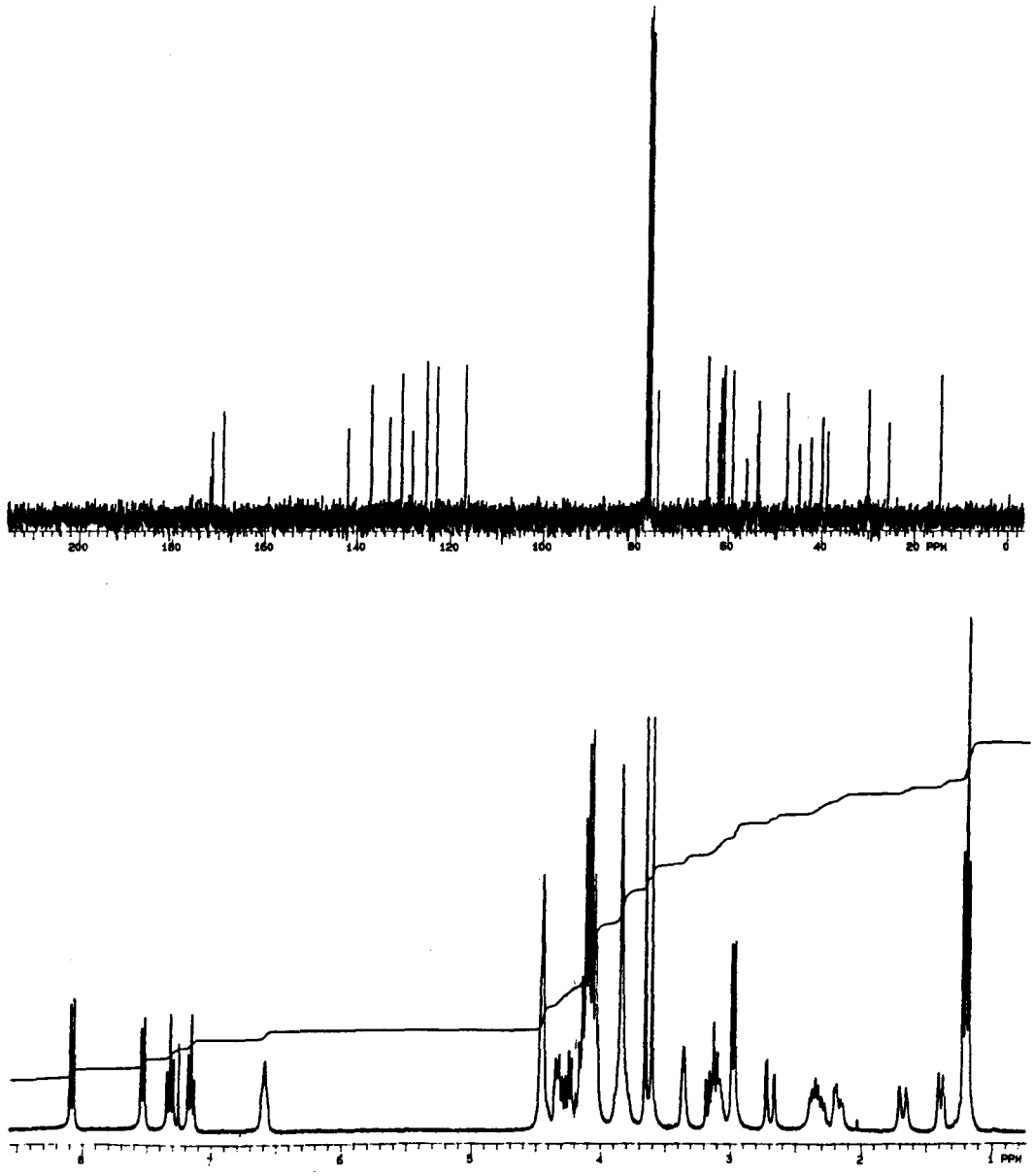

Strychnine-O,O,S-trimethylphosphorodithioate Salt (54a)

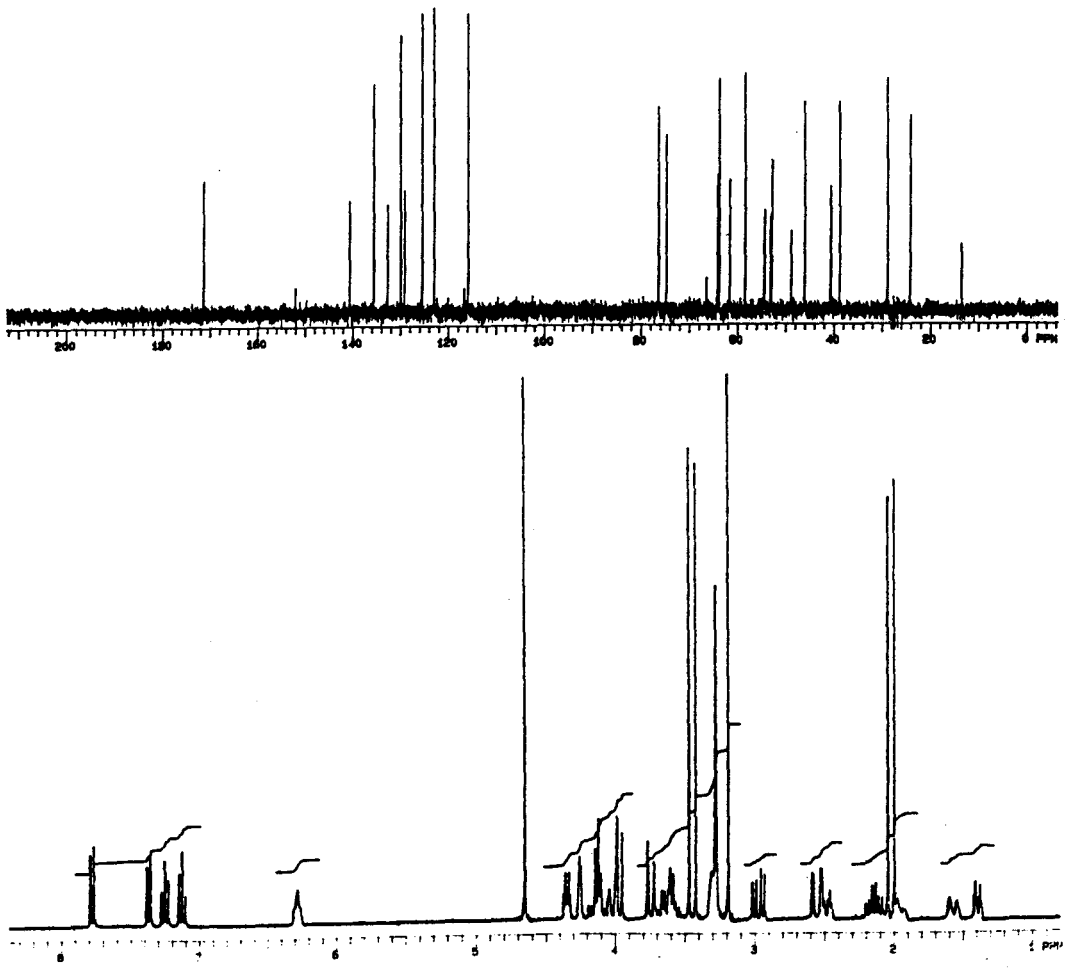

Strychnine-O,O,S-trimethylphosphorodithioate Salt (54b)

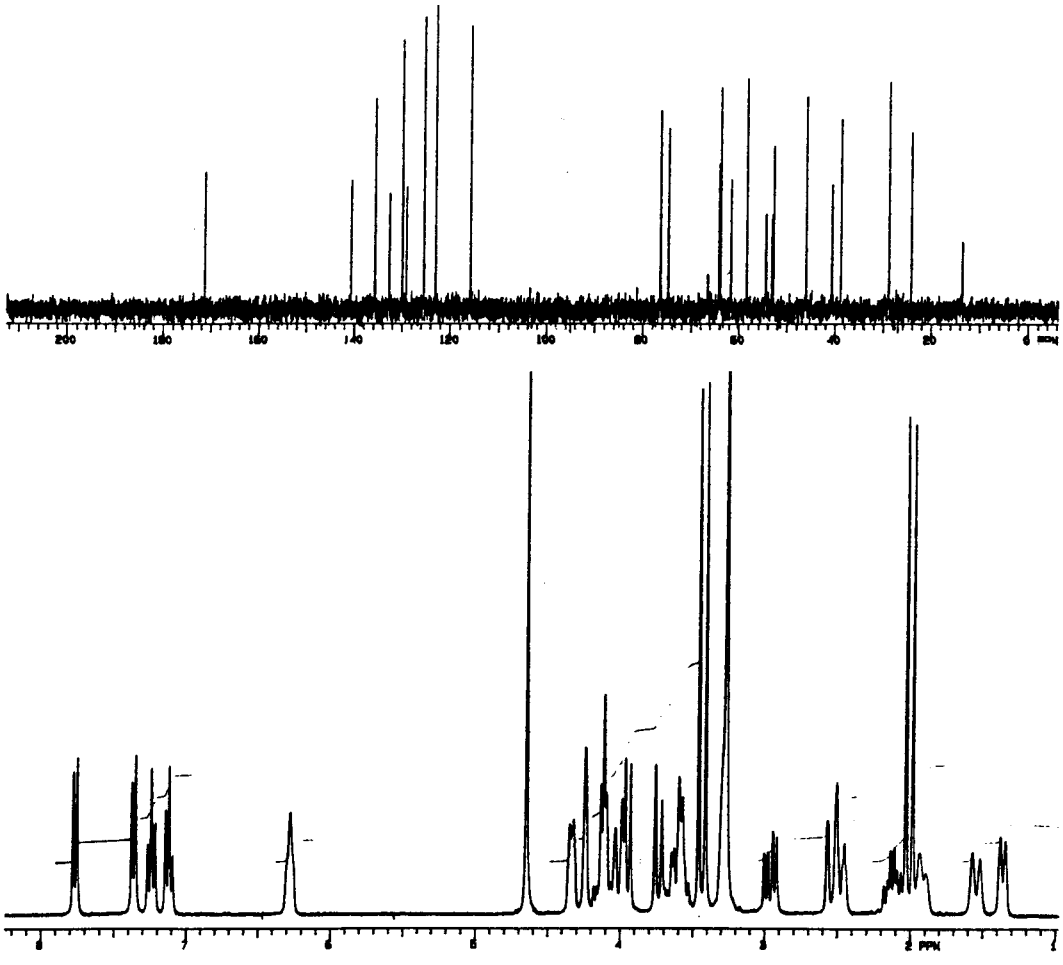

(*1R,3R*)-Isomalathion (12a)

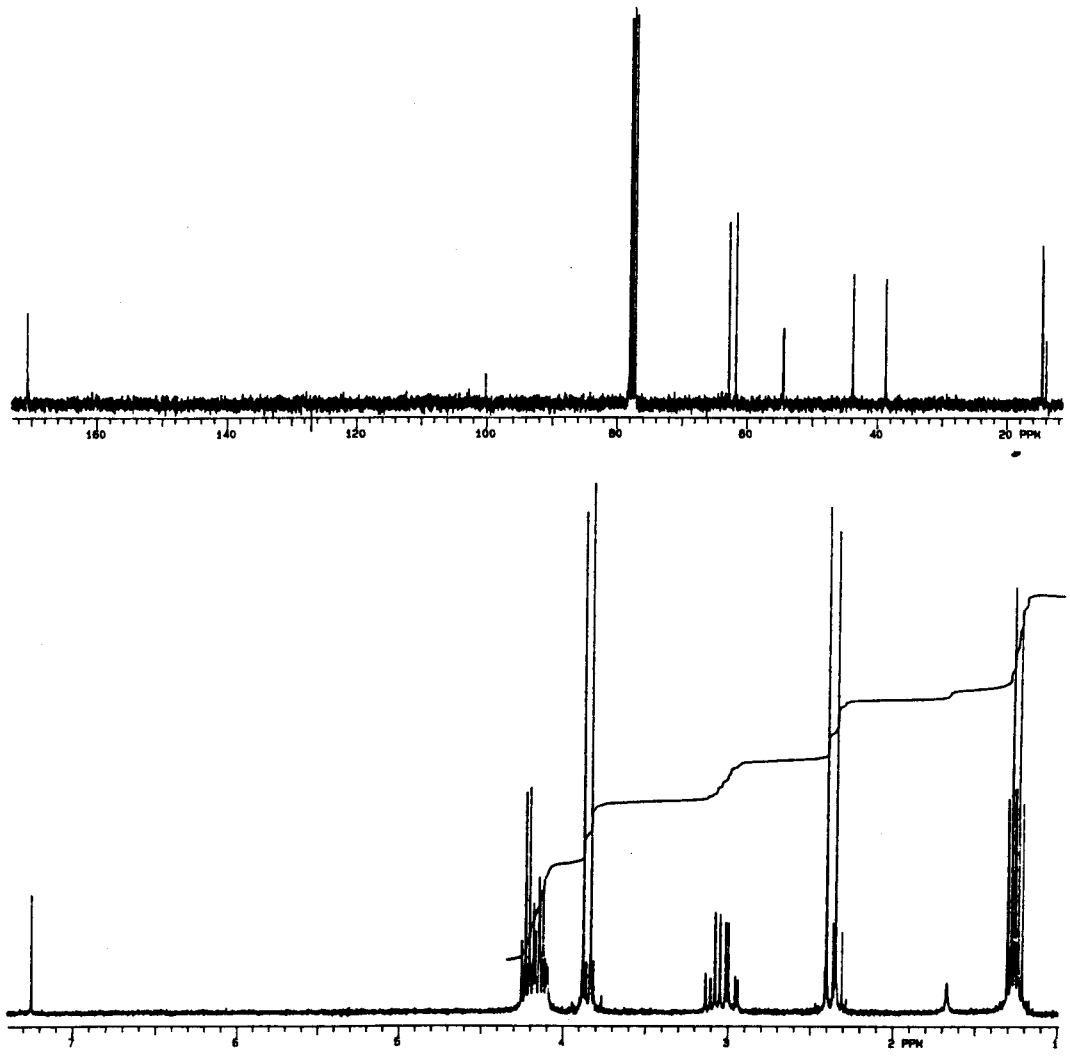

(*1R,3S*)-Isomalathion (12b)

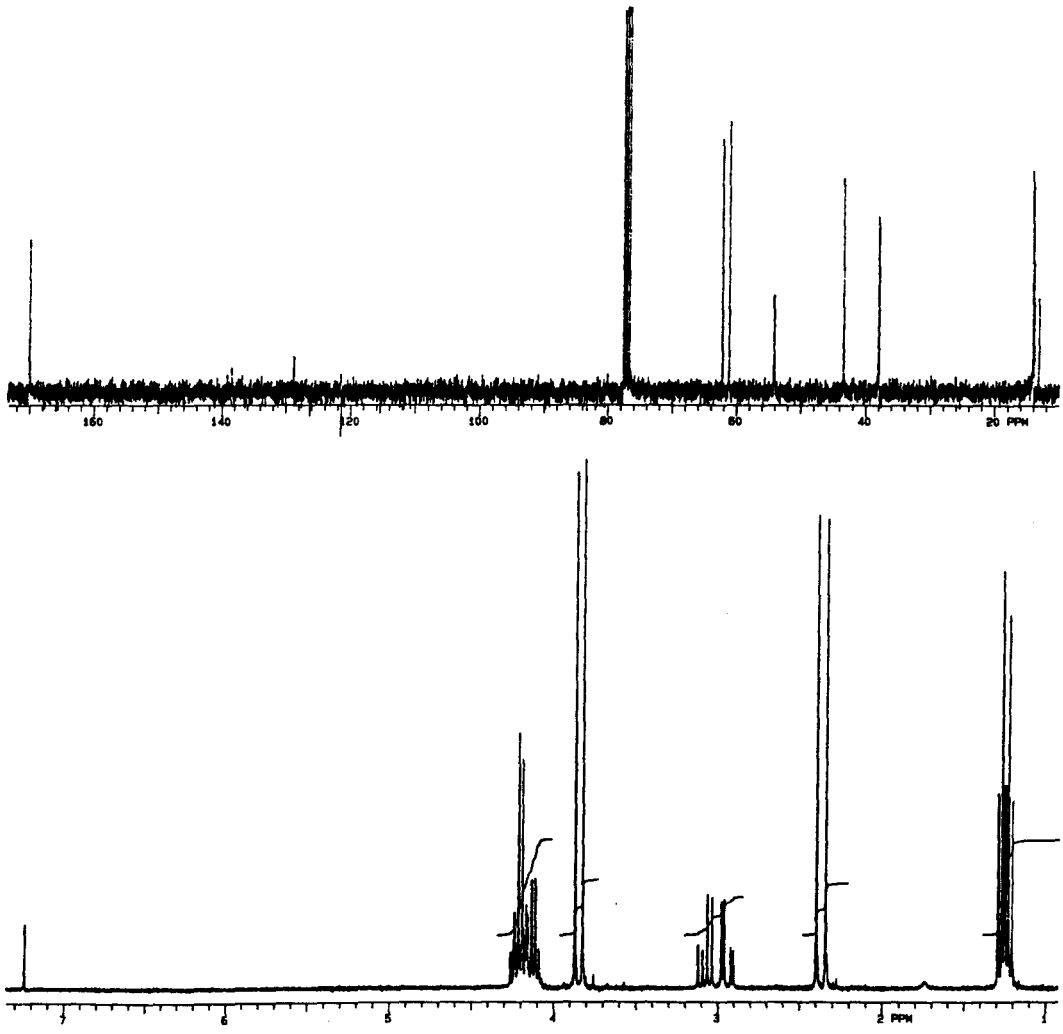

($^{13}CH_3S$)-(*1RS,3RS*)-Isomalathion (12')

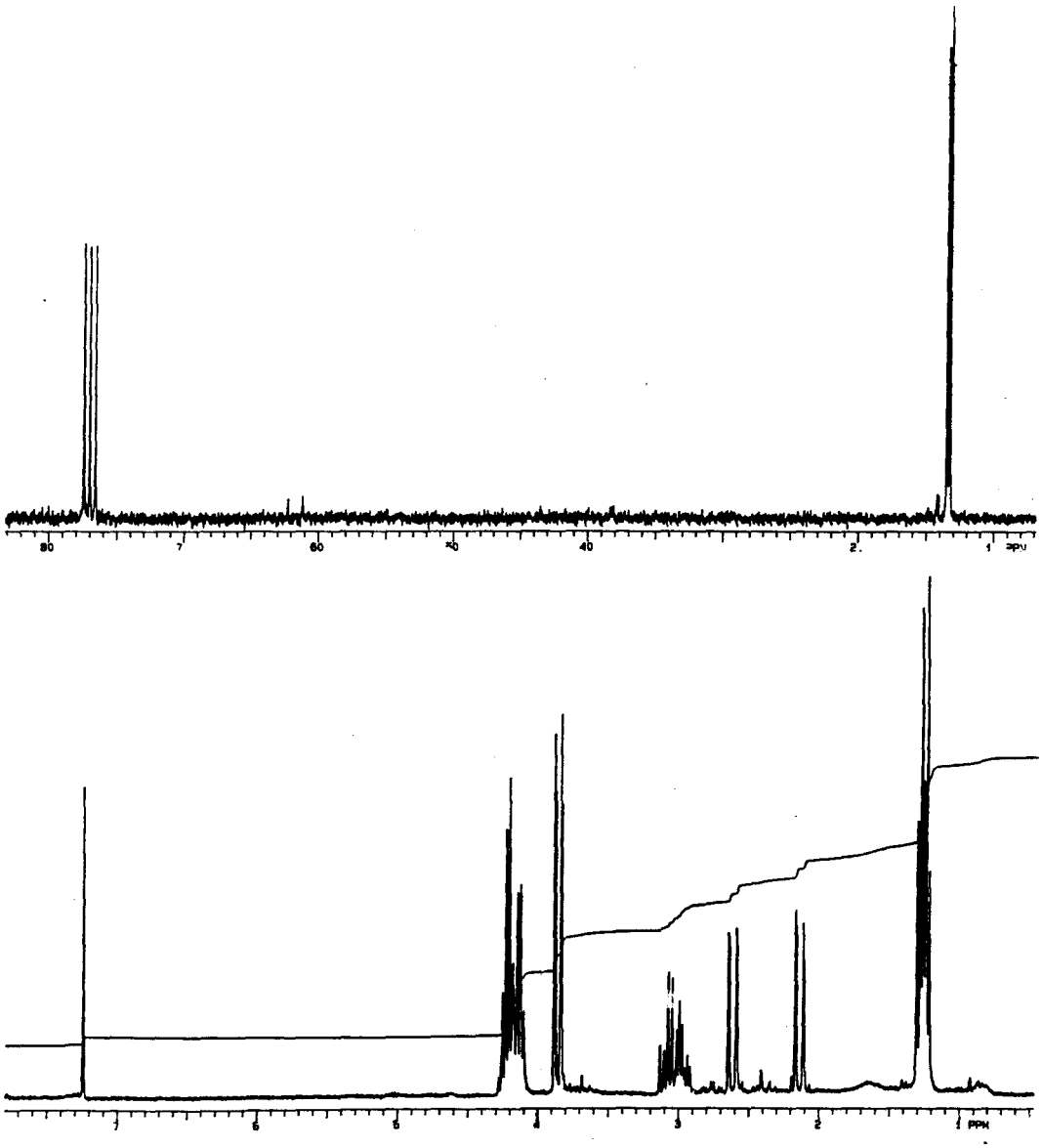

REFERENCES

Aaron, H. S., Shryne, T. M., Miller, J. I. The stereochemistry of asymmetric phosphorus compounds. I. The resolution of O-ethyl ethylphosphonothioic acid. *J. Am. Chem. Soc.* **1958**, *80*, 107-110.

Aaron, H. S., Braun, J., Shryne, T. M., Frack, H. F., Smith, G. E., Uyeda, R. T., Miller, J. I. The stereochemistry of asymmetric phosphorus compounds. III. The resolution of a series of O-alkyl alkylphosphonothioic acids. *J. Am. Chem. Soc.* **1960**, *82*, 596-598.

Ailman, D. E., Synthesis of O,O-dimethyl S-(1,2-dicarbethoxy)ethyl phosphorothioate (malaoxon) and related compounds form trialkyl phosphites and organic disulfides. *J. Org. Chem.*, **1965**, *30*, 1074-1077.

Aldridge, W. N. Some properties of specific cholinesterases with particular reference to the mechanism of inhibition by diethyl *p*-nitrophenyl thiophosphate (E605) and analogues. *Biochem. J.* **1950**, *46*, 451.

Aldridge, W. N., Miles, J. W., Mount, D. L., Verschoyle, R. D. The toxicological properties of impurities in malathion. *Arch. Toxicol.* **1979**, *42*, 95-106.

Ames, R. G., Brown, S. K., Mengle, D. C., Kahn, E., Stratton, J. W., Jackson, R. J. Protecting agricultural applicators from over-exposure to cholinesterase-inhibiting pesticides. *J. Soc. Occup. Med.* **1989**, *39*, 85-92.

Armstrong, D. J., Fukuto, T. R. Synthesis, resolution, and toxicological properties of the chiral isomers of O,S-dimethyl and -diethyl ethylphosphonothioate. *J. Agric. Food Chem.* **1987**, *35*, 500-503.

Baker, E. L., Zack, M., Miles, J. W., Alderman, L., Warren, McW., Dobbin, R. D Miller, S., and Teeters, W. R. (1978) Epidemic malathion poisoning in Pakistan malaria workers. *Lancet I,* 31-34.

Barinaga, M. A new buzz in the medfly debate. *Science*. **1991**, *253*, 1351.

Barnes, J. M. Hazards to People. In *Pesticides and Human Welfare*. **1976**, Gunn, D. L. and Stevens, J. G. R. Eds. Oxford University Press, Oxford.

Bedford, C. D., Howd, R. A., Dailey, O. D., Miller, A., Nolen, H. W., Kenley, R A., Kern, J. R., Winterle, J. S. Nonquaternary cholinesterase reactivators. 3. *J. Med. Chem.* **1986**, *29*, 2174-2183.

Bellet, E. M.; Casida, J. E. Products of peracid oxidation of organothiophosphorus compounds. *J. Agric. Food Chem.* **1974**, *22*, 207.

Benschop, H. P., DeJong, L. P. A. Nerve agent stereoisomers: Analysis, isolation and toxicology. *Acc. Chem. Res.* **1988**, *21*, 368-374.

Berkman, C. E., Fernandez, E. J., Thompson, C. M., Pavkovic, S. F. Structure of N-methylstrychninium (*S*)-[S-1, (*R*), 2-dicarbethoxyethyl]-O-methylphosphorodithioate. *Acta. Cryst.* **1993**, *C49*, 554-556.

Berman, H. A., Decker, M. M. Chiral nature of covalent methylphosphonyl conjugates of acetylcholinesterase. *J. Biol. Chem.* **1989**, *264*, 3951-3956.

Berman, H. A., Leonard, K. Chiral reactions of acetylcholinesterase probed with enantiomeric methylphosphonates. *J. Biol. Chem.* **1989**, *264*, 3942-3950.

Bhagwat, V. M., Ramachandran, B. V., Nair, P. M. Action of alkali and hydroxylamine on S-(1,2-dicarboxyethyl)-O,O-dimethylphosphorodithioate (malathion). *Indian J. Chem.* **1974**, *12*, 502-506.

Brougham, P.; Cooper, M. S.; Cummerson, D. A.; Heaney, H.; Thompson, N. *Synthesis*, **1987**, 1015.

Bucht, G., Puu, G. Aging and reactivatability of plaice cholinesterase inhibited by soman and its stereoisomers. *Biochem. Pharmacol.* **1984**, *33*, 3573-3577.

Caglioti, L. The two faces of chemistry. **1983**, MIT Press, Cambridge.

Cassida, J. E. Metabolism of organophosphorus insecticides in relation to their antiesterase activity, stability, and residual properties. *J. Agric. Food Chem.* **1956**, *4*, 772-785.

Cheminova Agro A/S, Data manual fyfanon technical. **1987**, Lemvig, Denmark.

Chen, P. R., Tucker, W. P., Dauterman, W. C. Inactivation of esterases by impurities isolated from technical malathion. *J. Agric. Food Chem.* **1969**, *7* 86-90.

Chukwudebe, A., March, R. B., Othman, M., and Fukuto, T. R. *J. Agric. Food Chem.* **1989**, *37*, 539-545.

Clothier, B., Johnson, M. K., Reiner, E. Interaction of some trialkyl phosphorothiolates with acetylcholinesterase. Characterization of inhibition, aging and reactivation. *Biochem. Biophys. Acta.* **1981**, *660*, 306-316.

Cohen, S, G. and Neuwirth, Z; Weinstein, S. Y. Association of substrates with α chymotrypsin, diethyl α-acetoxysuccinate, and diethyl malate. *J. Am. Chem. Soc.* **1966**, *88*, 5306-5315.

Cohen, S. D. Mechanisms of toxicological interactions involving organophosphate insecticides. *Fund. Appl. Toxicol.* **1984**, *4*, 315-324.

Connors, T. A. Mechanism of action of 2-choloroethylamine derivatives, sulfur mustards, epoxides, and aziridines. In *Anti-neoplastic and Immunosuppressive Agents, Part II. Handbook of Experimental Pharmacology.* Sartorelli, A. C. and Johns, D. G., Eds. **1975**, pp. 18-34, Springer-Verlag, Berlin.

Debord, J., Penicaut, B., Labadie, M. Kinetics of cholinesterase inhibition by organophosphorus compounds. *Phosphorus and Sulfur*, **1986**, *29*, 57-65.

de Jong, L. P. A., Wolring, G. Z. Stereospecific reactivation by some hagedorn-oximes of acetylcholinesterases from various species including man, inhibited by soman. *Biochem. Pharmacol.* **1984**, *33*, 1119-1125.

de Jong, L. P. A., Kossen, S. P. Stereospecific reactivation of human brain and erythrocyte acetylcholinesterase inhibited by 1,2,2-trimethylpropyl methylphosphonofluoridate (soman). *Biochem. Biophys. Acta* **1985**a, *830*, 345-348.

de Jong, L. P. A., Wolring, G. Z. Aging and stereospecific reactivation of mouse erythrocyte and brain acetylcholinesterase inhibited by soman. *Biochem.*

Pharmacol. **1985**b, *34*, 142-145.

De Matteis, F. Phosphorothionates. In *Sulphur Containing Drugs and Related Organic Compounds: Chemistry, Biochemistry, and Toxicology.* Damani, L. A. Ed. **1989**, Halsted Press, New York.

Ellman, G. L., Courtney, K. D., Andres, V., and Featherstone, R. M. A new and rapid colorimetric determination of acetylcholinesterase activity. *Biochem. Pharmacol.* **1961**, *7*, 88-95.

Eto, M. *Organophosphorus Pesticides: Organic and Biological Chemistry.* **1974**, CRC Press, Cleveland, OH.

Eya, B. K., Fukuto, T. R. The effect of chiral desbromoleptophos oxon isomers on acute and delayed neurotoxicity and their inhibitory activity against acetylcholinesterases and neurotoxic esterase. *J. Agric. Food Chem.* **1985**, *33*, 884-887.

Fest, C. Schmidt, K.-J. *The Chemistry of Organophosphorus Pesticides.* **1973**, Springer-Verlag, New York.

Forget, G. Pesticides in the third world. *J. Toxicol. Environ. Health*, **1991**, *32*, 11-31.

Fukuto, T. R. Mechanism of action of organophosphorus and carbamate insecticides. *Environ. Health Perspect.* **1990**, *87*, 245-254.

Furtick, W. R. Uncontrolled pests or adequate food? In *Pesticides And Human Welfare.* **1976**, Gunn, D. L. and Stevens, J. G. R. Eds. Oxford University Press, Oxford, pp 3-12.

Gallo, M. A. and Lawryk, N. J. Organic phosphorus pesticides. In *Handbook of Pesticide Toxicology.* Hayes, W. J. and Laws, E. R. Eds. **1991**, Academic Press, San Diego.

Glickman, A. H., Wing, K. D., Casida, J. E. Profenphos insecticide bioactivation in relation to antidote action and the stereospecificity of acetylcholinesterase inhibition, reactivation, and aging. *Toxicol. Appl. Pharmacol.* **1984**, *73*, 16-22.

Goodman and Gilman's The Parmacological Basis of Therapeutics, 7th Ed. **1985**,

Goodman, L. S.; Gilman, A.G.; Rall, T. W.; Murad, F. Eds. Macmillan, New York.

Gould, R. O., Walkinshaw, M. D. Molecular recognition in model crystal complexes: the resolution of D and L amino acids. *J. Am. Chem. Soc.* **1984**, 7840-7843.

Gould, R. O., Taylor, P., Walkinshaw, M. D. Stuctures of strychnine hydrogen (2*S*,3*S*)-tartrate trihydrate and strychnine (2*R*,3*R*)-tartrate hexahydrate. *Acta. Cryst.* **1987**, 2405-2410.

Gutmann, L., Besser, R. Organophosphate intoxication: pharmacologic, neurophysiologic, clinical, and therapeutic considerations. *Seminars in Neurology*. **1990**, *10*, 46-51.

Hassan, A., Dauterman, W. C. Studies on the optically active isomers of O,O-diethyl malathion and O,O-diethyl malaoxon. *Biochem. Pharmacol.* **1968**, *17*, 1431-1439.

Hayes, W. J. Introduction. In *Handbook of Pesticide Toxicology*. Hayes, W. J and Laws, E. R. Eds. **1991**, pp 1-37, Academic Press, San Diego.

Heath, D. F. *Organophosphorus poisons, anticholinesterases and related compounds.* **1961**, Pergamon, Oxford.

Helinski, J.; Skrzypczynski, Z,; Wasiak, J.; Michalski, J. Efficient oxygenation of thiophosphoryl and selenophosphoryl groups using trifluoroacetic anhydride. *Tetrahedron Lett.* **1990**, *31*, 4081.

Hilgetag, G., Lehmann, G. Optisch aktive thiophosphate. *J. Prak. Chem.* **1959**, *4*, 224-234.

Hilgetag, G. Optisch aktive dithiophosphorsaureester. *Z. Chem.* **1969**, *9*, 310-311.

Hirashima, A.; Eto, M. Synthesis of optically active cyclic phosphorothionates and phosphoramidothionates with insecticidal activity by using a chiral phosphorylating agent. *Agric. Biol. Chem.* **1983**, *47*, 2831-2839.

Hirashima, A., Leader, H., Holden, I., Casida, J. E. Resolution and stereoselective action of sulprofos and related *S*-propyl phosphorothiolates. *J. Agric. Food*

Chem. **1984**, *32*, 1302-1307.

Holmberg, B. Stereochemical studies. XIX. The diazotization of aspartic acid and its ethyl ester. *Z. Physik. Chem. Abt. A.* **1928**, *137*, 1893-1905.

Imamura, T.,; Gandy, J.; Fukuto, T. R.; Talbot, P. An impurity in malathion alters the morphology of rat lung bronchiolar epithelium. *Toxicology*, **1983**, *26*, 73-79.

Iyer, V. and Parmar, B. S. The isomalathion problem - a review. *Intern. J. Trop. Agric.* **1984**, *2*, 199-204.

Jackson, J. A.; Berkman, C. E.; Thompson, C. M. Stereoselective and chemoselective oxidation of phosphorothionates using MMPP. *Tetrahedron Lett.* **1992**, 6061-6064.

Jarv, J. Stereochemical aspects of cholinesterase catalysis. *Bioorg. Chem.* **1984**, *12*, 259-278.

Johnson, M. K. Delayed neurotoxicity induced by organophosphorus compounds - areas of understanding and ignorance. In *Mechanisms of Toxicity and Hazard Evaluation.* Holmstedt, B., Lauwerys, M., Mercier, M., Roberfroid, M. Eds. **1980**, pp. 27-38, Elsevier/North-Holland Biomedical Press, Amsterdam,

Johnson, M. K. Receptor or enzyme: the puzzle of NTE and organophosphate-induced delayed polyneuropathy. *TIPS*, **1987**, *8*, 174-179.

Kabachnik, M. F. and Mastryokova, T.A. Organophosphorus compounds. Dialkyl dithiophosphates. *Izvest. Akad. Nauk S.S.S.R., Otdel. Khim. Nauk*, **1953**, 121-125.

Kabalka, G. W.; Varma, M.; Varma, R. S. Tosylation of alcohols. *J. Org. Chem.*, **1986**, 2386-2388.

Koizumi, T., Amitani, H., Yoshii, E. A new method of preparing optically active alkyl phenyl phosphonates. *Tet. Lett.* **1978**, *39*, 3741-3742.

Langenberg, J. P., DeJong, L. P. A., Otto, M. F., Benschop, H. P. Spontaneous and oxime-induced reactivation of acetylcholinesterase inhibited by phosphoramidates. *Arch. Toxicol.* **1988**, *62*, 305-310.

Lanks, K. W., Seleznick, M. J. Spontaneous reactivation of acetylcholinesterase inhibited by diisopropylfluorophosphate. *Biochim. Biophys. Acta*, **1981**, *660*, 91-95.

Lee, P. W., Allahyari, R., Fukuto, T. R. Studies on the chiral isomers of fonofos and fonofos oxon. *Pestic. Biochem. Physiol.* **1978**, *8*, 146-157.

Lieske, C. N., Clark, J. H., Meyer, H. G., Lowe, J. R. Spontaneous and induced reactivation of eel acetylcholinesterase inhibited by three organophosphinates. *Pestic. Biochem. Physiol.* **1980**, *13*, 205-212.

Lieske, C. N., Gessner, C. E., Gepp, R. T., Clark, J. H., Meyer, H. G., Broomfield, C. A. pH effects in the spontaneous reactivity of phosphinylated acetylcholinesterase. *Life Sciences*, **1990**, *46*, 1189-1196.

Lin, A. R., Main, A. R., Tucker, W. P., Motoyama, N., Dauterman, W. C. Studies on organophosphorus impurities in technical malathion: inhibition of carboxylesterase and the stability of isomalathion. *Pestic. Biochem. Physiol.* **1984**, *21*, 223-231.

Lotti, M. Treatment of acute organophosphate poisoning. *Med. J. Aus.*, **1991**, *154*, 51-55.

Maelicke, A. Acetylcholinesterase: the structure. *TIPS.* **1991**, *16*, 355-356.

Mahieu, P., Lauwerys, R., Dive, A., Hanston, P. Poisoning by some insecticides, herbicides and fungicides. *Acta Clin. Belg. Suppl.* **1990**, *13*, 75-85.

Main, A. R. Affinity and phosphorylation constants for the inhibition of esterases by organophosphates. *Science.* **1964**, *144*, 992-993.17

Mallipudi, N. M., Talcott, R. E., Ketterman, A., Fukuto, T. R. Properties and inhibition of rat malathion carboxylesterase. *J. Toxicol. Environ. Health.* **1980**, *6*, 585-596.

March, R. B., Fukuto, T. R., Metcalf, R. L., Maxon, M. G. Fate of P^{32}-labeled malathion in the laying hen, white mouse, and american cockroach. *J. Econ. Entomol.* **1956**, *49*, 185-195.

Matolcsy, G., Nadasy, M., Andriska, V. *Pesticide Chemistry.* **1988**, Elsevier Science Publishing Co., Inc., New York.

Maxwell, D. M. and Brecht, K. M. Quantitative structure-activity analysis of acetylcholinesterase inhibition by oxono and thiono analogues of organophosphorus compounds. *Chem. Res. Toxicol.* **1992**, *5*, 66-71.

Metcalf, R. L., and March, R. B. The isomerization of organic thionophosphate insecticides. *J. Econ. Entomol.* **1953**, *46*, 288-294.

Miles, C. J., Takashima, S. Fate of malathion and O,O,S-trimethyl phosphorothioate by-product in Hawaiian soil and water. *Arch. Environ.Contam. Toxicol.* **1991**, *20*, 325-329.

Miller, A., Nolen, H. W., Jackson, S. E., Howd, R. A., Harris, R. N., Bedford, C. D. Comparison of three enzymatic models for evaluation of reactivators of organophosphorus ester inhibited acetylcholinesterase. *Proc. West. Pharmacol. Soc.*, **1984**, *27*, 297-301.

O'Brien, R.D. *Insecticides: Action and Metabolism.* **1967**, Academic Press, New York.

Ohkawa, H., Mikami, N., Kasamatsu, K., Miyamoto, J. Stereoselectivity in toxicity and acetylcholinesterase inhibition by the optical isomers of papthion and papoxon. *Agr. Biol. Chem.* **1976**, *40*, 1857-1861.

Ooms, A. J. J., Boter, H. L. Stereospecificity of hydrolytic enzymes in their reaction with optically active organophosphorus compounds. *Biochem. Pharmacol.* **1965**, *14*, 1839-1846.

Osweiler, G. D., Carson, T. L., Buck, W. B., Van Gelder, G. A. Clinical and Diagnostic Veterinary Toxicology. **1984**, Kendall/Hunt Publishing Company, Dubuque, IA.

Parr, J. A. Information Pamphlet: Pesticides. **1987**, Department of Governmental Relations and Science Policy, American Chemical Society, Washington, D.C.

Peerdeman, A. F. The absolute configuration of natural strychnine. *Acta Cryst.* **1956**, *9*, 824.

Perutz, M. Is science necessary? **1991**, Oxford University Press, Oxford.

Quinn, D. M. Acetylcholinesterase: Enzyme structure, reaction dynamics, and

virtual transition states. *Chem. Rev.* **1987**, *87*, 955-979.

Rosenstock, L., Keifer, M., Daniell, W. E., McConnel, R., Claypoole, K. Chronic central nervous system effects of acute organophosphate pesticide intoxication. *Lancet*, **1991**, *338*, 223-227.

Ryan, D. L., Fukuto, T. R. The effect of impurities on the toxicokinetics of malathion in rats. *Pestic. Biochem. Physiol.* **1985**, *23*, 413-424.

Ryu, S.; Jackson, J.; Thompson, C. M. Methanolysis of phosphoramidates with boron trifluoride-methanol complex. *J. Org. Chem.*, **1991**a, *56*, 4999-5002.

Ryu, S.; Lin, J.; Thompson, C. M. Comparative anticholinesterase potency of chiral isoparathion methyl. *Chem. Res. Toxicol.* **1991**b, *4*, 517-520.

Schuhmann, G. The economic impact of pesticides on advanced countries. In *Pesticides and Human Welfare*. Gunn, D. L. and Stevens, J. G. R. Eds. **1976**, pp. 55-71, Oxford University Press, Oxford.

Stec, W. J.; Okruszec, A.; Michalski, J. Organophosphorus compounds of sulfur and selenium. Stereochemistry of oxidation of thiono- and selenophosphoryl compounds with hydrogen peroxide. *J. Org. Chem.* **1976**, *41*, 233.

Stephens, T. Organophosphate pesticides: neurotoxins threaten farm workers. *J. NIH Research.* **1991**, *3*, 21-24.

Stone, J. F., Eichner, M. L., Kim, C., Koehler, K. Relationships between clothing and pesticide poisoning. *J. Environ. Health*, **1988**, *50*, 210-215.

Sussman, J. L., Harel, M., Frolow, F., Oefner, C., Goldman, A., Toker, L., Silman, I. Atomic structure of acetylcholinesterase from torpedo califonica; a prototypic acetylcholine-binding protein. *Science.* **1991**, *253*, 872-879.

Talcott, R. E. Hepatic and extrahepatic malathion carboxylesterase. Assay and localization in the rat. *Toxicol. Appl. Pharmacol.* **1979**, *47*, 145-150.

Talcott, R. E., Denk, H., Mallipudi, N. M. Inactivation of esterases by impurities isolated from technical malathion. *Toxicol. Appl. Pharmacol.* **1979**, *49*, 373-376.

Thompson, C. M., Fukuto, T. R. Mechanism of cholinesterase inhibition by

methamidophos. *J. Agric. Food Chem.* **1982**, *30*, 282-284.

Thompson, C. M., Frick, J. A., Natke, B. C., Hansen, L. K. Preparation, analysis, and anticholinesterase properties of O,O-dimethyl phosphorothioate isomerides. *Chem. Res. Toxicol.* **1989**, *2*, 386-391.

Thompson, C. M. Preparation, analysis, and toxicity of phosphorothiolates. In *Organophosphates: Chemistry, Fate and Effects*. Chambers, J. E. and Levi, P. E. Eds. **1992**, Academic Press, San Diego.

Thompson, C. M., Ryu, S., Berkman, C. E. Consequence of phosphorus stereochemistry upon the postinhibitory reaction kinetics of acetylcholinesterase poisoned by phosphorothiolates. *J. Am. Chem. Soc.* **1993**, *114*, 10710-10715.

Toia, R. F., March, R. B., Umetsu, N., Mallipudi, N. M., Allahyari, R., Fukuto, T. R. Identification and toxicological evaluation of impurities in technical malathion and fenthion. *J. Agric. Food Chem.* **1980**, *28*, 599-604.

Umetsu, N., Grose, F. H., Allahyari, R., Abu-El-Haj, S., Fukuto, T. R. Effect of impurities on the mammalian toxicity of technical malathion and acephate. *J. Agric. Food Chem.* **1977**, *4*, 946-953.

Valentine, D. Preparation of the enantiomers of compounds containing chiral phosphorus centers. In *Asymmetric Synthesis, Vol 4*, **1984**, Academic Press, Inc., San Diego.

Van Wazer, J. R. *Phosphorus and Its Compounds, Volume I: Chemistry.* **1958**, Interscience Publishers Inc., New York.

Wallace, K. B., Herzberg, U. Reactivation and aging of phosphorylated brain acetylcholinesterase from fish and rodents. *Toxicol. Appl. Pharmacol.* **1988**, *92*, 307-314.

Wallace, K. B.; Kemp, J. R. Species specificity in the chemical mechanism of organophosphorus, anticholinesterase activity. *Chem. Res. Toxicol.* **1991**, *4* 41-49.

Welling, W. Pesticides in Agriculture in *Stereoselectivity of Pesticides*, Ariens, E. J., Van Rensen, J. J. S., Welling, W. Eds. **1988**, Elsevier, Amsterdam.

Wester, R. C., and Cashman, J. R., Antiinfective skin preparations: Malathion. In *Sulphur Containing Drugs and Related Organic Compounds: Chemistry, Biochemistry, and Toxicology*. Damani, L. A. Ed. **1989**, Halsted Press, New York.

Wustner, D. A., Fukuto, T. R. Stereoselectivity in cholinesterase inhibition, toxicity, and plant systemic activity by the optical isomers of O-2-butyl S-2-(ethylthio)ethyl ethylphosphonothioate. *J. Agric. Food Chem.* **1973**, *21*, 756-761.

Zilberman, D., Schmitz, A., Casterline, G., Lichtenberg, E., Siebert, J. B. The economics of pesticide use and regulation. *Science*, **1991**, *253*, 518-522.

Zimmerman, N. Non-neurotoxic effects of malathion and malathion formulations. *Comments Toxicol.* **1990**, *4*, 39-58.

VITA

CLIFFORD E. BERKMAN

Clifford Berkman received a B.A. (with Honors) in Chemistry from Lake Forest College (Lake Forest, IL) in 1986. His senior thesis entitled "*Substrate Inhibition of Monoamine Oxidase*" was directed by William B. Martin. Berkman began his graduate studies at Loyola University of Chicago's Department of Chemistry in the Fall of 1988. During his career at Loyola University, he was awarded a Teaching Assistantship for General Chemistry in 1988, 1990, and 1992, and a Teaching Assistantship for Organic Chemistry in 1990. Research toward his Ph.D. thesis "*Synthesis of Malathion, Malaoxon, and Isomalathion Enantiomers and Examination of their Interactions with Acetylcholinesterase*" was guided by Prof. Charles M. Thompson and was successful defended November 1, 1993. He was awarded a Ph. D. in May of 1994. In February of 1993, prior to the successful defence of his thesis November 1, 1994, he began a post-doctoral fellowship at IGEN Research Institute (Seattle, WA) under the direction of John R. Cashman. Memberships in professional societies include the American Chemical Society (Organic and Agrochemical Divisions) and Sigma Xi. Awards include *First Place*

for Oral Presentation at the 21st Annual Graduate Student Forum of the Loyola University of Chicago Sigma Xi Chapter (May 1991) and *Young Scientist Research Award* from the Agrochemicals Division of ACS (203rd ACS National Meeting, San Francisco, April, 1992). Berkman's research interests include enzyme reaction mechanism and kinetics, protein-chiral substrate interactions, and asymmetric organophosphorus chemistry. A listing of his publications and presented papers can be found on the succeeding pages.

Publications

(1) Synthesis of Chiral Malathion and Chiral Isomalathion. Berkman, C. E., Thompson, C. M. *Tetrahedron Lett.* **1992**, *33*, 1415.

(2) Stereoselective and Chemoselective Oxidation of Phosphorothionates Using MMPP. Jackson, J. A., Berkman, C. E., Thompson, C. M. *Tetrahedron Lett.* **1992**, *33*, 6061.

(3) Consequence of Phosphorous Stereochemistry upon the Post-Inhibitory Reaction Kinetics of Acetylcholinesterase Poisoned by Phosphorothiolates. Thompson, C. M., Ryu, S., Berkman, C. E. *J. Am. Chem. Soc.*, **1992**, *114*, 10710.

(4) Kinetics of Post-Inhibitory Reactions of AChE Poisoned by Chiral Isomalathion: A Surprising Non-Reactivation Induced by the R_P Stereoisomers. Berkman, C. E., Ryu, S., Quinn, D. A., Thompson, C. M. *Chem. Res. Toxicol.* **1993**, *6*, 28.

(5) Structure of N-methylstrychninium *(S)*-[S-1,*(R)*,2-dicarbethoxyethyl]-O-methylphosphorodithioate. Berkman, C. E.; Fernandez, E. J.; Thompson, C. M.; Pavkovic, S. F. *Acta. Cryst.* **1993** *C49*, 554.

(6) Book Chapter: Stereochemical Aspects of Organophosphate Toxicity. Thompson, C. M.; Berkman, C. E.; Ryu, S.; Jackson, J. A.; Quinn, D. A; Larson, A. *Rev. Pest. Toxicol.* **1993** (in press).

(7) Interaction of AChE with Enantiomers of Malaoxon and Isomalathion. Berkman, C. E.; Quinn, D. A.; Thompson, C. M. *Chem. Res. Toxicol.* **1993** (in press).

(8) Synthesis, Absolute Configuration, and Analysis of Chiral Malathion, Malaoxon, and Isomalathion. Berkman, C. E.; Perrin, S.; Thompson, C. M *Chem Res. Toxicol.* **1993** (in press).

Presented Papers

(1) Synthesis and Preliminary Anti-Cholinesterase Potency by Chiral Impurities Found in Malathion Formulations. Berkman C. E.; Thompson, C. M. 21st Annual Graduate Student Forum, Loyola University Chicago Sigma Xi Chapter, Chicago,

IL. May 1991.

(2) Stereospecificity and Phosphorothiolate Mode of Action. Thompson, C. M.; Ryu, S.; Berkman, C. E.; Jackson, J. A. 203rd American Chemical Society Meeting, San Francisco, April 1992.

(3) Synthesis and Stereoselective Anticholinesterase Potency of Isomalathion Stereoisomers. Berkman, C. E.; Thompson, C. M. 203rd American Chemical Society Meeting, San Francisco, April 1992.

(4) Chiral Isoparathion Methyl as a Stereospecific Probe of Phosphorothiolate Mechanism of Action. 203rd American Chemical Society Meeting, San Francisco, April 1992.

(5) Stereospecificity and Phosphorothiolate Mode of Action. Thompson, C. M.; Ryu, S.; Berkman, C. E.; Jackson, J. A. ACS 25th Great Lakes Regional Meeting, June, 1992.

Education Ph. D. Chemistry, Loyola University of Chicago; 1993 (anticipated)
Thesis: *Synthesis of Malathion, Malaoxon, and Isomalathion Enantiomers and Examination of their Interactions with Acetylcholinesterase.*

B.A. Chemistry (Honors), Lake Forest College; 1986
Thesis: *Substrate Inhibition of Monoamine Oxidase.*

Research Experience 2/93 - present Post-Doctoral Fellow, IGEN Research Institute, John R. Cashman, Research Director.

8/88 - 2/93 Research Associate, Department of Chemistry, Loyola University of Chicago, Charles M. Thompson, Thesis Director.
8/81 - 5/82 Undergraduate Research Associate, Lake Forest College, William B. Martin, Thesis Director.

Teaching Experience Teaching Assistant:
General Chemistry 111, 112; 1988-1989, 1990 (Fall), 1992 (Fall).
Organic Chemistry 222; 1990 (Spring).

Research Interests Enzyme Reaction Mechanism and Kinetics.
Protein-Chiral Substrate Interactions.
Asymmetric Organophosphorus Chemistry.

Professional Societies American Chemical Society (Organic and Agrochemicals Division).
Sigma Xi

Awards *Young Scientist Research Award*; Agrochemicals Division, 203rd ACS National Meeting San Francisco, April 1992.

First Place Oral Presentation, 21st Annual Graduate Student Forum, Loyola University of Chicago Sigma Xi Chapter, May 1991.

References Prof. Charles M. Thompson, Department of Chemistry, Loyola University of Chicago, 6525 N. Sheridan Rd., Chicago, IL 60626. (312) 508-3123.

Prof. James H. Babler, Department of Chemistry, Loyola University of Chicago, 6525 N. Sheridan Rd., Chicago, IL 60626.

(312) 508-3113.

Dr. John R. Cashman, IGEN Research Institute, 130 5th Ave. N., Seattle, WA 98109. (206) 441-6684.

The dissertation submitted by Clifford E. Berkman has been read and approved by the following committee:

Dr. Charles M. Thompson, Director
Associate Professor, Chemistry
Loyola University of Chicago

Dr. Duarte Mota de Freitas
Associate Professor, Chemistry
Loyola University of Chicago

Dr. James H. Babler
Proffessor, Chemistry
Loyola University of Chicago

Dr. Stephen F. Pavkovic
Professor, Chemistry
Loyola University of Chicago

Dr. John R. Cashman
Assistant Director
IGEN Research Institute

The final copies have been examined by the director of the dissertation and the signature which appears below verifies the fact that any necessary changes have been incorporated and that the dissertation is now given final approval by the committee with reference to content and form.

The dissertation is, therefore, accepted in partial fulfillment of the requirements for the degree of doctor of philosophy.

April 6, 1994
Date

Charles M. Thompson
Director's Signature